University of Nevada

Reno

Soil Geochemical Study of the Altered Zones Associated with the Gooseberry Mine Area, Storey County, Nevada

A thesis submitted in partial fulfillment of the requirements for the degree of Master of Science in Geochemistry

by

Susan E. Royse

December 1986

The thesis of Susan E. Royse is approved:

Thesis Advisor

Department Chairman

Dean, Graduate School

University of Nevada

Reno

December 1986

ACKNOWLEDGEMENTS

My thanks to Westcoast Oil and Gas and Tom Nimsic for allowing me to do my thesis on the Gooseberry property and for allowing me to use their laboratory to analyze the samples.

I would also like to thank Precambrian Exploration for allowing me to use the lab to complete my analyses, and especially to Roy Laws for allowing me the time I needed to complete my thesis.

Special thanks to Dr. Li Hsu for his tremendous help and patience.

ABSTRACT

A soil geochemical study was conducted in the Gooseberry Mine area. The primary rock in the area which contains the ore deposit is the Kate Peak andesite.

Sampling was confined to the limonitic alteration zone which hosts the Gooseberry Au-Ag precious metal deposit, and the Red Top claims which contains a similar limonitic alteration zone and geology. Soil samples were taken on a 100-foot grid and analyzed for Au, Ag, Cu, Pb, Zn, Mn, Hg, K, As, and Sb.

The statistical and geochemical examination of the data exhibited a K-Pb and to a lesser extent Hg-As association in the Gooseberry alteration zone. An evident Hg-As, Cu and smaller Mn-Zn association was prominent in the Red Top alteration zone. Au and Ag anomalies were found in the Gooseberry zone but are believed to be due to contamination.

The statistical analysis showed the means and variances of the Red Top area to be different from the Gooseberry, but both areas have similar elemental composition and associations. A possible explanation for these elemental differences may be due to a deeper precious metal deposit in the Red Top area than in the Gooseberry area, forming a different secondary dispersion halo.

A geochemical signature of the alteration zones was established and in doing so a possible extension of the Gooseberry ore body was found and a possible new area was found in the Red Top zone.

TABLE OF CONTENTS

LIST OF FIGURES

LIST OF TABLES

LIST OF PLATES

INTRODUCTION

Systematic sampling of residual soil in search of ore deposits has been very successful in detailed geochemical exploration. During the process of weathering and leaching, anomalous concentrations of elements from underlying mineralization may become incorporated in the soil forming a secondary dispersion halo around the mineralization. Minerals formed under the primary conditions are often unstable in the secondary environment and will weather with the result that elements contained within them may be released, transported, and redistributed. Geochemical methods may then be used to find the primary source of these elements. (Levinson, 1974)

The purpose of this study is to determine the geochemical signature in the residual soil of the limonite-stained argillic alteration zone overlying the Gooseberry mineralized structure. Also included in this study are analyses of samples from the Red Top claims south of the Gooseberry mine which show a similar limonite-stained argillic alteration zone as that which hosts the Gooseberry precious metal veins. A comparison of the soil geochemistry between the two areas is made. It is hoped the data from this study will prove useful as an exploration tool for similar epithermal precious metal deposits.

The Gooseberry Mine property is in sections 25, 26 and 36, T19N, R22E, Storey County, Nevada and is approximately 24 miles east of Reno in the Virginia Range (Figure 1.).

The Gooseberry Mine property consists of some 1,280 acres comprised of one patented Gooseberry claim, 560 acres of fee property, 32 unpatented lode and fraction claims (section 25 and 26), and 21 unpatented Red Top lode claims (section 36).

The Gooseberry ore was originally discovered in 1906. APCO Oil Corporation assumed operational rights in 1974 and worked on the property 1974-1975. Westcoast Oil and Gas Corporation took over the mine in 1976 and continued to operate the mine until 1981. Asamera Minerals Inc. purchased the Gooseberry Mine property in late 1982. Reserves in the proven and probable categories total 607,000 tons at an average grade of 0.23 oz/ton gold and 9.71 oz/ton silver. (Asamera, 1984, unpubl. report)

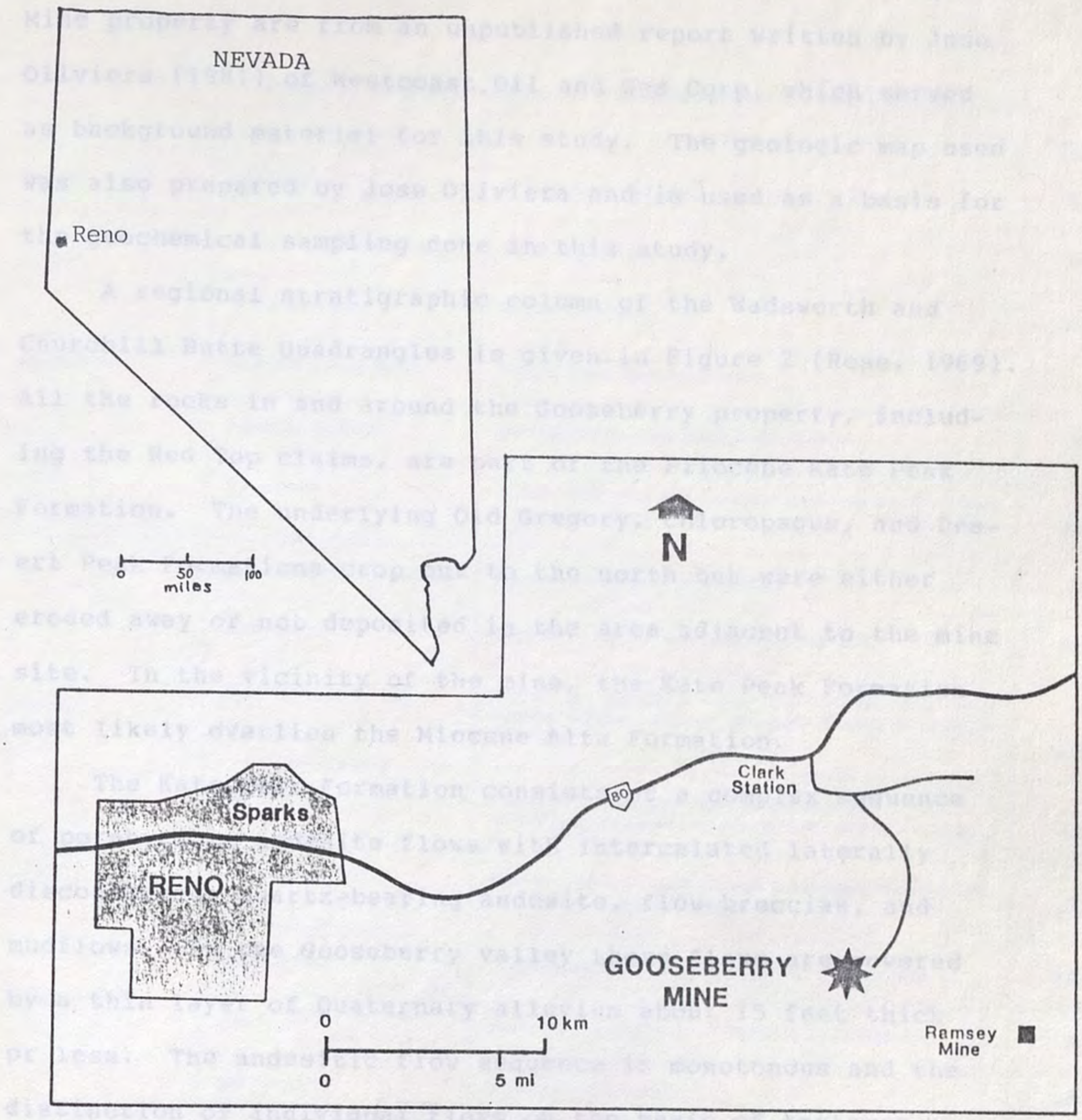

Figure 1. Location Map of Gooseberry Mine

GEOLOGY

The following geologic description of the Gooseberry Mine property are from an unpublished report written by Jose Oliviera (1981) of Westcoast Oil and Gas Corp. which served as background material for this study. The geologic map used was also prepared by Jose Oliviera and is used as a basis for the geochemical sampling done in this study.

A regional stratigraphic column of the Wadsworth and Churchill Butte Quadrangles is given in Figure 2 (Rose, 1969). All the rocks in and around the Gooseberry property, including the Red Top claims, are part of the Pliocene Kate Peak Formation. The underlying Old Gregory, Chloropagus, and Desert Peak Formations crop out to the north but were either eroded away or not deposited in the area adjacent to the mine site. In the vicinity of the mine, the Kate Peak Formation most likely overlies the Miocene Alta Formation.

The Kate Peak Formation consists of a complex sequence of porphyritic andesite flows with intercalated laterally discontinuous quartz-bearing andesite, flow breccias, and mudflows. In the Gooseberry valley these flows are covered by a thin layer of Quaternary alluvium about 15 feet thick or less. The andesitic flow sequence is monotonous and the distinction of individual flows on the basis of textures, phenocryst composition and ratios has proved impractical. Jose Oliviera distinguished four separate rock units and two alteration zones in the area (Plate 1). Based on field re-

Figure 2. **Generalized stratigraphic section in the Wadsworth and Churchill Butte quadrangles, Nevada.**

Age	Formation	Lithology	Approx. Max. Thickness
Recent	Alluvium	Gravel, sand, and silt.	50′
Pleistocene	Lake Lahontan deposits	Sand, silt, gravel.	125′
	Older alluvium	Gravel and sand.	35′
	McClellan Peak Basalt	Olivine basalt flows and cinders.	35′
	Mustang Andesite	Hornblende-pyroxene trachyandesite flows.	350′
	Lousetown	Basalts, andesites, and trachyandesites—mostly lava flows—some intrusives.	350′
	—Unconformity—		
Pliocene	Knickerbocker(?) Andesite	Pyroxene andesite dikes and plugs.	....
	Coal Valley	Sandstone, rhyolite tuff, shale, and diatomite.	500′
	Kate Peak	Dacite and rhyodacite flows, flow breccias, some interbedded rhyolite tuff, and diatomite. Dacitic to rhyolitic intrusives.	1,500′
	—Unconformity—		
	Desert Peak	Upper part: sandstone, shale, and diatomite. Lower part: dacite and rhyodacite flows and flow breccias.	3,000′?
Miocene	Chloropagus	Basaltic and andesitic flows with interbedded rhyolitic tuffs and sediments. Basaltic intrusives.	3,000′
	—Unconformity—		
	Old Gregory	Mainly rhyolitic tuffs, some shale and andesitic lava.	1,200′
	Alta	Andesitic and basaltic lavas, breccias, and intrusives.	1,000′
	Hartford Hill	Rhyolitic ash flow tuffs.	2,500′
	—Unconformity—		
Oligocene	Pre-Hartford Hill	Olive green claystone.	300′
	—Unconformity—		
Jurassic		Metamorphic dioritic and granitic rocks.	?

Source: Rose, 1969, p.10

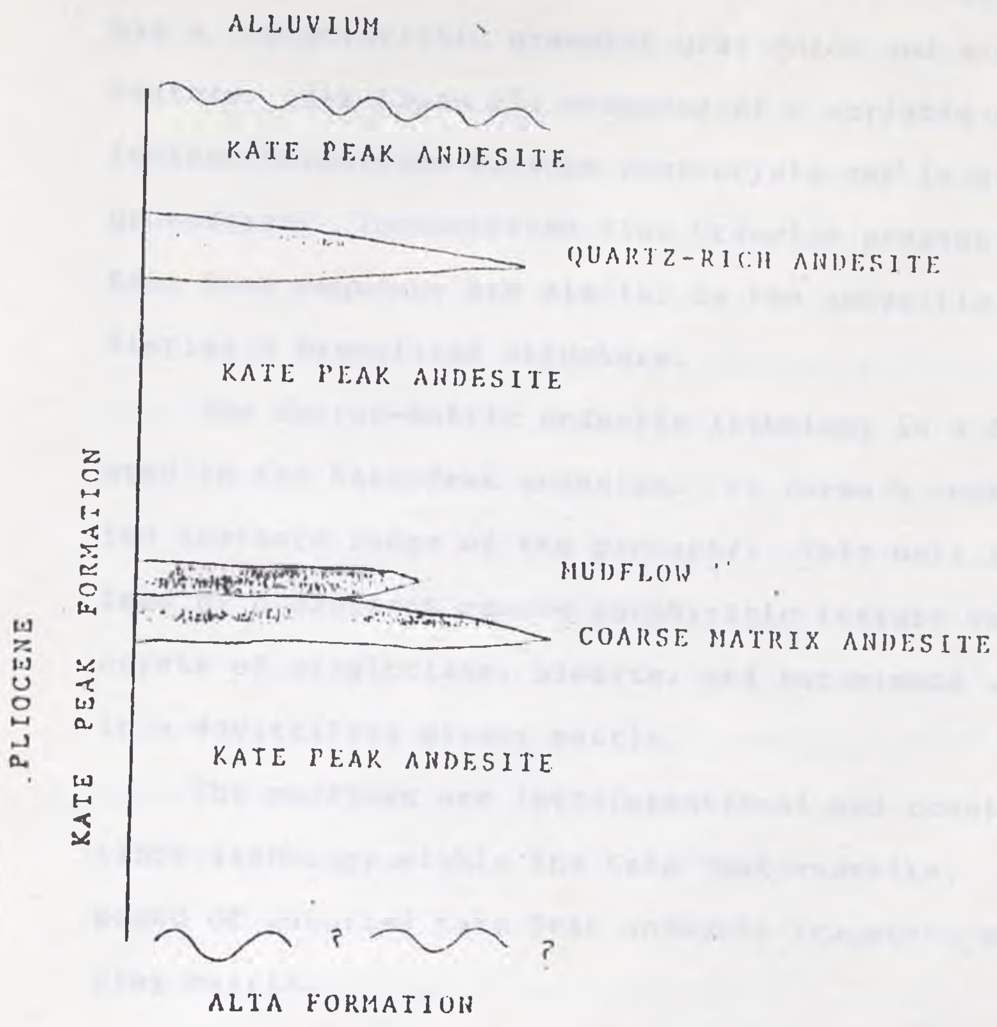

Figure 3. Stratigraphic Column at the Gooseberry Mine Property.

(Jose Oliviera, 1981)

lationships and geologic interpretation he also constructed a local stratigraphic column (Figure 3).

The Kate Peak andesite is the host rock for the epithermal veins and is the most abundant rock unit in the area. It has a characteristic greenish-gray color and a porphyritic texture. Its flows are composed of a variable ratio of plagioclase-hornblende-biotite phenocrysts set in an aphanitic groundmass. Intercalated flow breccias present within the Kate Peak sequence are similar to the andesitic flows but display a brecciated structure.

The Coarse-matrix andesite lithology is a flow intercalated in the Kate Peak andesite. It forms a continuous bed in the northern range of the property. This unit is characterized by a distinct coarse porphyritic texture where phenocrysts of plagioclase, biotite, and hornblende are embedded in a devitrified glassy matrix.

The mudflows are intraformational and constitute a distinct lithology within the Kate Peak andesite. They are composed of unsorted Kate Peak andesite fragments embedded in a clay matrix.

The Quartz-bearing andesite lithology outcrops only in the northwest portion of the property and forms a discontinuous interbedded flow. Quartz phenocrysts up to 2mm in diameter constitutes up to 5% of the unit.

The alteration zones present in the area are the argillic and limonite-stained argillic zones. The argillic zone is characterized by colors ranging from grayish-white to gray-green. Clays were formed along faults and fault intersections by pulverization of the rocks and hydrothermal fluid action which decreases in intensity away from the faults. Minimally altered andesite show kaolinized plagioclase phenocrysts embedded in a bleached grayish-green matrix.

The limonite-stained argillic zone coincides with the surface expression of the Gooseberry vein structure and extends 200 to 700 feet north and south of the vein and 4000 feet along the strike. It is also well-developed along the Dam fault (along east side of property) and the Red Top area. The zone is characterized by a rusty orange argillized material suggesting near-surface oxidation of the heavily propylitized andesite. In the Red Top area there is an extensive zone of leached and kaolinized porphyritic Kate Peak andesite.

A thin veneer of Quaternary alluvium debris covers portions of the valley and drainage courses. It consists of unconsolidated boulders, gravels, and sands derived from the Kate Peak Formation.

Structural Geology

The structural features associated with the Gooseberry property probably are intimately related to tectonic events which have taken place along the Walker Lane and other Basin and Range fault systems. Faults with large components of vertical or high angle oblique displacements predominate in the Gooseberry area, resulting from Post-Miocene regional extension which characterizes the Basin and Range Province.

Locally, faulting is evidenced by scarps, topographic lineaments, structurally controlled drainage, and fault gouge and brecciated zones. The Gooseberry area is bounded on the north, southwest, and southeast by an extensional fault system forming a triangular basin which developed during regional post-Miocene Basin and Range extension along pre-existing right-lateral wrench faults related to the Walker Lane fault system.

Three major intersecting sets of faults in the Gooseberry basin strike N25-55^{o}E, N40-60^{o}W, and E-W. Dips range from 45^{o} to vertical. The northeast and northwest fault sets intersect at angles of 60 to 90^{o} suggesting they originally developed as secondary or higher order shears related to earlier regional wrench fault movements. The Gooseberry ore was emplaced along an E-W trending pre-existing fault within the Kate Peak Formation.

Post-ore faults include the northeast and northwest sets, and a set along the E-W vein structure itself. The NW trending faults exhibit right-lateral movement, while the NE set exhibits left-lateral displacement. The third set parallel to the vein exhibits predominantly right-lateral displacement as indicated by slickensides formed along the Gooseberry fault. A component of vertical displacement is associated with all three sets of post-ore faults.

Alteration

In the vicinity of the Gooseberry vein the Kate Peak andesite has undergone intense propylitization and silicification. The rock has increased its pyrite content, up to 5%, and calcite has also been introduced. The propylitically altered rocks are characteristically dark greenish-gray with chalky white feldspar phenocrysts. Adjacent to the vein, the host rock contains finely disseminated pyrite and adularia in a zone that extends 5 to 30 feet from the vein. Calcite-quartz veinlets are also common. Plagioclase phenocrysts have been altered to calcite, adularia, chlorite, epidote and sericite. Hornblende and biotite have been altered to chlorite, magnetite and sphene. The groundmass is extremely altered and contains sericite, calcite, quartz, hornblende, and magnetite. As you go further from the vein the andesite remains propylitically altered with plagioclase replaced by calcite, sericite, and minor chlorite; and hornblende and biotite replaced by chlorite, magnetite, calcite, sphene, and epidote. The pyrite content decreases as you go further from the vein.

Therefore, the heavily propylitized wall rocks adjacent to the vein exhibit several types of alteration; chloritization, pyritization, carbonatization and sericitization. Chemically, this probably involved an introduction of water, CO_2, and S and extraction of SiO_2 that was probably transferred to the vein sites where it crystallized as quartz.

Mineralizing solutions laden with H_2O, CO_2, and S reacted with the andesites resulting in the binding of Fe, Ca, Mg, and Mn in the rocks to form calcite, chlorite and pyrite. (Jose Oliviera, 1981)

An analysis of the altered wall rock was done by Schafer (1976) for MgO, CaO, Na_2O, and K_2O. Schafer's study showed a decrease in calcium and magnesium toward the vein. Sodium and potassium concentrations increased as the vein was approached. This suggests the Ca and Mg ions were mobilized and moved from their mafic mineral and plagioclase sources by the introduction of the chemically active fluids, and precipitated as carbonates in the shear zone.

As a result of the mobilization and removal of the alkaline earth elements, the alkalis (Na and K) were enriched in the altered wall rock. The K and Na cations may also have been introduced by the hydrothermal waters. The adularia formed as a product of the alkali metasomatism. (Schafer, 1976)

Terry Sprecher conducted an alteration study on the Gooseberry mine as her M.S. thesis with the University of Nevada. She indentified 5 hydrothermal alteration assemblages based on outcrop appearance: propylitic (two types), smectite-quartz, dickite-silica, and silicification. Figure 4 lists the diagnostic minerals with each assemblage. Propylitized rock is the most common type of altered rock in the area, surrounding the Gooseberry fault as well as the Red Top fault structures. (Sprecher, 1985).

Summary of the Alteration Types Present at the Gooseberry Mine and their Diagnostic Minerals.

Assemblages:	Propylitic		M	I	D-S	S
Types:	P1	P2				
smectite	D	D	D	–	–	+/–
illite	+/–	+/–	+/–	D	–	+/–
mixed layer-clays	+/–	+/–	+/–	–	–	+/–
chlorite	D	+/–	–	–	–	–
calcite	D	+/–	+/–	–	–	–
albite	D	–	–	–	–	+/–
adularia	D	–	–	–	–	+/–
epidote	D	+/–	–	–	–	+/–
clinozoisite	D	+/–	–	–	–	+/–
hematite	+	+/–	–	–	–	+/–
pyrite	+/–	–	–	–	–	+/–
quartz	+/–	+/–	D	D	+/–	D
zeolites	+/–	+/–	–	–	–	–
dickite	–	–	–	–	D	–
alunite	–	–	–	–	+/–	–
cristobalite	–	–	–	–	+/–	–
opal	–	–	–	–	+/–	–

Symbols: P1 = propylitic type P1; P2 = propylitic type P2; M = smectite-quartz assemblage; I = illite-quartz assemblage; D-S = dickite-silica assemblage; S = silicification; D = diagnostic mineral; + = mineral present; – = mineral absent; +/– = mineral present or absent.

Figure 4. Alteration Assemblages present at Gooseberry Mine and their diagnostic minerals.
(Sprecher, 1985)

Vein Mineralization

The ore deposit at the Gooseberry mine is an epithermal Au-Ag calcite-quartz-adularia vein emplaced along the pre-existing Gooseberry fault. The fault served as a conduit for hydrothermal fluids and the locus for mineralization. The vein is dated at 10.3 million years by a K-Ar analysis of vein adularia (Silberman, 1977).

The Gooseberry ore bearing veins exist as a tabular body with thickness ranging up to 30 feet. The veins are fissure veins filling voids in the shear zone and partially replacing locally crushed wall rock. The ore zone consists of a hanging wall and a footwall structure which pinch and swell along strike and dip. The footwall (or northern part) generally carries the better grades. At various intervals the vein splits into offshoots which are separated by a few feet of wallrock. In detail, the vein deviates along strike from a straight line and can be divided into 3 sections; a western section striking N80W, a mid-section striking approximately E-W extending for 400 feet, and an eastern section which deviates from the E-W direction to S55E. The structure generally dips steeply to the south, however a northern dip was observed in a few places. The vein is thickest in the mid-section of the structure.

The vein is composed of calcite, quartz and lesser adularia. Pyrite is present in both the vein and alteration halo. Silver occurs as sulfides and sulfosalts (argentite, stephanite, polybasite), alloyed with gold in electrum, and in the native state.

Vein mineralization took place in 3 stages. The first stage is characterized by a brecciated calcite-quartz vein containing angular fragments of andesite and exhibits a "cockade" structure. The second stage is a granular mixture of quartz and calcite in places displaying banding and brecciation. The third stage is characterized by a coarsely crystalline calcite vein showing less deformation than the previous stages. Economic Au and Ag mineralization is associated mainly with the silicious portions of the vein while the coarsely crystalline calcite is relatively barren (low grade). (Jose Oliviera, 1981)

PREVIOUS GEOCHEMICAL WORK

During an underground study done in 1976 by Westcoast, vein samples from levels 500 to 1000 were analyzed for Au, Ag, Cu, Pb, and Zn. It showed that Ag values increased with depth, whereas Au decreased with depth. Cu, Pb, and Zn also increased with depth. This trend could be a result of supergene leaching of the upper levels, however, the absence of an enriched zone and the little visual evidence of leaching and secondary Cu minerals (malachite, azurite) occurring as oxidation rims around chalcopyrite favors the possibility that the increase in base metals with depth is a result of primary, hypogene ore deposition. (Jose Oliviera, 1981)

A soil geochemical survey done by APCO Oil Corp. (1974) was restricted to the central and western portion of the vein. It includes 7 geochemical lines spaced every 100 feet and samples at 25 foot intervals. Available Cu, Ag, Pb, Zn data for this zone showed a weak Cu and Ag anomaly over the vein. The anomaly was not continuous and may have shown some transport from the projected vein trace. (Jose Oliviera, 1981)

SOIL GEOCHEMICAL STUDY

Soil samples from the alteration zone which hosts the Gooseberry Au-Ag epithermal veins were taken and analyzed to determine the geochemical signature of this type of deposit. The alteration zone in the Red Top area was also sampled to compare elemental content with that of the Gooseberry area. The samples were analyzed for Au, Ag, As, Sb, Hg, Cu, Pb, Zn, Mn, and K. These elements were chosen based on known elemental associations with epithermal precious metal deposits in volcanics and on the mineral content of the epithermal veins in the Gooseberry structure. (Rose et al, 1979)

Mn was analyzed due to its adsorption effects on metals in the secondary environment. Comparisons of Mn abundance with the base metals may indicate the effect Mn oxides had on scavenging base metals. (Levinson, 1974)

K was used as an indicator element based on the possibility that the same hydrothermal event that redistributed the K also deposited the ore.

Soil Sampling

Soil sampling of the alteration zones around the Gooseberry mine and at the Red Top claims was done on a 100-foot grid. Although sampling was primarily confined to the alteration zones, one traverse line of sampling was extended 600 feet north and 500 feet south of the alteration zone to establish the background geochemical signature of the surrounding host geology. One soil sample was taken every 100 feet wherever possible. Rock outcrops prevented soil sampling in some areas and the mine and mill area was avoided.

A small pit was dug about 6 to 12 inches deep to avoid sampling the A-horizon and concentrate on the B-horizon of the soil profile. The B-horizon is the one normally sampled during geochemical exploration soil surveys because of its ability to accumulate elements due to the clay minerals and Fe and Mn oxides found there which have the capacity to absorb metals to varying degrees. (Levinson, 1974)

Sample Analysis

The samples were split with a riffle splitter to obtain a sample size of approximately 300g and this split was ground in a disc pulverizer. This 300g split was used for all analytical work.

Sample analysis for As and Sb was done in the laboratory set up at the Gooseberry mine by Westcoast. Analysis for Au, Ag, Hg, Cu, Pb, Zn, and K was done in the Precambrian Exploration laboratory in Wheatridge, Colorado. Due to expense of analysis and time involved, analysis became confined to samples at 200 foot spacings. When a higher than usual value was encountered the samples surrounding the higher valued ones were also analyzed so as not to miss any anomalous sample sites.

Reference standards with known concentrations were inserted at random in each batch of samples analyzed as a quality control on the analytical procedures. The analytical procedures used for each element are listed in Appendix B.

Results of the analyses are listed in Tables A-1 and A-2 for the Gooseberry and Red Top areas, respectively, in Appendix A. Sb was analyzed on samples from both areas but was not detected at the 5 ppm detection level, therefore Sb is not included in these tables and was not dealt with further in this study.

STATISTICAL TREATMENT OF DATA

UNIVARIATE ANALYSIS

To reduce the quantity of data to an easily interpretable form, a variety of statistical techniques were employed.

Background and threshold values are established through the computation of the mean, variances, and standard deviation of each element.

The mean, variance, standard deviation, and coefficient of variation for normal, uncensored distributions were determined from equations in Levinson (1974):

sample mean $= \bar{x} = \frac{\Sigma x}{n}$; sample variance $= s^2 = \frac{\Sigma(x-\bar{x})^2}{(n-1)}$;

standard deviation $= s = +\sqrt{s^2}$; coefficient of variation $= C = \frac{s}{\bar{x}}$; where n = no. of samples, and x = sample value. The threshold was determined from the equation $\bar{x}+2s = t =$ threshold (Levinson, 1974). The coefficient of variation, C, is a measure of relative variability which takes into account both mean and standard deviation. C is used as a guide to the form of the statistical distribution that should be applied for data analysis, based on the following general definitions:

$C < 0.5$ indicates a normal distribution.

$0.5 < C < 1.2$ indicates a log-normal distribution.

$C < 0.2$ indicates element generally present in major amounts.

$C > 2$ or 2.5 indicated a trace element.

(Koch and Link, 1971b)

Histograms and cumulative frequency plots were also used to determine whether the distribution was normal or log-normal. A cumulative frequency plot on arithmetic probability paper giving an approximately straight line indicates a normal distribution. A straight line cumulative frequency plot on log-probability paper indicates a log-normal distribution (Tennant & White, 1959). When it was determined the distribution was log-normal, two methods were employed to determine the mean, standard deviation and threshold values.

Lepeltier (1969) gives a graphical method for estimating the background (mean) and threshold values from the cumulative frequency plot on log-probability graph paper. The background (or geometric mean) b is given by the intersection of the line with the 50% ordinate. The standard deviation = s = log s' where s'(geometric deviation) = $\frac{\text{value read @ 16\%}}{\text{value read @ 50\%}}$. The coefficient of variation s" = $100\frac{s}{b}$. The threshold value can be read off the graph at the 2.5% ordinate or calculated from the equation $t = b \times s'^2$.

Miesch (1967) and Sichel (1952) gives a method for log-normal, uncensored distributions using an unbiased maximum-likelihood technique. The data is first transformed; x=log y. The biased sample mean $\bar{x}' = \frac{(\log y)}{n}$; biased standard deviation = $s' = \left[\frac{\Sigma x^2 - n\bar{x}'^2}{n}\right]^{\frac{1}{2}}$. Unbiased estimator for sample mean (T) is calculated from $\log_{10} T = \bar{x}' + \phi(V)$. $\phi(V)$ is determined from variance $V = 5.3019\left[m_2' - (\bar{x}')^2\right]$ where $m'_2 = \frac{\Sigma(\log y)^2}{n}$ and Sichel's Tables in Sichel (1952, p.288) (see Appendix C). Unbiased sample mean $T = \text{antilog}_{10}(\bar{x}' + \phi(V))$. Unbiased standard deviation $s = \frac{x^2 - n(T)^2}{n-1}^{\frac{1}{2}}$.

Before statistical work was done on the geochemical data, outlier values were omitted from the data in order to adequately describe the characteristics of the geochemical background population (Govett, 1983). Scatter plots made for each element pair focused attention on the relationship between the samples and helped identify outlier values. The scatter plots are given in Figures A-1 through A-16 for the Gooseberry data and Figures A-17 through A-29 for the Red Top. It was not feasible to label each sample number therefore only the samples deviating from the background cluster were labeled with the sample site number.

Figures A-30 through A-38 show the histograms and frequency distributions for elements in the Gooseberry area; Figures A-39 through A-45 for the Red Top area. Tables 1 and 2 lists the results of the univariate analysis of the Gooseberry and Red Top data respectively.

Descriptions of univariate analysis performed on Gooseberry are:

Copper (Fig. A-30)- A log transformed histogram gave a plot closer to the normal form. The cumulative frequency plot on log-probability gave an approximately straight line denoting a single population log-normally distributed (Lepeltier, 1969). The mean and threshold values were determined from the plot at the 50% and 2.5% ordinates respectively.

Lead (Fig. A-31)- A log transformed histogram plot approximately symmetrical, and a cumulative frequency plot giving a straight line on log-probability paper indicated a single, population log-normally distributed. Sichel's equations were used to determine the mean, standard deviation, and threshold values.

Zinc (Fig. A-32)- The histogram using ppm values was approximately symmetrical and the cumulative frequency plot on arithmetic-probability paper gave an approximate straight line indicating a single population normally distributed. Levinson's equations were used to determine mean, etc. A coefficient of variation (C)=0.17 indicates a normal distribution and element present in major amounts.

Manganese (Fig. A-33)- The cumulative frequency plot on arithmetic-probability paper gives a single straight line and symmetrical histogram using ppm values indicating a single population normally distributed. Levinson's equations were used to determine statistical data. A coefficient of variation (C)=0.17 indicates a normal distribution and element present in major amounts.

Mercury (Fig. A-34)- An approximately symmetrical histogram using log values and a cumulative frequency plot on log-probability paper giving a single straight line indicates a single population log-normally distributed. Sichel's equations were used to determine statistical data. C=0.7 also indicates log-normal distribution.

Potassium (Fig. A-35)- An approximately symmetrical histogram using ppm values and a cumulative frequency plot on arithmetic-probability paper giving a straight line indicates a normal population. The line on the cumulative frequency plot is broken suggesting two different populations, one population higher than the background population. In soil this may indicate two types of mineralization; one representative of the normal background content and the other a mineralization related to ore (lepeltier, 1969; Tennant & White, 1959). A coefficient of variation of 0.2 indicates an element present in major amounts. Levinson's equations were used to determine mean, etc.

Censored values occur when the concentration of an element is below the analytical limit of detection. This proved to be a problem when attempting to do a statistical analysis on Au, Ag, and As in the Gooseberry geochemical population. Data transformations are ineffective on highly censored data (Connor & Shacklette, 1975).

Arsenic (Fig. A-36)- As had 87% of data below the detection limit (5ppm). Highly censored data and poor analytical discrimination prevents the use of data transformations (Miesch, 1967). Histograms of ppm and log-transformed data both show a strong skewness. After a log transformation on the cumulative frequency plot, the line is still curved. The mean and standard deviation was therefore calculated from the analytical values above the limit of detection (5ppm) (Govett, 1983) using the following equations:

$\bar{x}'=\frac{\Sigma x}{n-n'}$ mean and $s'=\left[\frac{\Sigma x}{n-n'}-(\bar{x}')^2\right]^{\frac{1}{2}}$ standard deviation, where n=total number of samples and n'=number of samples below limit of detection (Miesch, 1967).

Silver (Fig. A-37)- Ag had 81% of data below the detection limit (0.2ppm). The histogram of ppm and log-transformed values both show a strong positive skewness. After log transformation the cumulative frequency plot on log-probability paper still shows a curved line. The censoring of data is too severe for any kind of adjustment. Therefore the mean and standard deviation was determined from the values above the limit of detection (0.2ppm) using the above equations used for arsenic.

Gold (Fig. A-38)- Au had 94% of data below the detection limit (0.02ppm). The histograms of ppm and log-transformed values show a strong positive skewness. The cumulative plots on log-probability paper still shows a curved line. As with the Ag, the censoring of the data is too severe for any kind of adjustment. The equation used for arsenic was used to find the mean and standard deviation.

Descriptions of univariate analysis done on Red Top area are:

Copper (Fig. A-39)- A log transformed histogram gave a plot closer to the norm and the cumulative frequency plot on log-probability paper gave an approximately straight line denoting a single population log-normally distributed. The mean and threshold values were determined from the plot at the 50% and 2.5% ordinates, respectively.

Lead (Fig. A-40)- A histogram using ppm values gave a plot closer to the norm. The cumulative frequency plot on arithmetic probability paper gave an approximately straight, broken line possibly due to ore mineralization. The coefficient of variation of 0.3 also indicates a normal distribution. The mean, standard deviation, and threshold was determined from Levinson's equations.

Zinc (Fig. A-41)- A histogram using ppm values and a cumulative frequency plot on arithmetic-probability paper giving an approximate straight line indicates a single population normally distributed. Levinson's equations were used to determine the mean, standard deviation, and threshold values.

Manganese (Fig. A-42)- The histogram using log transformed values gave a more symmetrical plot and coefficient of variation of 0.7 indicates a log-normal distribution. The cumulative frequency plot on log-probability paper shows a straight line with two breaks indicating a dual distribution. This suggests the existence of two populations which is also indicated in the double-peaked histogram (Lepeltier, 1969). A main background population (A) is mixed with another population of a higher average value (B) possibly due to ore mineralization. The mean, standard deviation, and threshold was calculated from Sichel's equations for log-normal distributions.

Mercury (Fig. A-43)- The histogram using log-transformed values gave a plot closer to the norm and a coefficient of variation of 0.9 indicates a log-normal distribution. The cumulative frequency plot gave a straight, broken line on log-probability paper indicating a log-normal distribution and two populations indicating an excess of high values possibly due to ore minerlization. Sichel's equations were used to determine the mean, standard deviation, and threshold values.

Potassium (Fig. A-44)- The histogram using ppm values was closer to the norm and the coefficient of variation of 0.27 indicates a normal distribution. The cumulative frequency plot gives a straight line with a slight change in slope. The negative break is an expression of a slight excess of low values (Lepeltier, 1969). The mean, standard deviation and threshold values were calculated using Levinson's equations.

Arsenic (Fig. A-45)- The histogram using log-transformed values gave a plot closer to the norm than the histogram with ppm values but still showed a slight skewness. The coefficient of variation of 0.56 and a straight line on the cumulative frequency plot on log-probability paper indicates a log-normal distribution. However, the line is broken indicating an excess of high values suggesting a possible ore mineralization. Since only two values were below the limit of detection, Sichel's equations for log-normal, uncensored distributions were used to calculate the mean, standard deviation, and threshold.

Plate 2 shows the geochemical distribution of the Gooseberry alteration zone. Plate 3 shows the geochemical distribution of the Red Top alteration zone.

Table 1. Statistical Data for Gooseberry mine area

Element	Observed Range Min. Max.	Mean	Variance	Standard Deviation	Coefficient of Variation	Threshold	Statistical Distribution
Cu	12 - 33	21	14.37	3.8	0.4	30	log-normal
Pb	3 - 33	8	9.0	3.1	0.4	14	log-normal
Zn	37 - 212	73	60	7.75	0.17	88	normal
Mn	196 - 1040	520	7582	87	0.17	694	normal
Hg	.02 - 1.00	0.11	0.006	0.08	0.7	0.265	log-normal
K	.56 -5.35%	1.69%	0.13	0.36	0.21	2.41%	normal
Au	L .02- .31	0.06	0.0009	0.03	–	0.12	censored
Ag	L .2- 12.0	0.5	0.16	0.4	–	1.3	censored
As	L 5 - 35	7	2.9	1.7	–	10	censored

L = less than
All values in ppm unless otherwise noted

Table 2. Statistical Data for Red Top area

Element	Observed Range Min. Max.	Mean	Variance	Standard Deviation	Coefficient of Variation	Threshold	Statistical Distribution
Cu	14 - 85	25	55.8	7.47	0.5	40	log-normal
Pb	2 - 13	6	3.69	1.9	0.3	9	normal
Zn	19 - 252	72	580	24	0.3	120	normal
Mn	16 - 1920	324	48488	220	0.7	764	log-normal
Hg	.035- 1.99	0.375	0.126	0.355	0.9	1.1	log-normal
K	.36- 2.04%	1.28%	0.12	0.35	0.27	1.9%	normal
As	L 5 - 40	8	20.3	4.5	0.56	17	log-normal

L = less than
All values in ppm unless otherwise noted

MULTIVARIATE ANALYSIS

Inspection of the raw data and individual frequency distributions tell nothing about inter-element relationships.

Cluster analysis groups samples together on the basis of their similarity in terms of their compositions. Scatter plots were used to pick out samples with anomalous elemental contents. Samples clustered together form a mutual group which is unlike that of the other samples lying a distance away from them on the plot. (Govett, 1983)

Correlation analysis measures the relationships between variables through the correlation coefficient. The correlation coefficient ranges from -1 for a perfect inverse linear relationship to +1 for a perfect positive linear relationship, and values tending toward zero indicate no linear relationship. The correlation coefficient for each element pair was calculated using the equation:

$$r_{xy} = \frac{\dfrac{\Sigma(x-\bar{x})(y-\bar{y})}{n-1}}{\left[\dfrac{\Sigma(x-\bar{x})^2}{n-1} \cdot \dfrac{\Sigma(y-\bar{y})^2}{n-1}\right]^{\frac{1}{2}}}$$

where x & y are the raw values from sample populations x & y, $\bar{x}$ & $\bar{y}$ are the means, and n is the number of samples. (Koch and Link, 1971a).

The correlation matrix in Table 3 lists the correlation coefficients for each element pair for the Gooseberry area.

Table 4 lists the correlation coefficients for the Red Top area. Again just the uncensored part of the data was used in determining r for correlations involving Au, Ag, and As in the Gooseberry population.

The correlation coefficients are arranged into a hierarchy so objects with the highest mutual similarity are placed together. This forms a dendogram (tree diagram). The clustering technique used was the weighted pair-group method with arithmetic averages (Davis, 1973). Two dendograms were made for the Gooseberry area, one using all element associations and the other omitting Au, Ag, and As associations. This was done to check the effect the censored variables would have on the dendogram using uncensored data. Figure 5 compares the two dendograms for the Gooseberry area. It appears that the addition of Au, Ag, and As did not have an affect on the major cluster groups formed. Figure 6 lists the Red Top dendogram with the Gooseberry dendogram (including Au, Ag, and As) to be used for comparison later in this study.

F and T tests are used to test the equality between the variances and means as an indication of similarity (or dissimilarity) between two populations. These values are compared to critical values tabulated for different levels of significance and a wide range of degrees of freedom. F and T tests are used as one step in comparing the mineralization from both alteration zones.

Table 3. Correlation matrix for Gooseberry area

Au	1.00								
Ag	0.90	1.00							
Cu	-0.48	-0.36	1.00						
Pb	0.55	0.47	0.07	1.00					
Zn	0.22	0.01	0.18	0.31	1.00				
Mn	0.09	-0.10	0.18	0.10	0.21	1.00			
Hg	-0.13	0.13	0.03	0.29	-0.01	-0.17	1.00		
K	-0.02	-0.37	0.01	0.53	-0.09	0.30	0.11	1.00	
As	0.14	0.15	0.37	-.003	-0.26	-0.19	0.50	0.48	1.00
	Au	Ag	Cu	Pb	Zn	Mn	Hg	K	As

Table 4. Correlation matrix for Red Top area

Cu	1.00						
Pb	-0.16	1.00					
Zn	0.49	-0.12	1.00				
Mn	-0.12	-0.16	0.30	1.00			
As	0.34	0.22	0.20	-0.01	1.00		
Hg	0.51	-0.02	-0.11	-0.24	0.19	1.00	
K	.003	-0.37	-0.59	0.02	-0.29	-0.13	1.00
	Cu	Pb	Zn	Mn	As	Hg	K

Figure 5. Dendograms for Gooseberry area; a) including Au, Ag, and As; b) excluding Au, Ag, and As

a)

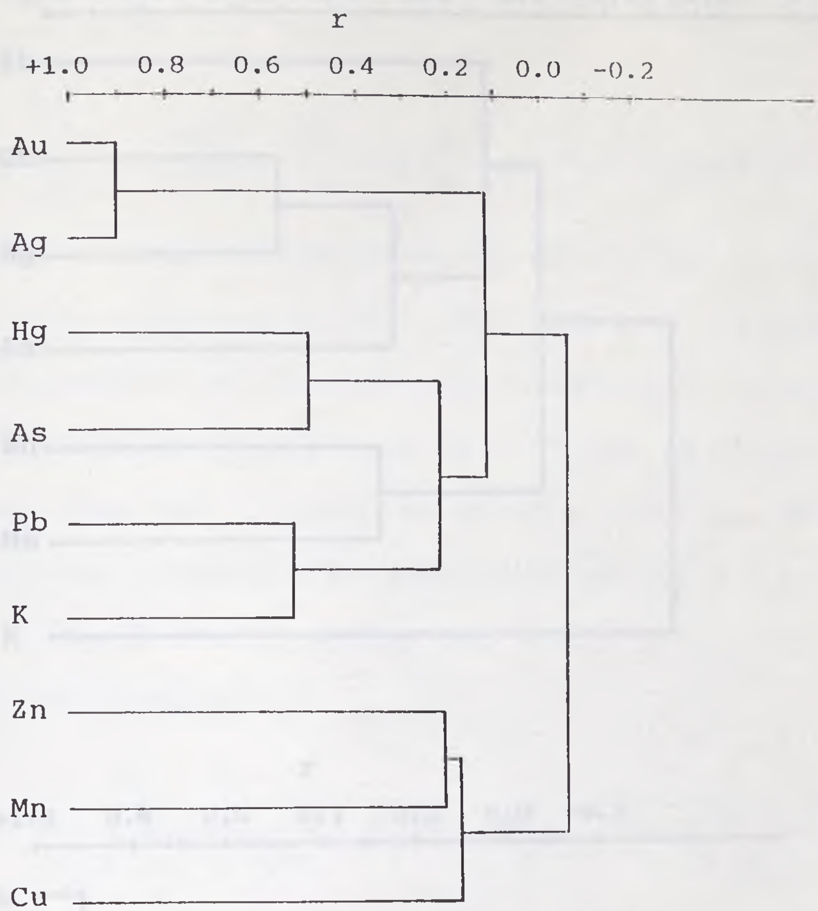

b)

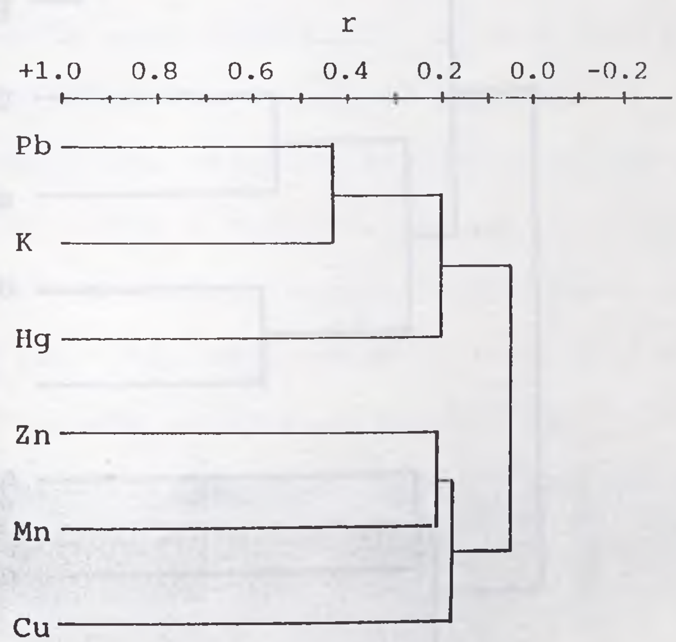

Figure 6. Dendograms for: a) Red Top area and b) Gooseberry area

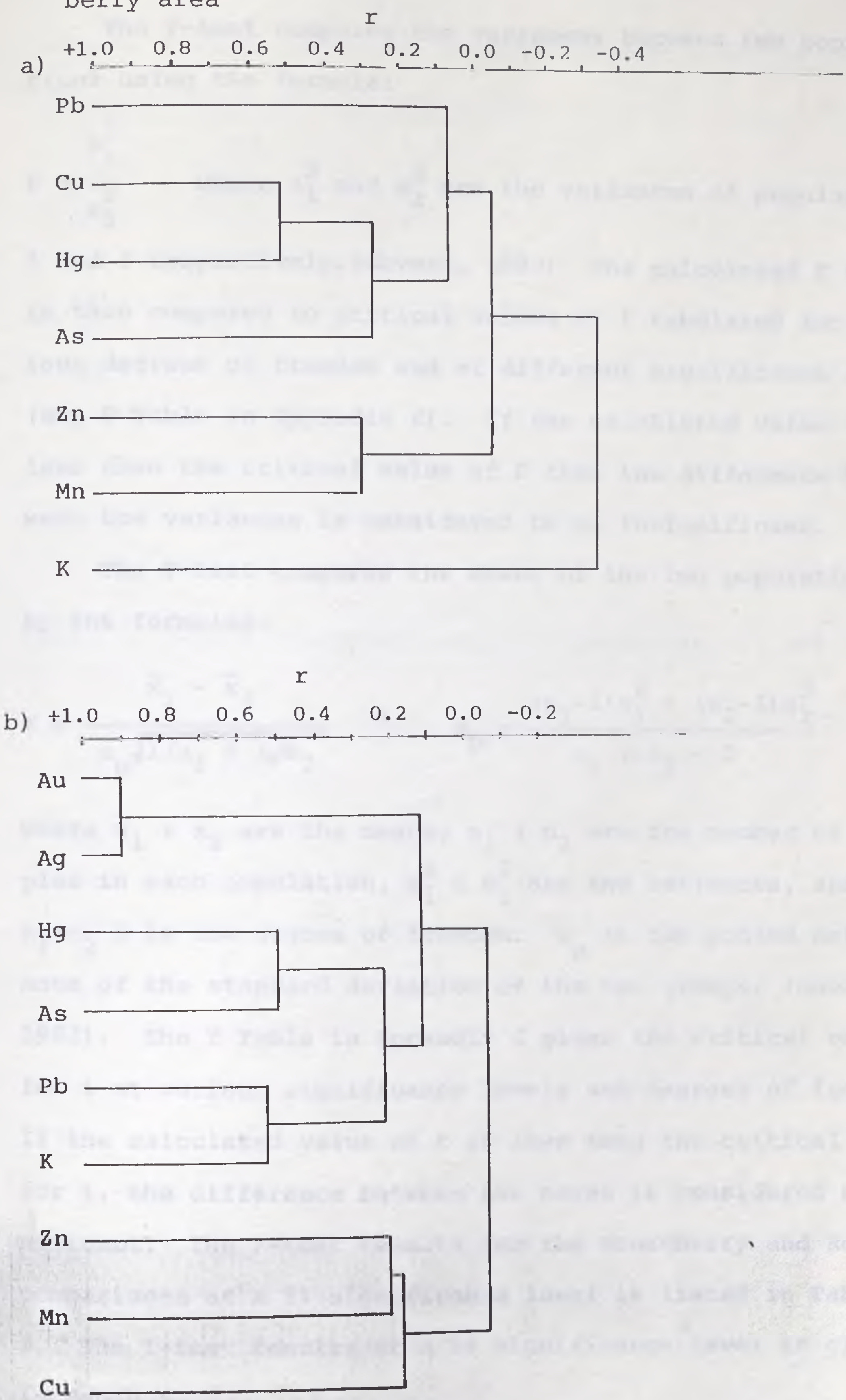

The F-test compares the variances between two populations using the formula:

$$F = \frac{s_1^2}{s_2^2}$$ where s_1^2 and s_2^2 are the variances of populations 1 and 2 respectively. (Govett, 1983) The calculated F value is than compared to critical values of F tabulated for various degrees of freedom and at different significance levels (see F Table in Appendix C). If the calculated value of F is less than the critical value of F then the difference between the variances is considered to be insignificant.

The T-test compares the means of the two populations by the formulas:

$$t = \frac{\bar{x}_1 - \bar{x}_2}{s_p\sqrt{1/n_1 + 1/n_2}} \quad ; \quad s_p = \frac{(n_1-1)s_1^2 + (n_2-1)s_2^2}{n_1 + n_2 - 2}$$

where $\bar{x}_1$ & $\bar{x}_2$ are the means, n_1 & n_2 are the number of samples in each population, s_1^2 & s_2^2 are the variances, and n_1+n_2-2 is the degree of freedom. s_p is the pooled estimate of the standard deviation of the two groups. (Govett, 1983). The T Table in Appendix C gives the critical values for t at various significance levels and degrees of freedom. If the calculated value of t is less than the critical value for t, the difference between the means is considered significant. The F-test results for the Gooseberry and Red top comparisons at a 5% significance level is listed in Table 5. The T-test results at a 5% significance level is given in Table 6.

Table 5. F-test comparison between Gooseberry and Red Top

Element	F(cal)	F(table @ 5%)
Cu	3.9	1.3
Pb	2.4	1.3
Zn	9.7	1.3
Mn	6.4	1.3
Hg	21	1.2
K	1.08	1.3
As	7.0	1.2

Table 6. T-test comparison between Gooseberry and Red Top

Element	T(cal)	T(table @ 5%)
Cu	1.17	1.6
Pb	2.3	1.6
Zn	0.35	1.6
Mn	0.076	1.6
Hg	43	1.6
K	25	1.6
As	1.1	1.6

INTERPRETATION OF DATA

Looking at the Gooseberry scatter plots (Figs. A-1 through A-16) samples #115, 122, 130, 145, 149, and 151 are anomalous in Hg and K. On the geochemical map (Plate 2) these sample sites occur near the projected vein structure along the northwestern and southeastern portions of the fence surrounding the mining area. Sample numbers 239, 250, 277, 285, and 295 are anomalous in Mn and are in the northwest portion of the alteration zone. These samples occur in an area with some enrichment in Zn (samples #239, 265, and 279) and Hg (#264, 265, 277, and 295). However, the occurrences in the northern portion of the alteration zone are isolated and probably less likely related to ore mineralization.

Looking at the Red Top scatter plots (Figs. A-17 through A-29) sample numbers 3, 14, 21, and 29 show anomalous values in Hg and Mn and to a lesser extent Zn, with other Hg anomalies at 28, 30, 32, 36, 39, and 41 all located together in the Red Top alteration zone. Some enrichment in Zn and Mn is indicated with samples 56, 59, and 68 located in the lower mid-section of the alteration zone.

From the Gooseberry dendogram (Figure 6b) three distinct clusters are apparent at approximately r=0.2: 1) Au and Ag; 2) Pb, K, Hg, and As; and 3) Zn, Mn, and Cu.

Group 1) Au and Ag, is intensely anomalous and least correlated with the rest of the elements. This is indicative of contamination (Obial and James, 1972). Looking at the geochemical map for the Gooseberry area (Plate 2) the anomalous values for Au and Ag are at sites next to the mine and mill area or down drainage from there, also indicative of contamination from the mine.

Group 2) Pb, K, Hg, and As, contains the highest correlations, without apparent relation to contamination. Pb-K and Hg-As groupings occur at approximately r=0.5 and could be due to ore mineralization. Looking at the geochemical map (Plate 2) K and Pb show a loose association in the mid-section of the Gooseberry alteration zone (near the Post location, site #1). Hg and As show a clustering with K along the western rim of the fence (surrounding the mining area) and in the eastern portion of the zone. K appears to be the most interesting showing a cluster of anomalous values in the eastern part of the zone. The cumulative frequency curve for K (Figure A-35) shows a positive break in the line, indicating an excess over the background concentrations (Lepeltier, 1969).

K is a useful indicator of mineralization because it is commonly enriched periphreal to ore body emplacement (Scherkenbach and Noble, 1984). With a low ionic potential, K can go into solution during weathering and become mobile (Levinson, 1974). Therefore, it is reasonable to conclude that K could be a good indicator of mineralization in the Gooseberry area.

Group 3) Zn, Mn and Cu, shows an association with Mn and Fe oxides common in the secondary environment. Mn and

Fe oxides are insoluble minerals commonly formed in the secondary environment and have the ability to adsorb base metals (Cu, Zn) which are otherwise mobile in the secondary environment (Levinson, 1974). Looking at the geochemical map (Plate 2), there aren't any remarkable clusters of anomalous groupings of Mn, Zn, and Cu. On the dendogram the Zn-Mn and Cu groupings occur at a low correlation level. It is probable that this grouping is due more to the secondary environment than to ore mineralization. Low order Cu anomalies occur in the central portion of the zone but are probably due to adsorption onto Mn and Fe oxides.

Looking at the Red Top dendogram (Figure 6a), four groups are evident at a correlation level of r=0.3: 1) Pb; 2) Cu, Hg, and As; 3) Zn and Mn; and 4) K. Looking at the geochemical map for the Red Top area (Plate 3) Pb does not show any apparent clustering of highly anomalous values or any associations with the other elements.

Group 2) Cu, Hg and As, is the most interesting of the groupings. There is an obvious cluster of anomalous Hg values in the southeastern region of the alteration zone. Overlapping the southwestern part of the Hg anomaly and continuing south is a cluster of anomalous As values. This is also seen in the cumulative frequency plots for Hg and As (Figures A-43 and A-45), indicating an excess of high values. A cluster of anomalous Cu values overlays the union of the Hg and As clusters and extends north-northwest. In intimate proximity to the intersection of the anomalous Hg, As and Cu clusters is a small anomalous cluster of Mn-Zn values.

Group 3), the Zn and Mn grouping with a fairly low correlation of r=0.3 may again be due to the secondary environment as in the Gooseberry area. However, referring to the cumulative frequency plot (Figure A-42) Mn did show a dual distribution. On the geochemical map (Plate 3) some associations of Mn and Zn is obvious but the occurrences are generally isolated and scattered. This association alone may not be representative of ore mineralization but it does show an above background mineralization.

Group 4), K shows no association with any other elements. There is a small clustering of anomalous K values in the northern section of the alteration zone.

Comparing the Gooseberry zone with Red Top zone, the F and T tests showed a significant difference between the two areas (Tables 5 & 6). With the exception of K, the variances showed a significant difference between the elements and when comparing the means, K also showed a difference. The geochemical background value for Hg and As was higher for the Red Top area than the Gooseberry, however, the background values for Pb, Mn, and K runs lower. Although the means for Zn and Cu were similar their variances differed.

The dendograms for the Gooseberry and Red Top areas showed some differences in groupings (Figure 6). The Zn and Mn grouping is present in both areas and is likely due to adsorption in the secondary environment. K and Pb showed no correlations to the other elements in the Red Top as they did in the Gooseberry. However, the grouping of Hg and As exists in both areas.

EXPLANATION AND PROPOSED MODEL

Differences in the elemental concentrations in the Gooseberry and Red Top areas may be due to several reasons:

1) Different composition of the country rock. This can affect the mobility of the elements (e.g. The mobility of many heavy metals in acidic water can be reduced when subjected to neutralization by reaction with carbonates). (Levinson, 1974)

2) Different amount of fluid activity which aids in the dispersion of elements from the ore zone to the primary and secondary environments; by complexing, distribution, etc.

3) Complexing and adsorption of elements within the secondary environment. Insoluble minerals, such as Mn and Fe oxides and clay minerals, formed through weathering and oxidation in the secondary environment have controlling factors in the fixation of metals in soils. (Levinson, 1974)

4) A precious metal deposit located deeper underground, further away from the surface of erosion, can give a different secondary dispersion halo. Figure 7 shows three variants of the erosion surface of an ore body ((1) blind, in which only the primary halo is exposed; (2) weakly eroded; and (3) ore body partially destroyed by erosion.)

Figure 7. Variations in the quantity of metal in secondary dispersion halos depending on the level of the erosion surface of the ore-bearing zones.
1 - bedrock; *2* - eluvial-diluvial formations; *3* - ore body; *4* - primary halos; *5* and *6* - secondary halos (*5* - with a low content of the metal; *6* - with a high content); M - metal reserves in the secondary halo.

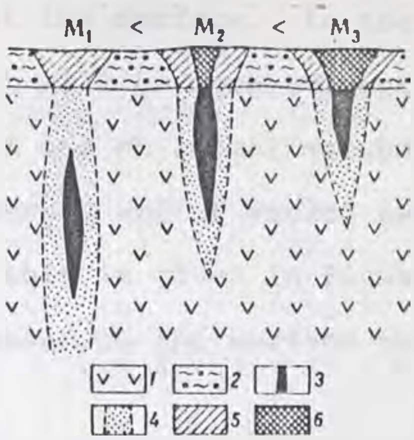

(Beus and Grigorian, 1977, p.186)

In the surficial environment: Hg, As and Zn are moderately mobile, and K and Mn are slightly mobile (Rose et al, 1979). However, it is commonly believed that a considerable amount of Hg released from an oxidizing deposit disperses in the vapor state, making it very mobile (Glover et al, 1979). Based on mobilities, Hg, As, and Zn would give wider haloes than K and Pb. According to Polikarpochkin and Kitaev (1971), the search for deep ore bodies in steeply dipping veins is best done by using zonation haloes for As, Sb, Hg and Cu. Generally, higher concentrations of Hg and As are good indications that one is high above the zone of optimal Au-Ag mineralization.

A possible model for the different elemental concentrations in both areas: A deeper precious metal ore deposit in the Red Top area would be indicated by a Hg-As-(Zn-Cu) halo expressed at the surface. In the Gooseberry area, a shallower deposit will be more evident by the surface expression of the K and Pb anomalies where the Hg and As halo may have been leached and/or eroded away. A schematic representation of this is given in Figure 8. This is an interpretation based on the surface geochemistry and geology.

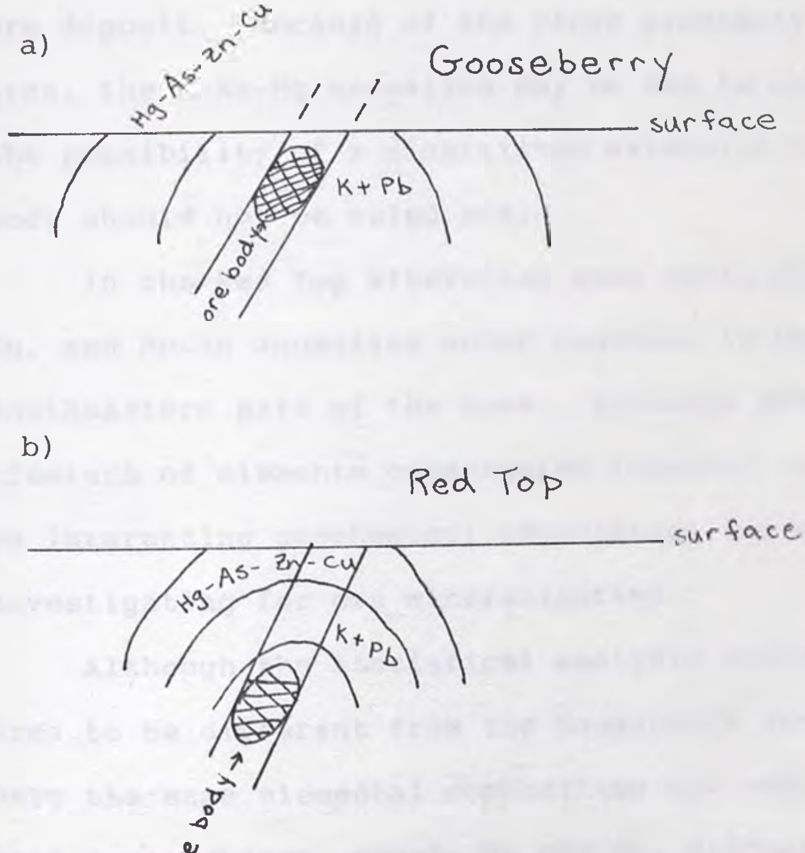

Figure 8. a) Hypothesis for Gooseberry ore deposit; b) Hypothesis for Red Top ore deposit.

CONCLUSIONS

A geochemical signature for the Gooseberry alteration zone was established and two areas of possible mineralization was found in the Gooseberry alteration zone and one area in the Red Top alteration zone. Plate 4 shows the locations of these areas.

In the Gooseberry alteration zone K-As-Hg anomalies were found northwest and southeast of the fence surrounding the mining area. Both of these anomalies are located over the projected extension of the vein structure hosting the ore deposit. Because of the close proximity to the mining area, the K-As-Hg anomalies may be due to contamination but the possibility of a mineralized extension from the main ore body should not be ruled out.

In the Red Top alteration zone small clusters of Hg, As, Cu, and Mn-Zn anomalies occur together in one area in the southeastern part of the zone. Although weak, these small clusters of elements congregated together in one area gives an interesting geochemical association and would be worth investigating for ore mineralization.

Although the statistical analysis showed the Red Top area to be different from the Gooseberry area, both areas have the same elemental composition and some similar element associations, namely Hg and As, differing only in the concentration of the elements. Given the strength of the Hg-As anomaly and the common association of these elements with Au-Ag precious metal deposits, there exists potential for this type of mineralization in the Red Top area.

RECOMMENDATIONS

Further studies should be made on the lithology and underground geology of the Red Top area. Studies of the primary dispersion halo would contribute to the soil study in the interpretation of the elemental associations characteristic of this type of deposit.

Also more detailed sampling is recommended in the anomalous areas to confirm the initial anomaly and further delineate the geometry and nature of the occurrence.

APPENDIX A

Table A-1. Analytical Results for Gooseberry Mine area.

No.	Sample Location	Au (ppm)	Ag (ppm)	Cu (ppm)	Pb (ppm)	Zn (ppm)	As (ppm)	Hg (ppm)	K(%)	Mn (ppm)
1	0-0 post	L(0.02)	L(0.2)	35	25	105	L(5)	-	-	-
2	0-1N	L(0.02)	L(0.2)	31	14	82	8	0.380	2.14	922
3	0-2N	-	-	-	-	-	L(5)	0.110	-	-
4	0-3N	L(0.02)	L(0.2)	20	12	80	L(5)	0.135	1.77	542
5	0-4N	L(0.02)	L(0.2)	-	-	-	L(5)	-	-	-
6	0-5N	-	-	21	8	83	L(5)	0.045	1.75	470
7	0-6N	L(0.02)	L(0.2)	-	-	-	L(5)	-	-	-
8	0-1S	L(0.02)	L(0.2)	19	14	75	L(5)	0.100	1.98	532
9	0-2S	-	L(0.2)	-	-	-	L(5)	-	-	-
10	0-3S	L(0.02)	L(0.2)	18	8	68	L(5)	0.100	2.00	636
11	0-4S	L(0.02)	L(0.2)	-	-	-	L(5)	-	-	-
12	1E-0	L(0.02)	L(0.2)	20	11	78	L(5)	0.090	-	462
13	1E-1N	-	-	23	11	70	5	0.130	2.09	596
14	1E-2N	L(0.02)	L(0.2)	29	10	77	L(5)	0.160	-	542
15	1E-3N	-	-	21	10	76	L(5)	-	1.61	640
16	1E-4N	L(0.02)	L(0.2)	24	10	76	L(5)	0.055	-	500
17	1E-5N	-	-	21	8	76	L(5)	0.255	-	476
18	1E-6N	L(0.02)	L(0.2)	-	-	-	L(5)	-	-	-
19	1E-1S	-	-	29	9	63	L(5)	-	1.88	632
20	1E-2S	L(0.02)	L(0.2)	30	11	72	L(5)	0.100	1.91	618
21	1E-3S	L(0.02)	L(0.2)	25	8	73	L(5)	-	-	578
22	2E-0	L(0.02)	L(0.2)	27	9	78	5	0.155	1.82	476
23	2E-1N	-	-	31	9	70	L(5)	-	2.15	628
24	2E-2N	L(0.02)	L(0.2)	-	-	-	L(5)	0.060	-	-
25	2E-3N	L(0.02)	L(0.2)	12	12	37	L(5)	0.300	2.11	196
26	2E-4N	-	-	-	-	-	-	0.050	-	-
27	2E-5N	L(0.02)	L(0.2)	20	9	73	L(5)	0.235	1.75	476
28	2E-6N	-	-	-	-	-	-	0.085	-	-
29	2E-7N	L(0.02)	L(0.2)	20	6	46	L(5)	-	1.70	546
30	2E-1S	L(0.02)	L(0.2)	16	7	60	L(5)	0.095	1.79	516
31	2E-2S	-	-	-	-	-	L(5)	0.040	-	-
32	2E-3S	-	-	23	6	63	-	-	-	512
33	3E-0	L(0.02)	L(0.2)	19	12	72	L(5)	0.120	1.78	560
34	3E-2N	L(0.02)	L(0.2)	24	9	71	L(5)	0.070	0.90	662
35	3E-4N	L(0.02)	L(0.2)	20	11	82	L(5)	0.050	2.05	524
36	3E-6N	L(0.02)	0.2	24	7	71	L(5)	-	-	524
37	3E-2S	L(0.02)	L(0.2)	17	10	68	L(5)	0.050	1.97	492
38	4E-0	L(0.02)	L(0.2)	20	8	65	L(5)	0.050	1.86	586
39	4E-1N	L(0.02)	L(0.2)	29	9	75	L(5)	0.020	2.18	602
40	4E-2N	-	-	-	-	-	10	-	-	-
41	4E-3N	L(0.02)	L(0.2)	26	9	68	L(5)	0.030	2.06	584
42	4E-5N	L(0.02)	L(0.2)	17	9	74	L(5)	0.050	2.06	528
43	4E-7N	L(0.02)	L(0.2)	18	6	65	L(5)	0.060	1.58	590
44	4E-8N	L(0.02)	L(0.2)	-	-	-	L(5)	-	-	-
45	4E-1S	L(0.02)	L(0.2)	18	12	75	L(5)	0.090	2.10	496
46	4E-3S	L(0.02)	L(0.2)	24	9	76	L(5)	0.085	1.99	542
47	5E-0	L(0.02)	L(0.2)	18	9	71	L(5)	0.175	1.81	510
48	5E-2N	L(0.02)	L(0.2)	29	11	68	6	0.045	2.07	548
49	5E-3N	-	-	-	-	-	L(5)	-	-	-
50	5E-4N	L(0.02)	L(0.2)	26	13	77	L(5)	0.080	1.89	620

Table A-1. Analytical Results for Gooseberry Mine area (continued)

No.	Sample Location	Au (ppm)	Ag (ppm)	Cu (ppm)	Pb (ppm)	Zn (ppm)	As (ppm)	Hg (ppm)	K(%)	Mn (ppm)
51	5E-6N	L(0.02)	L(0.2)	20	8	85	L(5)	0.055	1.85	592
52	5E-8N	L(0.02)	L(0.2)	15	5	60	L(5)	-	2.23	444
53	5E-1S	L(0.02)	L(0.2)	-	-	-	-	-	-	-
54	5E-2S	L(0.02)	L(0.2)	19	7	73	L(5)	-	-	-
55	5E-4S	L(0.02)	L(0.2	20	8	71	L(5)	0.070	1.72	544
56	6E-1N	L(0.02)	L(0.2)	27	10	76	L(5)	0.045	1.81	602
57	6E-2N	-	-	-	-	-	5	-	-	-
58	6E-3N	L(0.02)	L(0.2)	29	10	77	L(5)	0.050	1.86	650
59	6E-5N	L(0.02)	L(0.2)	26	6	82	L(5)	-	1.72	616
60	6E-7N	L(0.02)	L(0.2)	20	6	75	L(5)	-	-	480
61	6E-8N	-	L(0.2)	-	-	-	L(5)	-	-	-
62	6E-1S	L(0.02)	L(0.2)	19	8	70	L(5)	0.125	1.95	566
63	6E-3S	L(0.02)	L(0.2)	20	7	70	L(5)	0.040	1.90	518
64	7E-0	L(0.02)	L(0.2)	18	7	68	L(5)	0.045	1.84	518
65	7E-3/4N	L(0.02)	L(0.2)	-	-	-	L(5)	-	1.61	-
66	7E-3N	L(0.02)	L(0.2)	27	10	75	L(5)	0.120	1.01	550
67	7E-4N	L(0.02)	L(0.2)	-	-	-	L(5)	-	-	-
68	7E-6N	L(0.02)	L(0.2)	30	6	74	L(5)	-	-	536
69	7E-2S	L(0.02)	L(0.2)	21	8	72	L(5)	0.060	1.82	584
70	7E-4S	L(0.02)	0.2	18	7	72	L(5)	0.030	-	534
71	7E-5S	L(0.02)	L(0.2)	-	-	-	L(5)	-	-	-
72	8E-0	-	L(0.2)	-	-	-	-	-	-	-
73	8E-1N	L(0.02)	L(0.2)	18	14	62	L(5)	0.070	1.75	520
74	8E-3N	L(0.02)	L(0.2)	21	13	70	L(5)	0.060	1.96	570
75	8E-5N	L(0.02)	L(0.2)	25	8	71	L(5)	0.075	1.81	570
76	8E-6N	L(0.02)	L(0.2)	-	-	-	L(5)	-	-	-
77	8E-8N	L(0.02)	L(0.2)	19	5	69	L(5)	0.105	-	390
78	8E-10N	L(0.02)	L(0.2)	18	4	60	L(5)	0.105	1.70	426
79	8E-12N	L(0.02)	L(0.2)	19	3	58	L(5)	-	-	500
80	8E-14N	L(0.02)	L(0.2)	18	3	58	L(5)	-	-	512
81	8E-15N	L(0.02)	L(0.2)	-	-	-	L(5)	-	-	-
82	8E-1S	L(0.02)	L(0.2)	20	5	60	L(5)	0.170	2.19	354
83	8E-1Sa pit	0.02	L(0.2)	18	6	77	35	-	-	364
84	8E-3S	L(0.02)	L(0.2)	19	9	79	L(5)	0.050	1.81	480
85	8E-4S	L(0.02)	0.4	-	-	-	-	-	-	-
86	8E-5S	L(0.02)	L(0.2)	22	8	75	L(5)	0.070	1.51	560
87	8E-8S	L(0.02)	L(0.2)	21	6	78	L(5)	0.055	-	438
88	8E-9S	L(0.02)	L(0.2)	-	-	-	L(5)	-	-	-
89	9E-0	L(0.02)	0.4	19	8	68	L(5)	0.105	2.11	530
90	9E-1N	-	L(0.2)	-	-	-	-	-	-	-
91	9E-2N	L(0.02)	L(0.2)	30	10	66	L(5)	0.100	1.62	484
92	9E-4N	L(0.02)	L(0.2)	22	16	79	L(5)	0.055	1.70	482
93	9E-6N	L(0.02)	L(0.2)	22	7	72	L(5)	0.090	-	542
94	9E-8N	L(0.02)	L(0.2)	22	6	64	L(5)	-	-	454
95	9E-1S	L(0.02)	-	-	-	-	-	-	2.22	-
96	9E-2S	L(0.02)	L(0.2)	26	6	66	L(5)	0.080	1.50	416
97	9E-3S	-	-	19	8	88	-	-	-	420
98	9E-4S	L(0.02)	L(0.2)	21	8	78	L(5)	0.080	1.35	468
99	10E-0	-	L(0.2)	-	-	-	-	-	1.81	-
100	10E-1N	L(0.02)	L(0.2)	24	7	56	L(5)	0.085	-	428

Table A-1 Analytical Results for Gooseberry Mine area (continued)

No.	Sample Location	Au (ppm)	Ag (ppm)	Cu (ppm)	Pb (ppm)	Zn (ppm)	As (ppm)	Hg (ppm)	K(%)	Mn (ppm)
101	10E-2N	-	-	-	-	-	L(5)	-	1.65	-
102	10E-3N	L(0.02)	L(0.2)	21	10	73	5	0.105	-	396
103	10E-4N	-	-	-	-	-	L(5)	-	-	-
104	10E-5N	L(0.02)	L(0.2)	18	13	75	L(5)	0.085	1.82	482
105	10E-7N	L(0.02)	L(0.2)	24	8	72	L(5)	-	1.84	642
106	10E-1S	L(0.02)	0.2	29	8	68	L(5)	0.085	2.67	594
107	10E-2S	L(0.02)	L(0.2)	-	-	-	-	-	1.51	-
108	10E-3S	L(0.02)	L(0.2)	18	6	69	L(5)	0.090	1.37	412
109	11E-0	L(0.02)	0.2	20	8	63	L(5)	-	2.02	568
110	11E-1N	L(0.02)	L(0.2)	26	7	73	L(5)	0.070	1.83	598
111	11E-5N	L(0.02)	L(0.2)	-	-	-	L(5)	-	-	-
112	11E-6N	L(0.02)	L(0.2)	17	10	68	L(5)	0.090	-	410
113	11E-8N	L(0.02)	L(0.2)	-	-	-	L(5)	-	-	-
114	11E-1S	L(0.02)	0.3	-	-	-	5	0.085	2.12	-
115	11E-2S	0.20	2.4	23	8	73	10	0.450	2.39	568
116	11E-3S	L(0.02)	0.3	-	-	-	L(5)	0.085	1.61	-
117	12E-0	-	-	-	-	-	L(5)	-	1.46	-
118	12E-1N	L(0.02)	L(0.2)	17	10	74	5	0.100	-	586
119	12E-6N	L(0.02)	L(0.2)	-	-	-	L(5)	-	-	-
120	12E-7N	-	L(0.2)	16	7	71	L(5)	0.145	-	760
121	12E-8N	L(0.02)	L(0.2)	-	-	-	L(5)	-	-	-
122	12E-1S	L(0.02)	L(0.2)	21	7	69	10	0.360	2.10	552
123	13E-0	L(0.02)	L(0.2)	25	9	79	L(5)	0.175	1.58	468
124	13E-1N	L(0.02)	0.2	22	7	79	L(5)	0.210	1.72	592
125	13E-7N	L(0.02)	L(0.2)	24	7	69	L(5)	-	-	586
126	13E-8N		L(0.2)	-	-	-	L(5)	-	-	-
127	13E-1S	L(0.02)	0.2	22	9	78	5	0.070	2.10	524
128	14E-0	L(0.02)	0.3	-	-	-	L(5)	-	-	-
129	14E-1N	L(0.02)	L(0.2)	25	20	84	L(5)	0.130	1.67	504
130	14E-1S	0.03	0.8	29	33	212	20	0.350	1.64	596
131	15E-1N	L(0.02)	0.5	19	10	76	L(5)	-	1.79	500
132	16E-1N	L(0.02)	0.3	19	10	76	L(5)	0.120	1.29	472
133	17E-0	0.10	1.6	17	20	88	L(5)	0.175	1.72	520
134	17E-1N	0.03	0.6	-	-	-	L(5)	-	1.32	-
135	18E-0	0.11	3.0	19	11	78	L(5)	0.120	1.55	516
136	18E-½N	0.07	1.4	-	-	-	-	-	-	-
137	18E-1N	0.08	1.1	16	8	72	-	0.050	1.41	434
138	19E-0	0.05	0.5	18	9	80	L(5)	0.100	2.21	578
139	20E-0	0.08	1.4	20	8	73	L(5)	0.120	1.77	538
140	21E-0	0.10	1.1	17	7	76	-	-	-	558
141	21E-1S	L(0.02)	0.4	18	8	80	L(5)	0.050	1.48	622
142	22E-0	0.02	0.7	-	-	-	-	-	-	-
143	22E-1S	L(0.02)	L(0.2)	18	8	77	L(5)	0.110	1.74	564
144	22E-2S	L(0.02)	0.4	-	-	-	L(5)	-	1.85	-
145	22E-3S	0.03	0.6	21	6	75	L(5)	0.175	2.90	570
146	23E-0	L(0.02)	L(0.2)	19	9	82	L(5)	0.140	-	628
147	23E-2S	L(0.02)	0.5	18	9	80	L(5)	0.165	1.88	592
148	23E-3S	-	0.3	-	-	-	L(5)	-	2.30	-
149	23E-4S	L(0.02)	L(0.2)	23	7	76	L(5)	0.290	2.58	658
150	23E-5S	L(0.02)	-	-	-	-	25	-	2.54	-

Table A-1 Analytical Results for Gooseberry Mine area (continued)

No.	Sample Location	Au (ppm)	Ag (ppm)	Cu (ppm)	Pb (ppm)	Zn (ppm)	As (ppm)	Hg (ppm)	K(%)	Mn (ppm)
151	23E-6S	L(0.02)	0.2	21	8	72	10	0.300	5.35	310
152	24E-0	–	0.3	–	–	–	–	–	–	–
153	24E-1S	L(0.02)	L(0.2)	23	9	72	L(5)	0.085	1.78	418
154	24E-2S	–	0.3	–	–	–	–	–	–	–
155	24E-3S	L(0.02)	0.2	22	8	74	L(5)	0.110	2.23	542
156	24E-4S	L(0.02)	–	–	–	–	–	–	–	–
157	24E-5S	L(0.02)	0.2	20	6	84	L(5)	0.125	2.33	536
158	24E-5½S	–	–	–	–	–	5	–	–	–
159	25E-0	L(0.02)	0.2	17	9	69	L(5)	0.080	1.81	674
160	25E-1N	–	0.2	–	–	–	–	–	–	–
161	25E-2S	L(0.02)	0.3	18	8	81	L(5)	0.110	2.51	564
162	25E-3S	–	L(0.2)	–	–	–	–	–	–	–
163	25E-4S	L(0.02)	L(0.2)	26	7	77	L(5)	0.205	1.91	590
164	26E-0	L(0.02)	L(0.2)	21	8	74	L(5)	0.060	1.55	494
165	26E-1N	L(0.02)	0.2	22	9	75	L(5)	0.135	–	434
166	26E-1S	–	–	20	9	80	–	–	–	564
167	26E-2S	L(0.02)	L(0.2)	18	8	81	L(5)	0.130	1.83	598
168	26E-3S	–	1.1	–	–	–	–	–	–	–
169	26E-4S	L(0.02)	L(0.2)	19	5	73	L(5)	–	1.61	506
170	27E-0	L(0.02)	–	–	–	–	–	–	–	–
171	27E-1N	L(0.02)	L(0.2)	24	7	74	L(5)	0.120	1.26	494
172	27E-1S	L(0.02)	0.3	21	9	78	L(5)	0.135	1.85	566
173	27E-2S	–	0.5	–	–	–	–	–	–	–
174	27E-3S	L(0.02)	L(0.2)	28	7	77	L(5)	0.150	1.50	516
175	28E-0	0.07	1.7	21	9	73	L(5)	0.200	1.54	506
176	28E-1N	L(0.02)	L(0.2)	–	–	–	L(5)	0.080	–	–
177	28E-2N	–	–	21	6	82	–	–	–	590
178	28E-1S	L(0.02)	L(0.2)	–	–	–	–	–	–	–
179	28E-2S	0.31	12.0	20	12	78	L(5)	0.135	1.87	664
180	28E-3S	L(0.02)	L(0.2)	–	–	–	–	–	–	–
181	29E-0	L(0.02)	L(0.2)	–	–	–	–	–	–	–
182	29E-1N	L(0.02)	L(0.2)	28	9	62	L(5)	0.070	1.59	622
183	29E-1S	L(0.02)	0.3	19	8	78	L(5)	0.030	2.03	586
184	29E-2S	L(0.02)	L(0.2)	–	–	–	–	–	–	–
185	30E-0	L(0.02)	L(0.2)	16	8	59	L(5)	0.075	1.87	596
186	30E-2N	–	L(0.2)	16	7	66	–	–	–	486
187	30E-1S	–	0.2	–	–	–	–	–	–	–
188	31E-0	L(0.02)	L(0.2)	19	9	77	L(5)	0.030	–	616
189	32E-0	L(0.02)	L(0.2)	19	7	75	–	–	–	602
190	1W-1N	L(0.02)	L(0.2)	20	12	78	L(5)	0.080	1.82	502
191	1W-3N	L(0.02)	L(0.2)	20	12	81	L(5)	0.080	1.63	614
192	1W-5N	L(0.02)	L(0.2)	23	6	70	L(5)	–	1.59	504
193	1W-1S	L(0.02)	L(0.2)	21	11	75	L(5)	0.085	1.26	450
194	1W-3S	L(0.02)	L(0.2)	23	8	85	L(5)	0.045	1.44	486
195	2W-0	L(0.02)	L(0.2)	20	9	79	L(5)	0.090	1.63	458
196	2W-2N	L(0.02)	L(0.2)	19	9	77	L(5)	0.080	1.47	392
197	2W-4N	L(0.02)	L(0.2)	23	6	74	L(5)	0.090	1.70	644
198	2W-2S	L(0.02)	L(0.2)	19	9	68	L(5)	0.135	1.31	436
199	2W-3S	L(0.02)	L(0.2)	–	–	–	L(5)	–	–	–
200	3W-0	L(0.02)	L(0.2)	16	8	55	L(5)	0.150	1.20	376

Table A-1 Analytical Results for Gooseberry Mine area (continued)

No.	Sample Location	Au (ppm)	Ag (ppm)	Cu (ppm)	Pb (ppm)	Zn (ppm)	As (ppm)	Hg (ppm)	K(%)	Mn (ppm)
201	3W-1N	L(0.02)	0.2	-	-	-	10	0.165	2.26	-
202	3W-2N	L(0.02)	L(0.2)	22	9	69	7	0.240	1.78	552
203	3W-5N	L(0.02)	L(0.2)	22	6	73	L(5)	0.075	-	486
204	3W-2S	L(0.02)	L(0.2)	22	7	74	L(5)	0.095	1.24	498
205	4W-0	L(0.02)	L(0.2)	30	9	76	L(5)	0.075	1.93	478
206	4W-1N	-	-	-	-	-	-	-	1.14	-
207	4W-2N	L(0.02)	L(0.2)	15	12	63	L(5)	0.125	2.19	426
208	4W-4N	L(0.02)	L(0.2)	25	6	72	L(5)	0.060	1.58	486
209	4W-1S	L(0.02)	L(0.2)	25	8	74	L(5)	0.095	1.65	552
210	5W-0	L(0.02)	L(0.2)	-	-	-	L(5)	-	1.46	-
211	5W-1N	L(0.02)	L(0.2)	25	9	85	L(5)	0.135	1.56	544
212	5W-3N	L(0.02)	L(0.2)	19	11	73	L(5)	0.080	1.48	386
213	5W-5N	L(0.02)	L(0.2)	19	7	77	L(5)	0.150	-	470
214	6W-0	L(0.02)	L(0.2)	23	7	76	L(5)	0.150	1.33	474
215	6W-2N	L(0.02)	L(0.2)	18	9	63	L(5)	0.110	0.95	202
216	6W-4N	L(0.02)	L(0.2)	23	6	74	L(5)	0.080	1.61	472
217	7W-1N	L(0.02)	L(0.2)	23	6	75	L(5)	0.095	1.51	486
218	7W-3N	L(0.02)	L(0.2)	17	8	84	L(5)	0.115	1.42	566
219	7W-5N	L(0.02)	L(0.2)	24	5	77	L(5)	0.065	1.60	444
220	7W-6N	-	L(0.2)	-	-	-	L(5)	-	-	-
221	8W-2N	L(0.02)	L(0.2)	26	8	78	L(5)	0.075	1.41	482
222	8W-4N	L(0.02)	L(0.2)	22	8	82	L(5)	0.150	1.10	282
223	8W-6N	L(0.02)	L(0.2)	24	5	67	L(5)	0.155	1.70	504
224	9W-3N	L(0.02)	L(0.2)	22	7	75	L(5)	0.060	1.29	446
225	9W-5N	L(0.02)	L(0.2)	19	6	69	L(5)	0.080	1.80	516
226	9W-6N	-	-	-	-	-	-	-	1.45	-
227	9W-7N	L(0.02)	L(0.2)	18	4	72	L(5)	-	-	486
228	10W-3N	L(0.02)	L(0.2)	-	-	-	L(5)	-	1.31	-
229	10W-4N	L(0.02)	L(0.2)	19	8	78	L(5)	0.070	1.02	492
230	10W-6N	L(0.02)	L(0.2)	21	5	58	L(5)	0.090	1.92	524
231	10W-7N	-	-	-	-	-	-	-	1.60	-
232	10W-8N	L(0.02)	L(0.2)	14	5	67	L(5)	0.120	1.94	614
233	11W-4N	L(0.02)	L(0.2)	-	-	-	L(5)	0.060	1.39	-
234	11W-5N	L(0.02)	L(0.2)	22	6	76	L(5)	-	1.67	450
235	11W-6N	-	-	-	-	-	-	0.065	-	-
236	11W-7N	L(0.02)	L(0.2)	17	5	72	L(5)	0.135	1.91	566
237	12W-4N	L(0.02)	L(0.2)	21	7	73	L(5)	-	1.64	540
238	12W-5N	-	-	-	-	-	-	0.075	-	-
239	12W-6N	L(0.02)	L(0.2)	16	12	97	L(5)	-	1.30	776
240	12W-7N	-	-	-	-	-	-	0.095	-	-
241	12W-8N	L(0.02)	L(0.2)	17	5	72	L(5)	0.120	1.44	424
242	12W-9N	-	L(0.2)	-	-	-	L(5)	-	-	-
243	13W-6N	L(0.02)	L(0.2)	20	8	72	L(5)	0.090	1.34	410
244	13W-7N	-	L(0.2)	-	-	-	L(5)	-	1.70	-
245	13W-8N	L(0.02)	L(0.2)	16	4	61	L(5)	0.060	1.99	488
246	13W-10N	-	L(0.2)	14	4	67	L(5)	0.080	1.96	542
247	14W-6N	L(0.02)	L(0.20	-	-	-	L(5)	-	1.69	-
248	14W-7N	L(0.02)	L(0.2)	17	10	69	10	0.045	1.41	452
249	14W-8N	-	-	-	-	-	5	-	-	-
250	14W-9N	L(0.02)	L(0.2)	18	8	76	8	0.135	1.57	696

Table A-1. Analytical Results for Gooseberry Mine area (continued)

No.	Sample Location	Au (ppm)	Ag (ppm)	Cu (ppm)	Pb (ppm)	Zn (ppm)	As (ppm)	Hg (ppm)	K(%)	Mn (ppm)
251	14W-11N	L(0.02)	L(0.2)	15	7	66	L(5)	0.060	1.76	604
252	15W-7N	L(0.02)	L(0.2)	23	8	79	L(5)	0.060	-	542
253	15W-9N	L(0.02)	L(0.2)	18	9	70	L(5)	0.205	1.33	480
254	15W-10N	-	-	-	-	-	-	0.080	-	-
255	15W-11N	L(0.02)	L(0.2)	20	8	72	L(5)	0.085	1.38	466
256	15W-12N	-	-	-	-	-	L(5)	-	-	-
257	16W-8N	L(0.02)	L(0.2)	19	7	77	L(5)	-	-	360
258	16W-10N	L(0.02)	L(0.2)	20	7	70	L(5)	0.240	1.32	478
259	16W-12N	L(0.02)	L(0.2)	20	10	82	L(5)	0.085	1.15	504
260	16W-13N	-	-	-	-	-	L(5)	-	-	-
261	16W-14N	-	-	25	10	87	L(5)	-	-	436
262	17W-8N	L(0.02)	L(0.2)	-	-	-	L(5)	-	-	-
263	17W-9N	L(0.02)	-	25	6	74	L(5)	0.035	-	538
264	17W-11N	L(0.02)	L(0.2)	19	7	73	L(5)	0.300	1.53	536
265	17W-13N	L(0.02)	L(0.2)	16	10	82	5	0.300	1.14	550
266	17W-14N	-	-	-	-	-	L(5)	0.040	-	-
267	17W-15N	-	L(0.2)	20	8	75	L(5)	-	0.76	418
268	17W-16N	L(0.02)	L(0.2)	-	-	-	5	0.100	-	-
269	18W-10N	L(0.02)	L(0.2)	24	7	82	L(5)	0.135	1.57	642
270	18W-11N	-	-	-	-	-	L(5)	-	-	-
271	18W-12N	L(0.02)	L(0.2)	21	6	88	5	0.170	1.35	468
272	18W-13N	-	-	-	-	-	10	-	-	-
273	18W-14N	L(0.02)	L(0.2)	23	10	84	L(5)	0.065	1.08	596
274	19W-10N	L(0.02)	L(0.2)	-	-	-	L(5)	-	-	-
275	19W-11N	L(0.02)	L(0.2)	18	5	47	L(5)	0.100	0.73	412
276	19W-12N	-	-	21	5	70	5	-	-	526
277	19W-13N	L(0.02)	L(0.2)	18	9	73	7	1.00	1.58	1040
278	19W-14N	-	-	-	-	-	-	0.255	-	-
279	19W-15N	L(0.02)	L(0.2)	24	8	93	L(5)	0.175	0.61	502
280	19W-16N	L(0.02)	L(0.2)	-	-	-	8	-	-	-
281	20W-12N	L(0.02)	L(0.2)	23	5	78	8	0.085	1.41	516
282	20W-13N	-	-	-	-	-	L(5)	-	-	-
283	20W-14N	L(0.02)	L(0.2)	33	6	75	L(5)	0.120	1.41	514
284	20W-16N	L(0.02)	-	25	9	73	L(5)	0.040	1.02	754
285	21W-12N	L(0.02)	L(0.2)	-	-	-	L(5)	-	-	-
286	21W-13N	L(0.02)	L(0.2)	20	3	69	5	0.075	1.68	558
287	21W-15N	L(0.02)	L(0.2)	22	6	66	L(5)	0.095	1.10	582
288	21W-17N	L(0.02)	-	18	7	76	L(5)	0.175	-	438
289	21W-18N	-	L(0.2)	-	-	-	L(5)	-	-	-
290	22W-14N	L(0.02)	L(0.2)	23	6	66	L(5)	0.130	1.60	578
291	22W-16N	L(0.02)	L(0.2)	23	6	60	L(5)	0.250	0.56	208
292	22W-17N	-	L(0.2)	-	-	-	L(5)	-	-	-
293	23W-14N	L(0.02)	L(0.2)	19	6	70	8	0.255	-	370
294	23W-15N	-	-	-	-	-	L(5)	-	-	-
295	23W-16N	L(0.02)	L(0.2)	24	5	78	7	0.220	-	914

L( ) = less than indicated detection limit

Detection limits are as follows: Au 0.02ppm; Ag 0.2ppm; Cu-Pb-Zn-Mn 1ppm; As 5ppm; Hg 0.005ppm; K 0.05%

Table A-2. Analytical Results for Red Top area.

No.	Sample Location	Au (ppm)	Ag (ppm)	Cu (ppm)	Pb (ppm)	Zn (ppm)	As (ppm)	Hg (ppm)	K(%)	Mn (ppm)
1	RT 0-0	L(0.02)	L(0.2)	27	5	61	15	0.345	1.29	420
2	RT 0-1N	–	–	–	–	–	10	–	–	–
3	RT 0-2N	L(0.02)	L(0.2)	22	7	108	8	0.525	0.45	1300
4	RT 0-4N	L(0.02)	L(0.2)	29	3	77	5	0.230	1.65	260
5	RT 0-1S	–	–	–	–	–	15	–	–	–
6	RT 0-2S	L(0.02)	L(0.2)	31	4	71	15	0.325	1.49	230
7	RT 1E-0	L(0.02)	L(0.2)	–	–	–	8	–	–	–
8	RT 1E-1N	L(0.02)	L(0.2)	25	3	47	8	0.190	1.18	210
9	RT 1E-3N	L(0.02)	L(0.2)	33	4	85	5	0.145	1.30	546
10	RT 1E-4N	L(0.02)	–	–	–	–	5	–	–	–
11	RT 2E-3N	L(0.02)	L(0.2)	31	3	98	5	0.110	1.29	602
12	RT 1W-0	–	–	–	–	–	8	–	–	–
13	RT 1W-1N	L(0.02)	L(0.2)	26	13	60	20	0.270	0.43	244
14	RT 1W-2N	–	–	33	5	93	15	1.55	–	350
15	RT 1W-3N	L(0.02)	L(0.2)	32	3	85	8	0.175	1.35	532
16	RT 1W-1S	L(0.02)	L(0.2)	30	6	59	15	0.265	1.06	80
17	RT 1W-2S	–	–	–	–	–	5	–	–	–
18	RT 2W-0	L(0.02)	L(0.2)	21	8	72	15	0.410	0.65	536
19	RT 2W-1N	–	–	–	–	–	8	–	–	–
20	RT 2W-2N	L(0.02)	L(0.2)	37	5	48	40	1.190	1.44	48
21	RT 2W-3N	–	–	38	2	148	10	0.795	–	1340
22	RT 2W-4N	L(0.02)	L(0.2)	39	2	124	8	0.400	1.24	1920
23	RT 2W-5N	L(0.02)	L(0.2)	38	3	90	10	–	1.34	318
24	RT 2W-1S	–	–	–	–	–	15	–	–	–
25	RT 2W-2S	L(0.02)	L(0.2)	85	6	83	10	0.155	1.48	330
26	RT 3W-0	–	–	–	–	–	8	–	–	–
27	RT 3W-1N	L(0.02)	L(0.2)	33	5	61	5	0.290	1.45	170
28	RT 3W-2N	–	–	–	–	–	5	1.99	–	–
29	RT 3W-3N	L(0.02)	L(0.2)	27	2	78	5	0.475	1.65	888
30	RT 3W-4N	–	–	41	4	76	–	0.855	–	46
31	RT 3W-5N	L(0.02)	L(0.2)	46	7	74	10	0.465	1.47	294
32	RT 3W-1S	L(0.02)	L(0.2)	20	7	52	18	0.865	0.76	70
33	RT 4W-0	L(0.02)	L(0.2)	25	6	21	8	0.445	1.29	48
34	RT 4W-2N	L(0.02)	L(0.2)	28	5	44	8	0.205	1.59	106
35	RT 4W-3N	–	–	–	–	–	–	0.855	–	–
36	RT 4W-4N	L(0.02)	L(0.2)	23	3	55	8	1.00	1.42	40
37	RT 4W-5N	–	–	–	–	–	–	0.100	–	–
38	RT 4W-2S	L(0.02)	L(0.2)	31	7	76	7	0.440	0.98	246
39	RT 5W-1N	L(0.02)	L(0.2)	19	5	42	5	1.48	1.48	52
40	RT 5W-2N	–	–	–	–	–	–	0.330	–	–
41	RT 5W-3N	L(0.02)	L(0.2)	29	3	83	10	1.37	0.93	158
42	RT 5W-4N	–	–	–	–	–	–	0.325	–	–
43	RT 5W-5N	L(0.02)	L(0.2)	34	6	87	10	0.410	0.80	340
44	RT 5W-9N	L(0.02)	L(0.2)	27	6	82	15	0.920	0.81	144
45	RT 5W-11N	L(0.02)	L(0.2)	23	7	68	10	0.285	0.58	640
46	RT 5W-1S	L(0.02)	L(0.2)	32	4	74	8	0.530	1.37	44
47	RT 6W-0	L(0.02)	L(0.2)	37	7	92	10	0.805	1.63	186
48	RT 6W-1N	–	–	–	–	–	–	0.360	–	–
49	RT 6W-2N	L(0.02)	L(0.2)	45	6	104	10	1.01	0.67	194
50	RT 6W-3N	–	–	–	–	–	–	0.595	–	–

Table A-2. Analytical Results for Red Top area (continued)

No.	Sample Location	Au (ppm)	Ag (ppm)	Cu (ppm)	Pb (ppm)	Zn (ppm)	As (ppm)	Hg (ppm)	K(%)	Mn (ppm)
51	RT 6W-4N	L(0.02)	L(0.2)	14	10	44	10	0.140	0.61	50
52	RT 6W-5N	–	–	41	7	110	–	–	–	38
53	RT 6W-6N	L(0.02)	L(0.2)	–	–	–	7	0.285	1.16	–
54	RT 6W-8N	L(0.02)	L(0.2)	22	4	62	7	0.170	1.74	352
55	RT 6W-10N	L(0.02)	L(0.2)	19	4	48	7	0.120	2.04	552
56	RT 6W-12N	L(0.02)	L(0.2)	24	3	94	7	0.120	1.41	666
57	RT 6W-2S	L(0.02)	L(0.2)	26	6	64	5	0.745	1.17	42
58	RT 7W-0	–	–	–	–	–	10	–	–	–
59	RT 7W-1N	L(0.02)	L(0.2)	36	5	132	7	0.130	1.59	644
60	RT 7W-2N	–	–	30	3	158	–	0.080	–	716
61	RT 7W-3N	L(0.02)	L(0.2)	21	4	51	7	0.980	1.73	62
62	RT 7W-4N	–	–	–	–	–	–	0.245	–	–
63	RT 7W-5N	L(0.02)	L(0.2)	22	6	69	5	0.245	1.15	300
64	RT 7W-7N	L(0.02)	L(0.2)	21	4	57	10	0.860	1.67	260
65	RT 7W-9N	–	–	19	4	61	–	–	–	500
66	RT 7W-11N	L(0.02)	L(0.2)	–	–	–	8	0.120	1.73	–
67	RT 7W-1S	L(0.02)	L(0.2)	19	7	83	5	0.225	0.87	472
68	RT 8W-0	L(0.02)	L(0.2)	27	4	252	25	0.140	1.10	972
69	RT 8W-1N	–	–	27	4	130	7	–	–	158
70	RT 8W-2N	L(0.02)	L(0.2)	25	7	91	7	0.420	0.95	78
71	RT 8W-3N	–	–	–	–	–	–	0.075	–	–
72	RT 8W-4N	L(0.02)	L(0.2)	26	6	97	7	0.360	0.87	184
73	RT 8W-6N	L(0.02)	L(0.2)	24	6	59	8	0.265	1.56	50
74	RT 8W-8N	L(0.02)	L(0.2)	22	3	47	5	0.775	1.64	258
75	RT 8W-10N	L(0.02)	L(0.2)	23	4	57	5	0.240	1.49	110
76	RT 8W-12N	L(0.02)	L(0.2)	23	6	76	L(5)	0.190	1.10	388
77	RT 8W-1S	–	–	–	–	–	7	–	–	–
78	RT 8W-2S	L(0.02)	L(0.2)	20	6	68	7	0.100	1.50	504
79	RT 9W-1N	L(0.02)	L(0.2)	22	4	19	5	0.280	1.61	16
80	RT 9W-3N	L(0.02)	L(0.2)	27	6	45	5	0.160	1.69	90
81	RT 9W-5N	L(0.02)	L(0.2)	21	6	53	5	0.130	1.66	336
82	RT 9W-7N	L(0.02)	L(0.2)	25	7	83	7	0.035	1.50	450
83	RT 9W-9N	L(0.02)	L(0.2)	27	7	99	5	0.160	1.50	1380
84	RT 9W-11N	L(0.02)	L(0.2)	23	5	72	7	0.095	1.60	362
85	RT 9W-1S	L(0.02)	L(0.2)	19	7	62	7	0.100	1.46	556
86	RT 10W-0	L(0.02)	L(0.2)	23	6	88	8	0.145	1.09	404
87	RT 10W-2N	L(0.02)	L(0.2)	22	8	62	5	0.195	1.37	28
88	RT 10W-4N	L(0.02)	L(0.2)	20	6	58	5	0.135	1.13	340
89	RT 10W-6N	L(0.02)	L(0.2)	22	5	72	8	0.170	1.08	346
90	RT 10W-8N	L(0.02)	L(0.2)	22	3	88	7	0.095	1.19	802
91	RT 10W-10N	L(0.02)	L(0.2)	20	5	45	5	0.170	0.92	126
92	RT 10W-12N	L(0.02)	L(0.2)	22	5	71	5	0.065	1.03	540
93	RT 10W-2S	L(0.02)	L(0.2)	24	6	98	7	0.140	0.67	306
94	RT 11W-1N	L(0.02)	L(0.2)	23	7	51	5	0.490	1.43	128
95	RT 11W-3N	L(0.02)	L(0.2)	25	8	56	7	0.205	1.51	360
96	RT 11W-5N	L(0.02)	L(0.2)	21	4	46	L(5)	0.210	1.64	154
97	RT 11W-7N	L(0.02)	L(0.2)	23	5	49	5	0.120	1.68	120
98	RT 11W-9N	L(0.02)	L(0.2)	25	6	95	7	0.170	1.14	284
99	RT 11W-11N	L(0.02)	L(0.2)	14	5	62	5	0.520	1.51	124
100	RT 11W-1S	L(0.02)	L(0.2)	19	6	55	7	0.155	1.55	768

Table A-2 Analytical Results For Red Top area (continued)

No.	Sample Location	Au (ppm)	Ag (ppm)	Cu (ppm)	Pb (ppm)	Zn (ppm)	As (ppm)	Hg (ppm)	K(%)	Mn (ppm)
101	RT 11W-1Sa	L(0.02)	L(0.2)	-	-	-	7	-	-	-
102	RT 12W-1N	-	-	19	7	47	-	-	-	250
103	RT 12W-2N	L(0.02)	L(0.2)	16	7	34	5	0.320	0.36	28
104	RT 12W-4N	L(0.02)	L(0.2)	21	6	70	5	0.125	1.65	460
105	RT 12W-6N	L(0.02)	L(0.2)	26	6	87	10	0.170	1.27	262
106	RT 12W-8N	L(0.02)	L(0.2)	24	6	57	5	0.520	1.15	254
107	RT 12W-10N	L(0.02)	L(0.2)	24	4	88	7	0.405	1.16	184
108	RT 12W-12N	L(0.02)	L(0.2)	26	6	86	7	0.135	-	404
109	RT 12W-2S	L(0.02)	L(0.2)	23	6	81	8	0.340	1.17	362
110	RT 13W-1N	L(0.02)	L(0.2)	23	7	61	8	0.300	1.28	124
111	RT 13W-3N	L(0.02)	L(0.2)	22	12	26	5	0.770	0.98	82
112	RT 13W-5N	L(0.02)	L(0.2)	25	9	67	7	0.470	1.24	280
113	RT 13W-7N	L(0.02)	L(0.2)	21	6	59	8	0.200	1.67	422
114	RT 13W-9N	L(0.02)	L(0.2)	25	6	80	10	0.185	1.33	420
115	RT 13W-12N	L(0.02)	L(0.2)	-	-	-	8	0.140	-	-
116	RT 13W-1S	L(0.02)	L(0.2)	22	5	70	7	0.225	1.54	762
117	RT 14W-0	L(0.02)	L(0.2)	19	9	56	7	0.380	1.27	410
118	RT 14W-2N	L(0.02)	L(0.2)	24	7	71	7	0.290	1.67	600
119	RT 14W-4N	L(0.02)	L(0.2)	21	7	59	10	0.275	1.69	368
120	RT 14W-6N	L(0.02)	L(0.2)	23	10	65	10	0.200	1.52	570
121	RT 14W-9N	L(0.02)	L(0.2)	25	6	86	7	0.190	-	320
122	RT 14W-10N	L(0.02)	L(0.2)	-	-	-	7	-	-	-
123	RT 14W-1S	L(0.02)	L(0.2)	-	-	-	7	-	1.14	-
124	RT 14W-2S	L(0.02)	L(0.2)	20	5	74	5	0.095	1.47	652
125	RT 15W-1N	L(0.02)	L(0.2)	18	6	58	5	0.110	1.59	462
126	RT 15W-6N	L(0.02)	L(0.2)	-	-	-	8	-	-	-
127	RT 15W-7N	L(0.02)	L(0.2)	20	6	52	8	0.270	-	364
128	RT 15W-1S	L(0.02)	-	18	6	82	7	0.385	1.41	798
129	RT 16W-0	L(0.02)	-	18	5	62	8	0.540	1.53	318
130	RT 16W-1N	L(0.02)	-	-	-	-	7	-	-	-
131	RT 16W-1S	L(0.02)	-	-	-	-	7	-	-	-

L( ) = less than indicated detection limit

Detection limits are as follows: Au 0.02ppm; Ag 0.2ppm; Cu-Pb-Zn-Mn 1ppm; As 5ppm; Hg 0.005ppm; K 0.05%

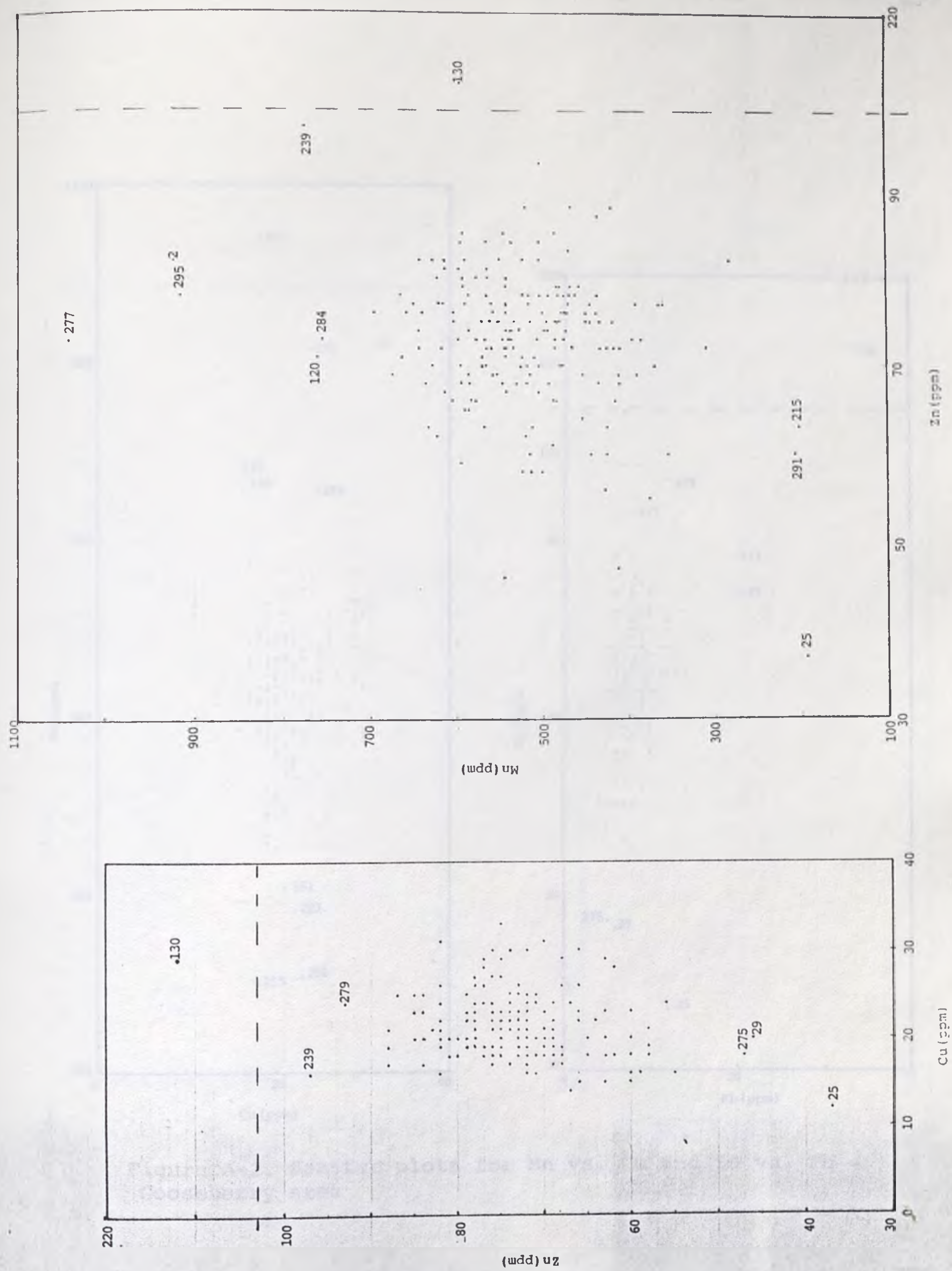

Figure A-1. Scatter plots for Mn vs. Zn and Zn vs. Cu -
Gooseberry area

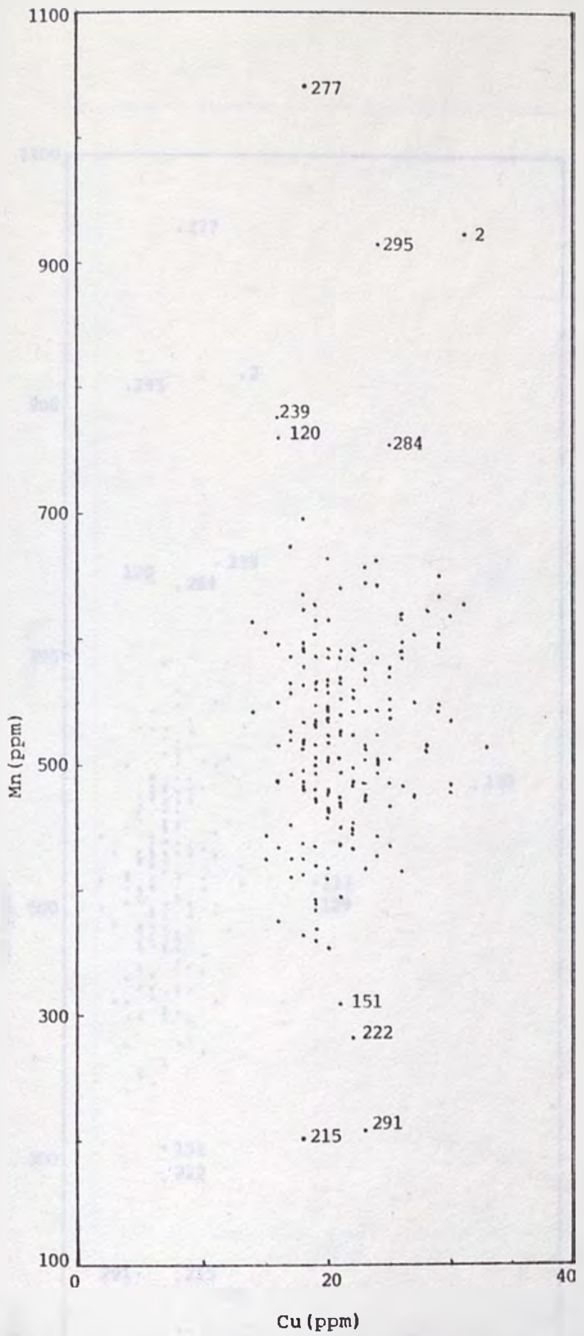

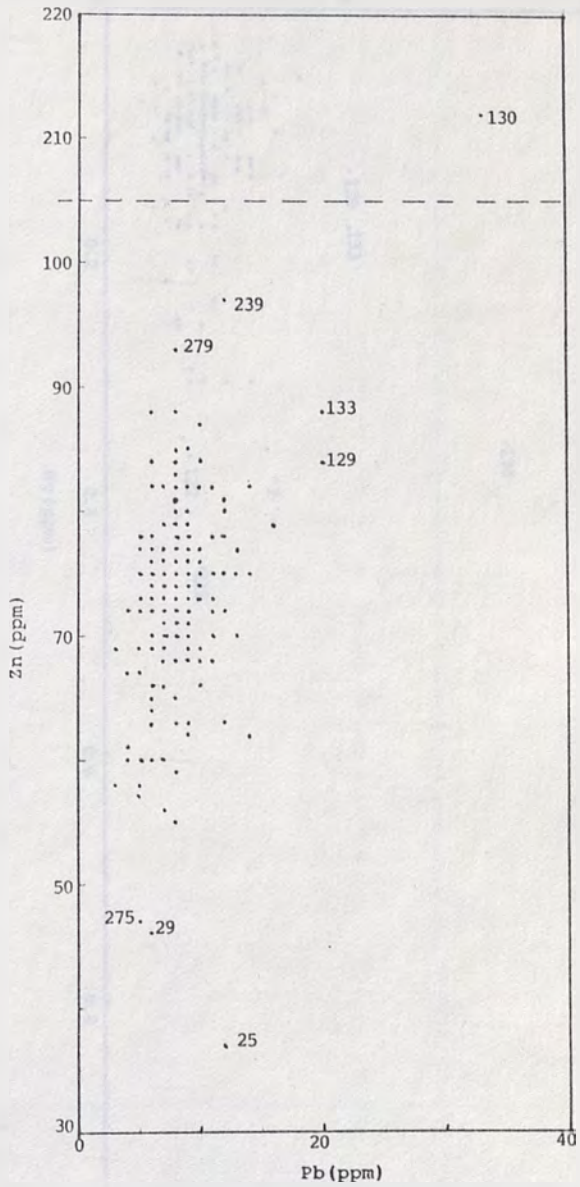

Figure A-2. Scatter plots for Mn vs. Cu and Zn vs. Pb - Gooseberry area

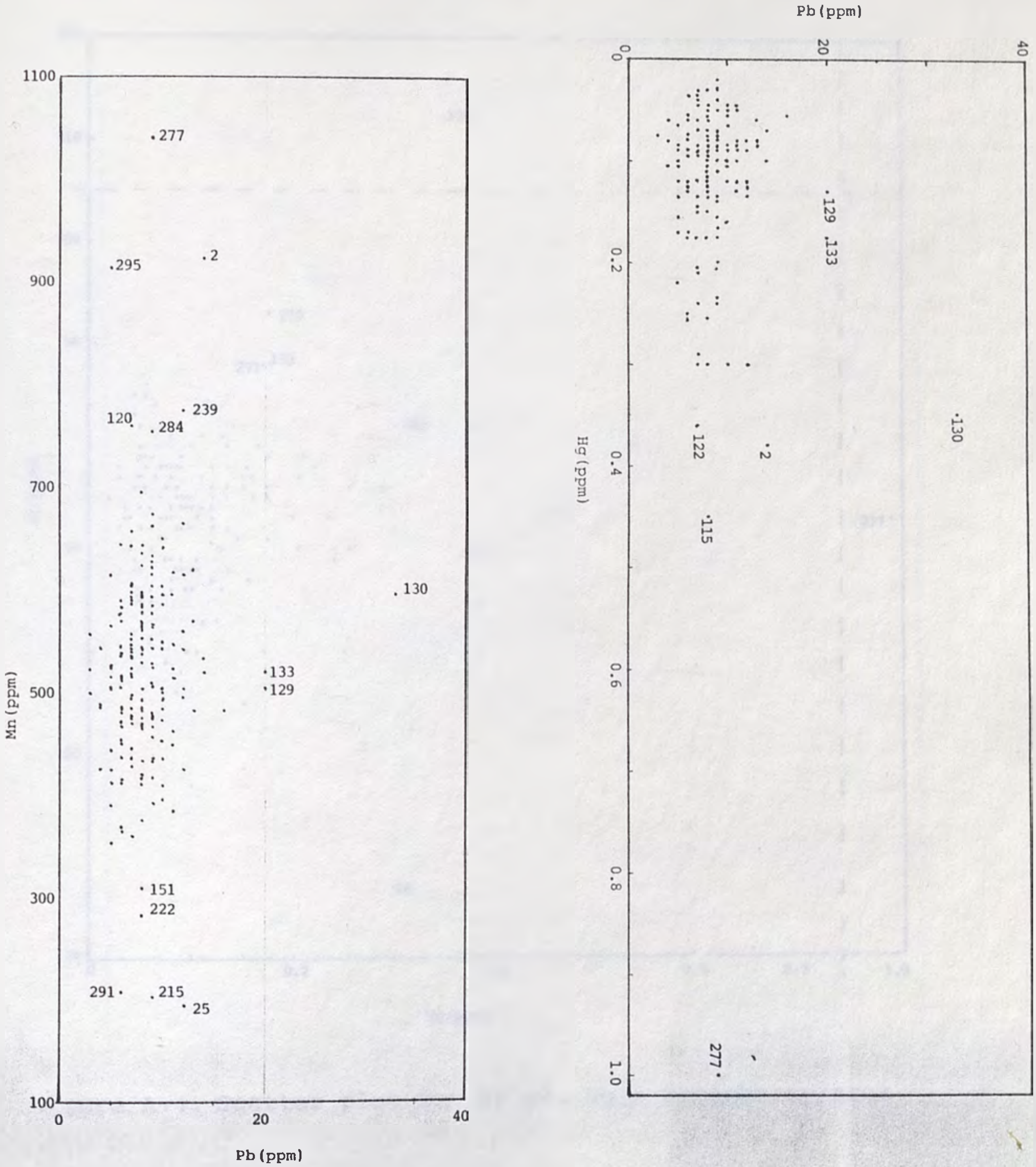

Figure A-3. Scatter plots for Mn vs. Pb and Pb vs. Hg - Gooseberry area

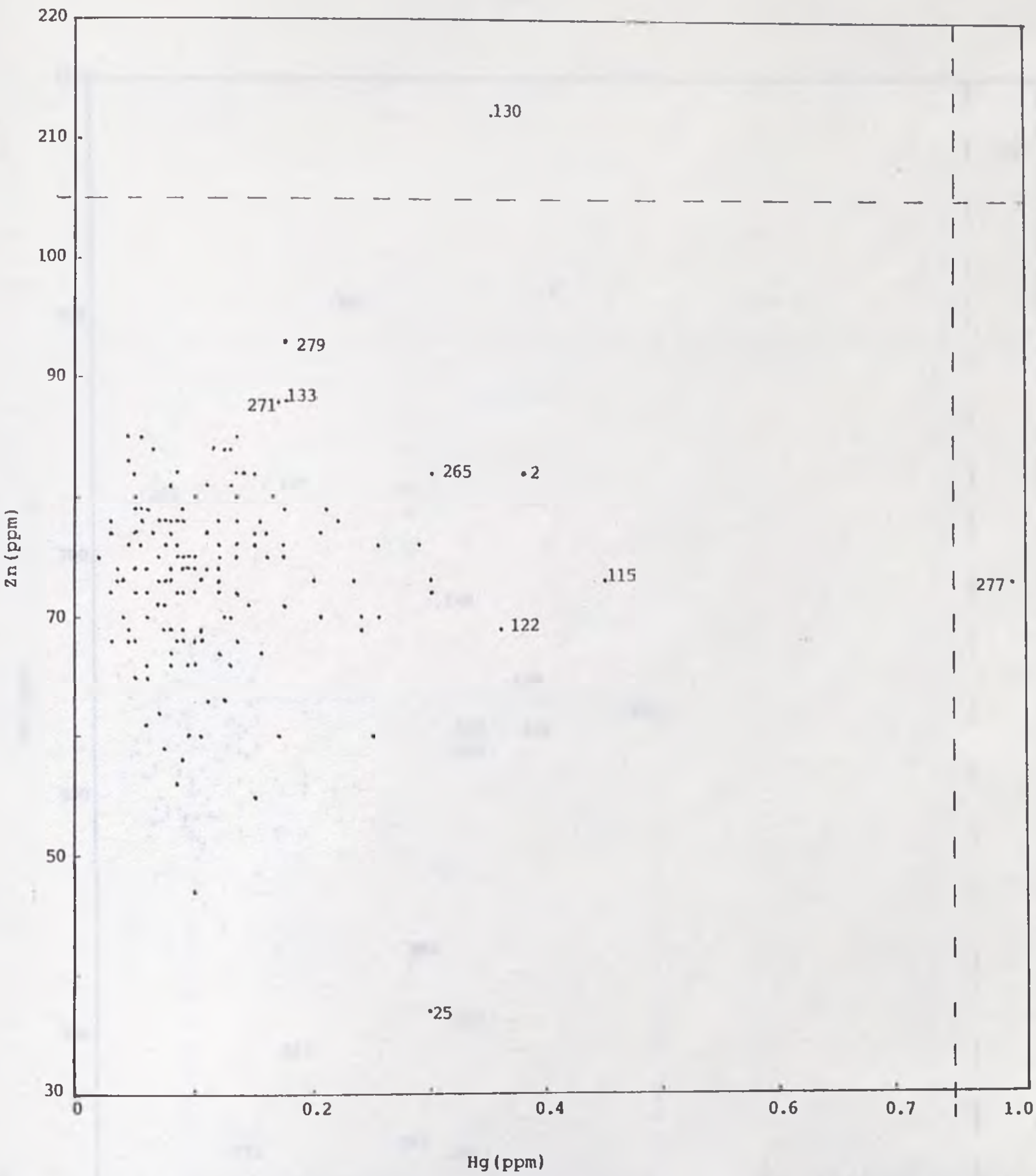

Figure A-4. Scatter plot for Zn vs. Hg - Gooseberry area

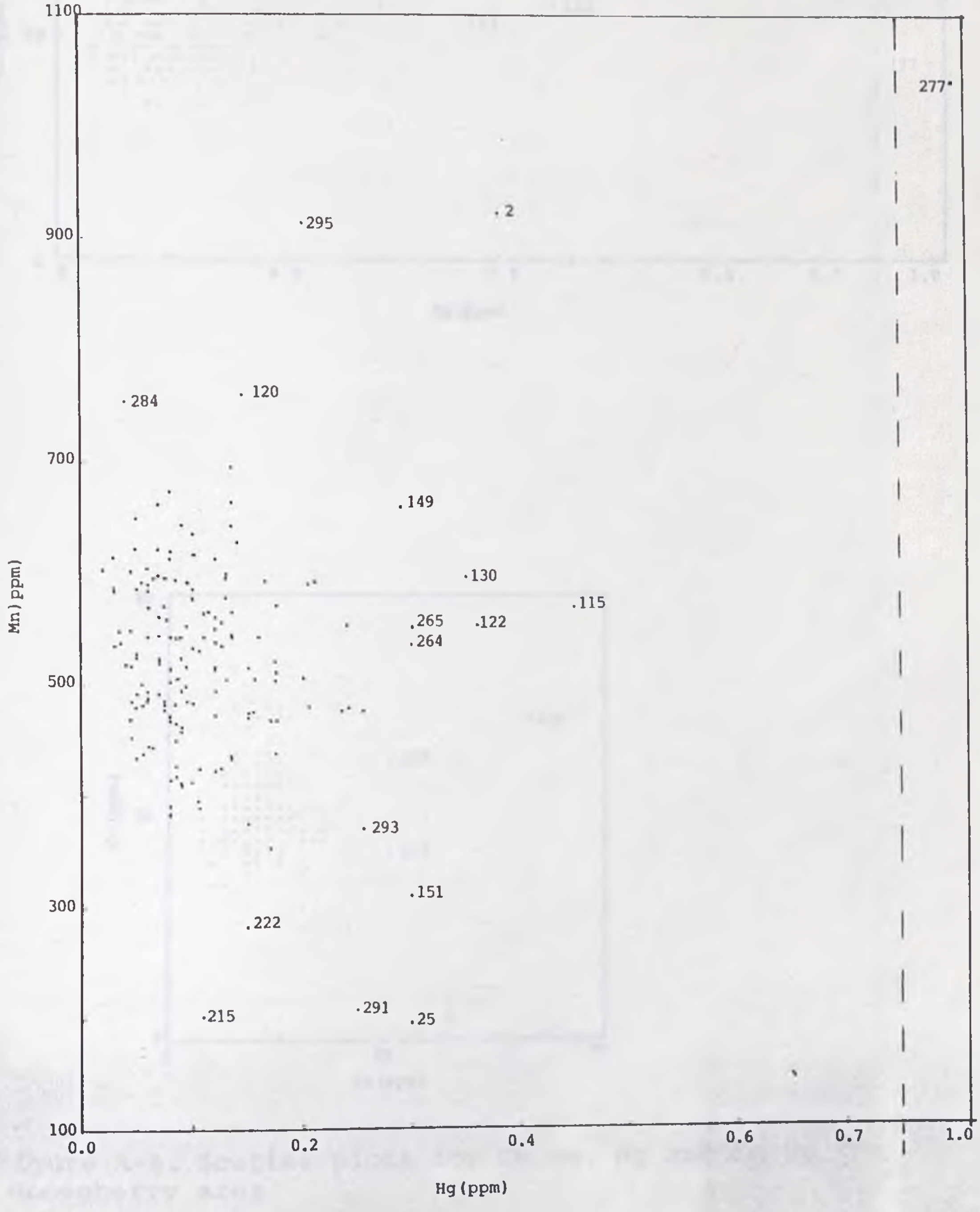

Figure A-5. Scatter plot for Mn vs. Hg - Gooseberry area

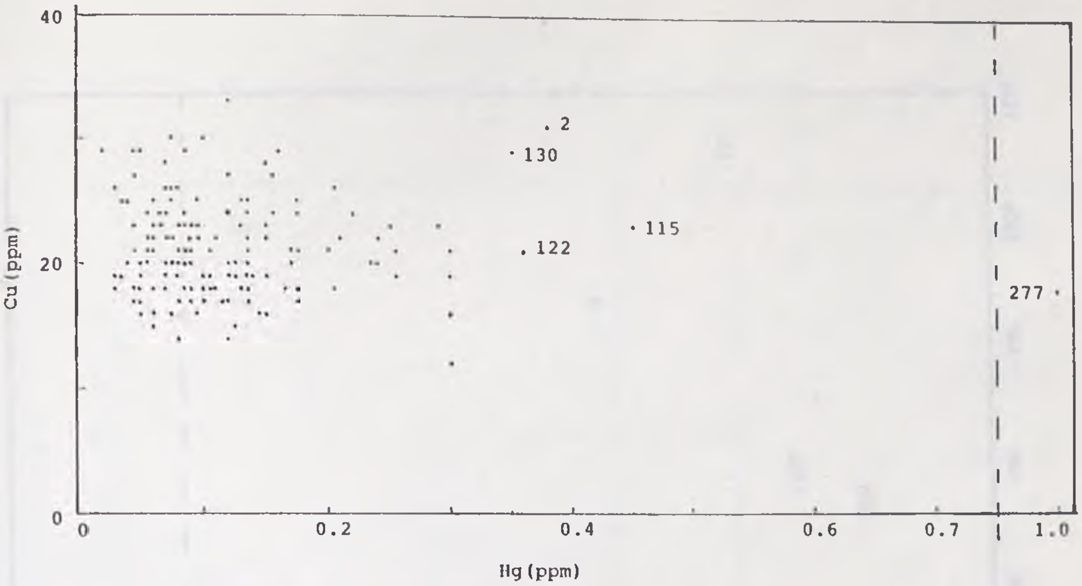

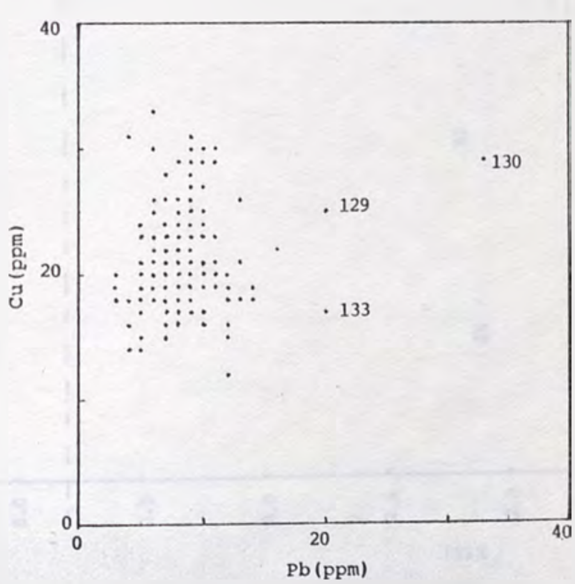

Figure A-6. Scatter plots for Cu vs. Hg and Cu vs. Pb - Gooseberry area

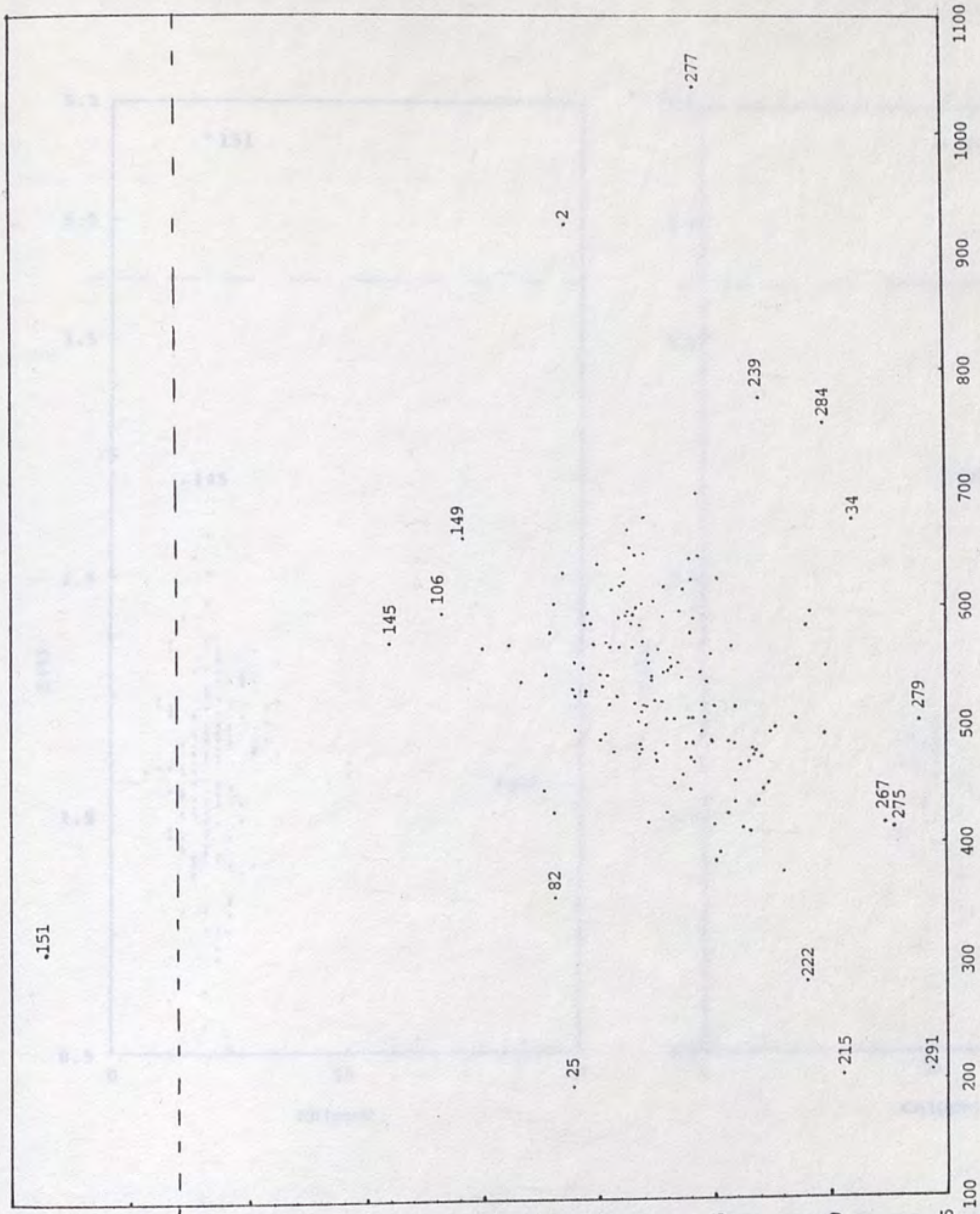

Figure A-7. Scatter plot for K vs. Mn - Gooseberry area

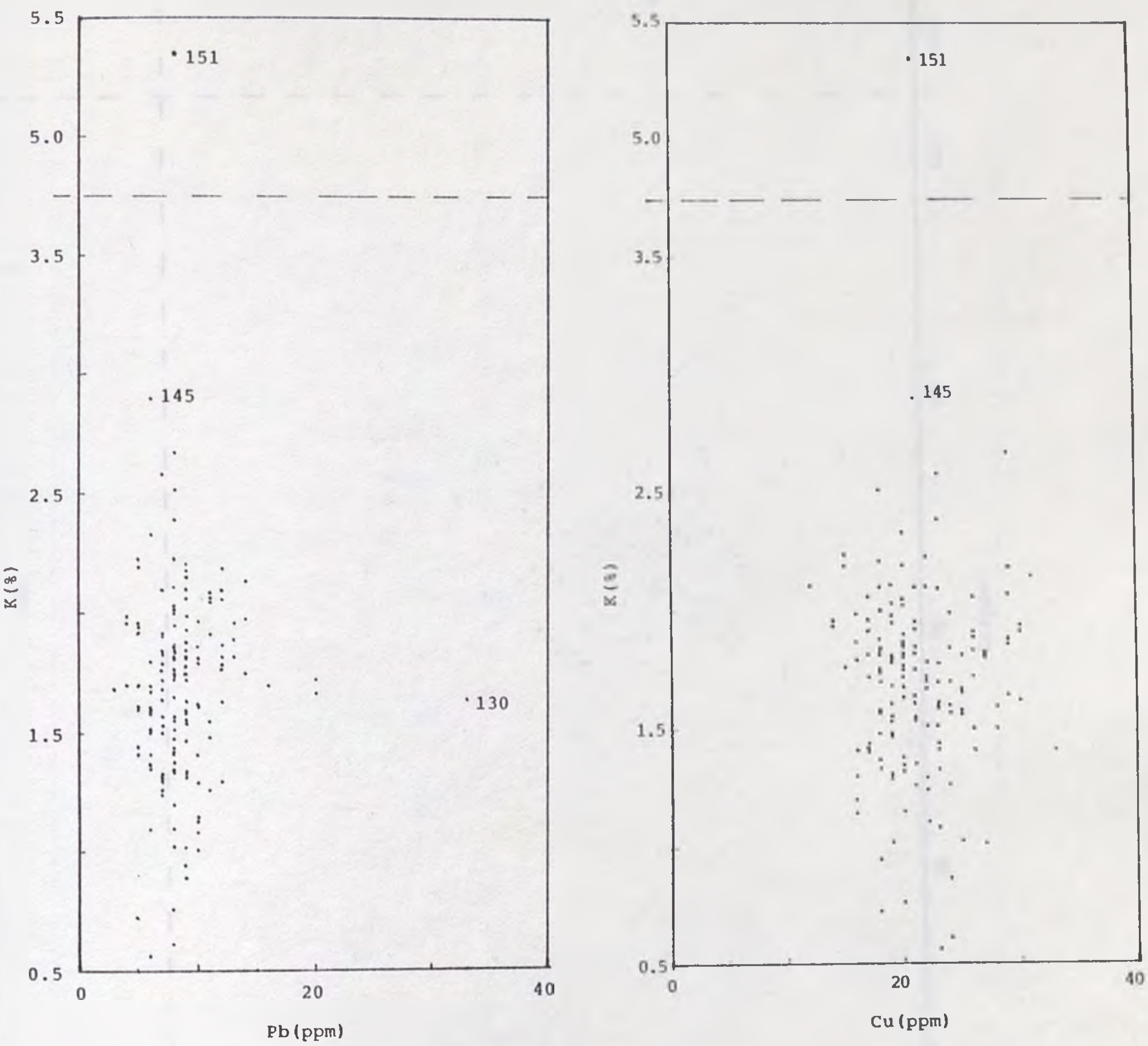

Figure A-8. Scatter plots for K vs. Pb and K vs. Cu - Gooseberry area

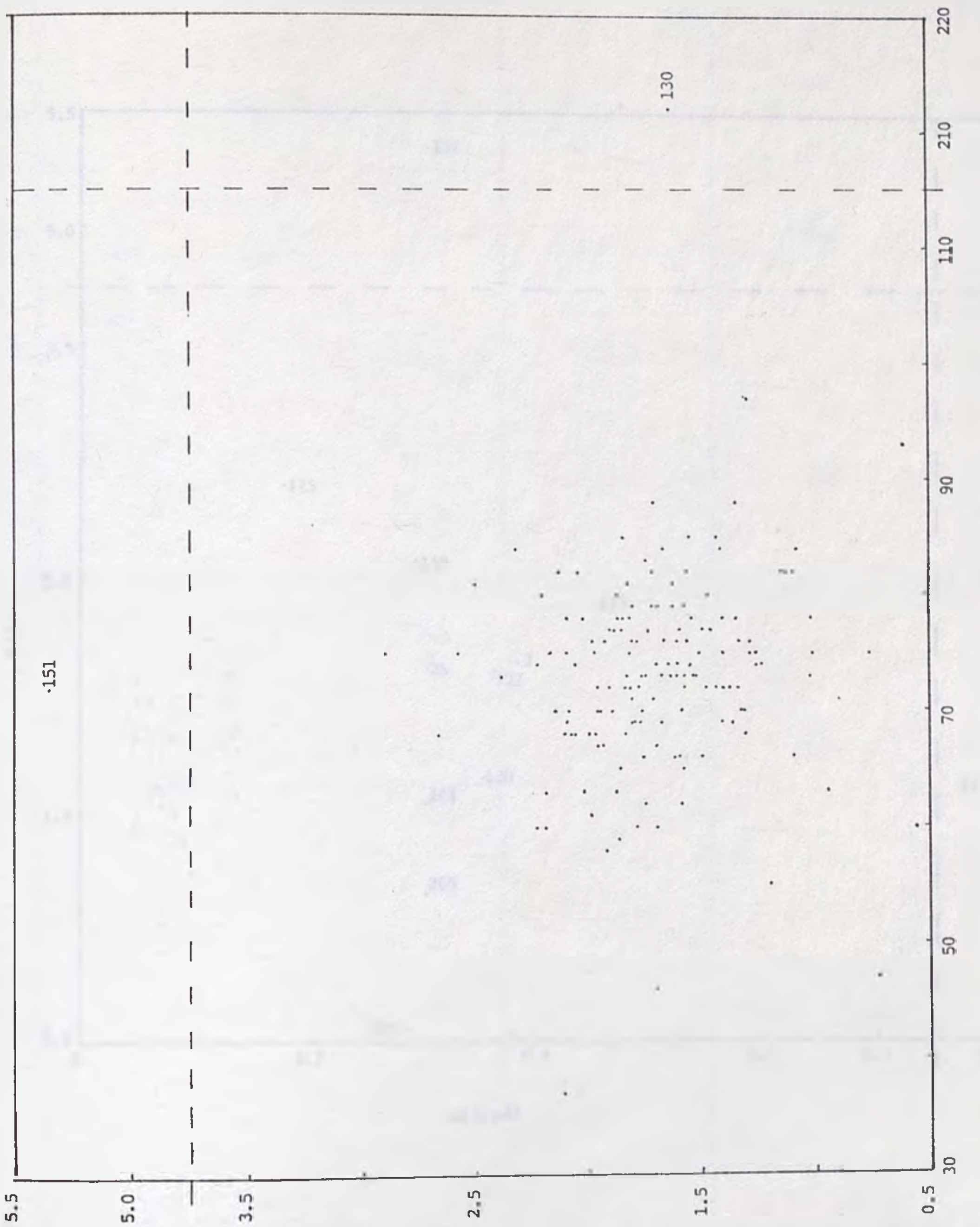

Figure A-9. Scatter plot for K vs. Zn - Gooseberry area

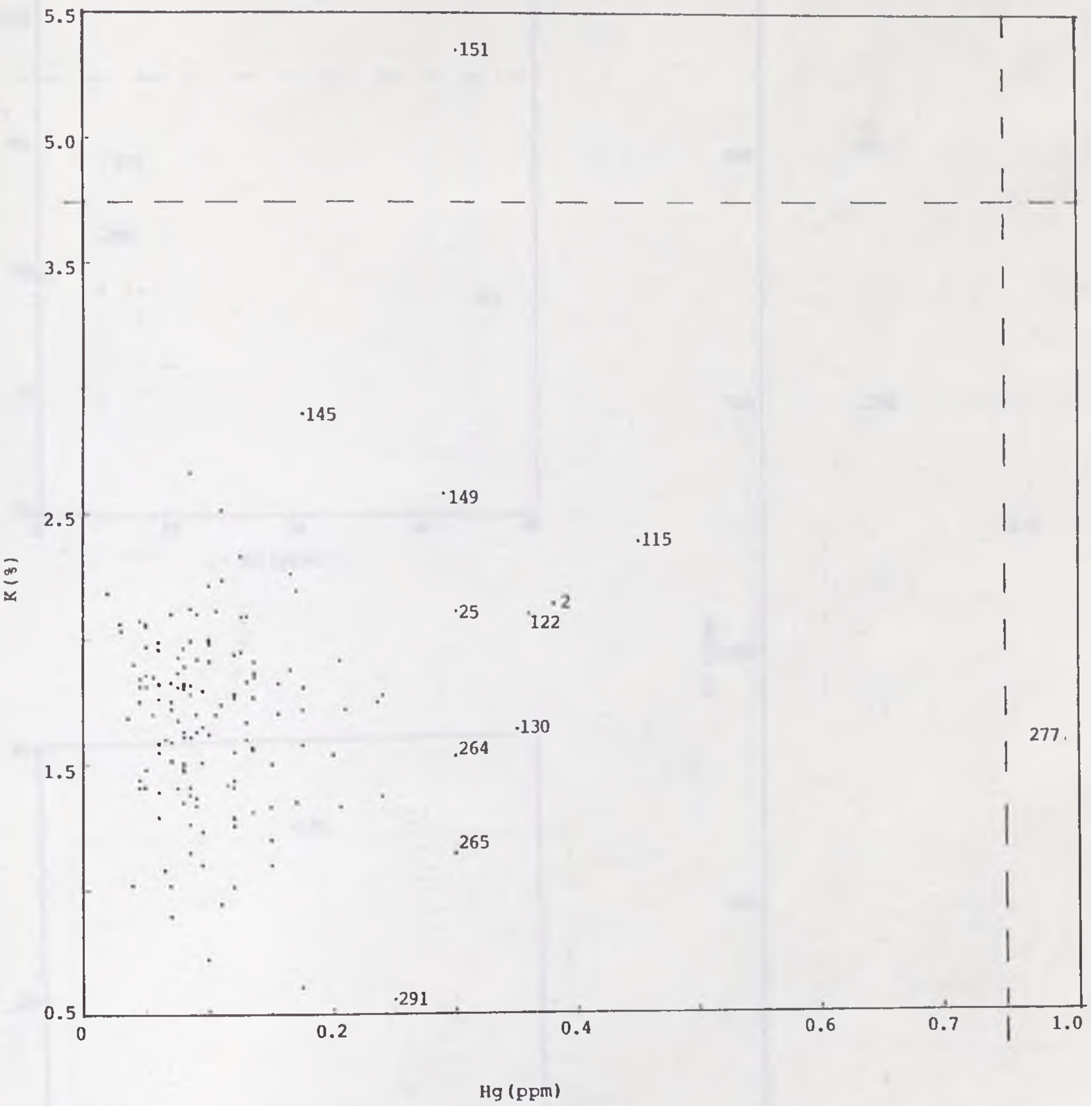

Figure A-10. Scatter plot for K vs. Hg - Gooseberry area

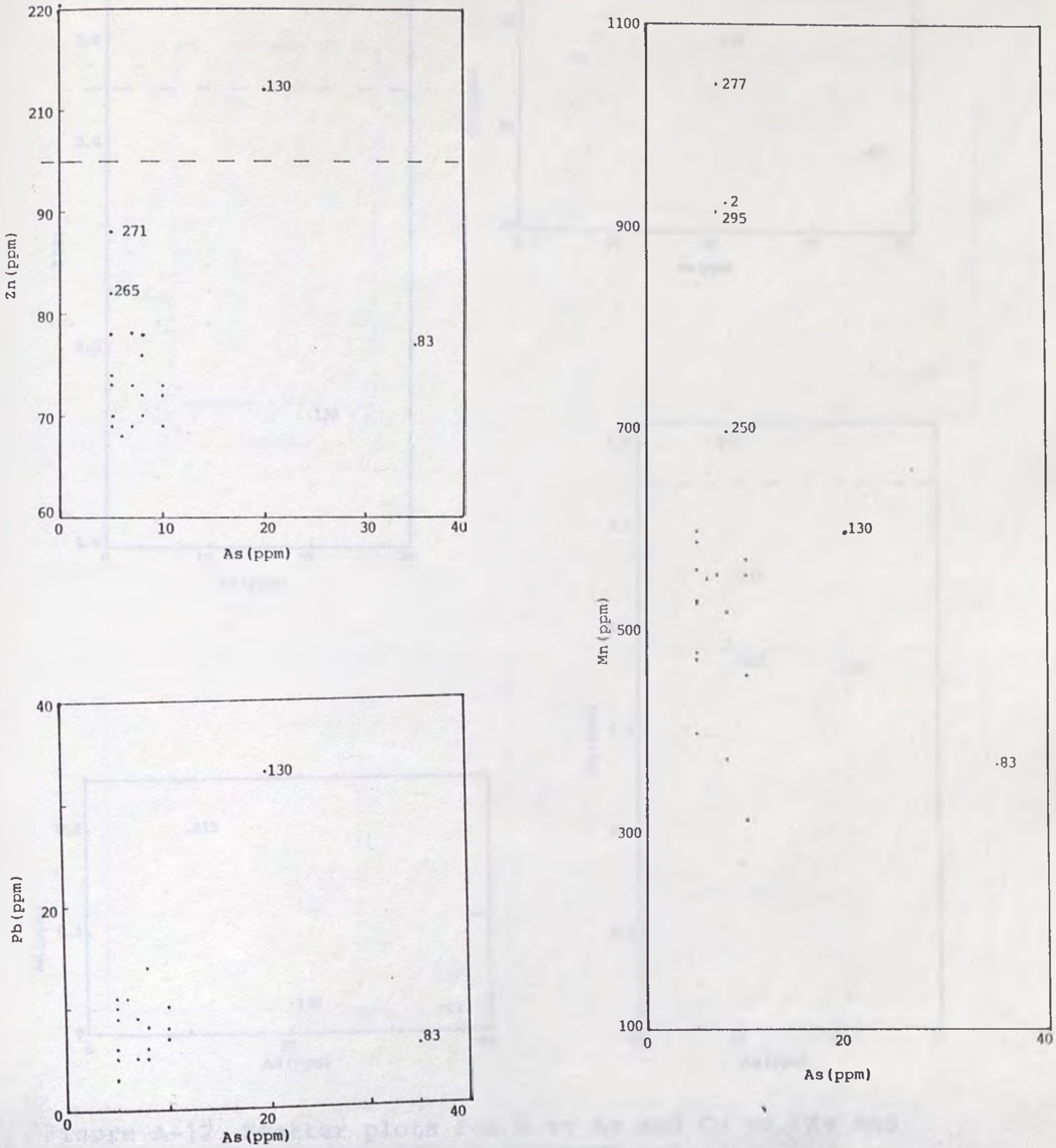

Figure A-11. Scatter plots for Zn vs. As and Pb vs. As and Mn vs. As - Gooseberry area

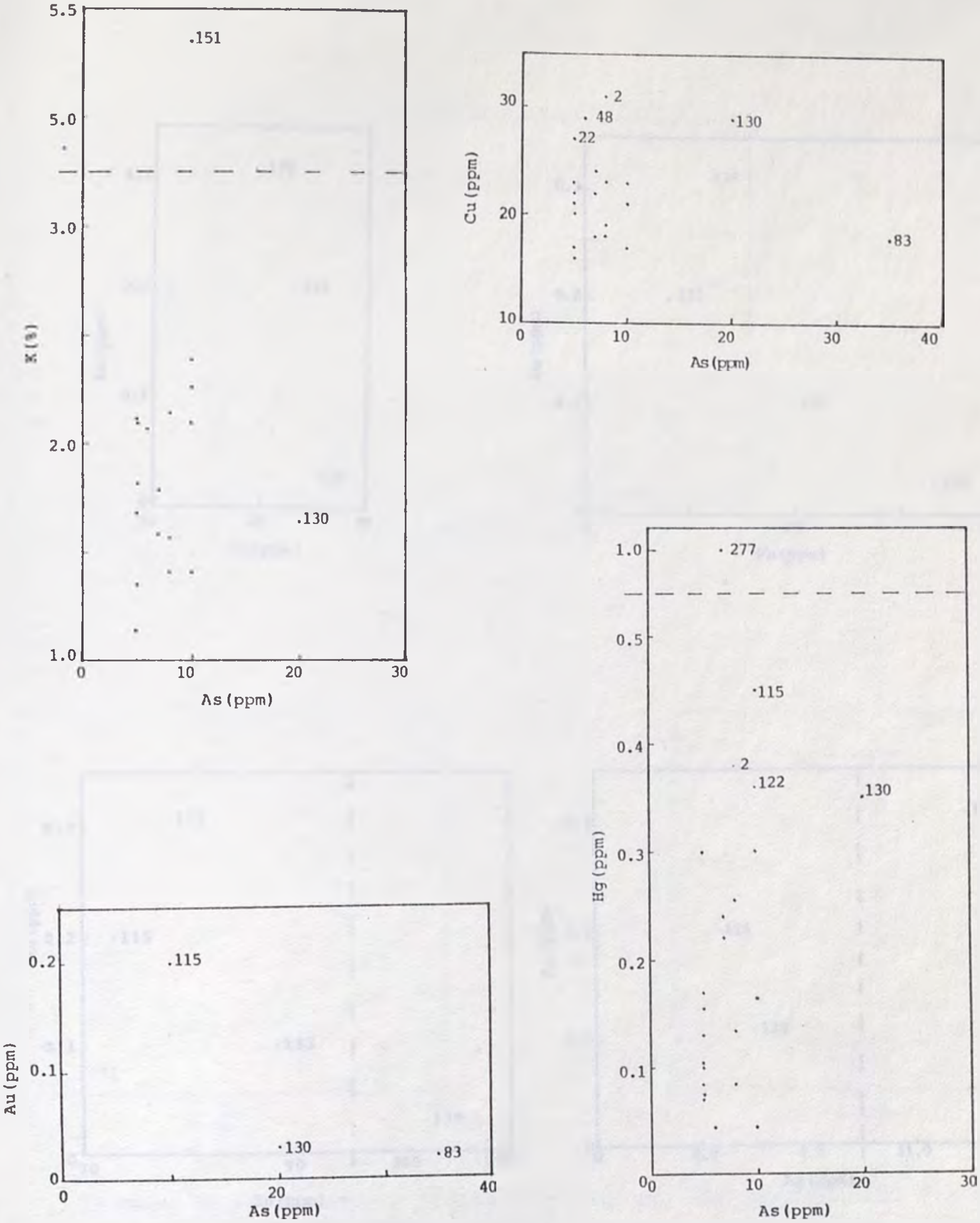

Figure A-12. Scatter plots for K vs As and Cu vs. As and Au vs. As and Hg vs. As - Gooseberry area

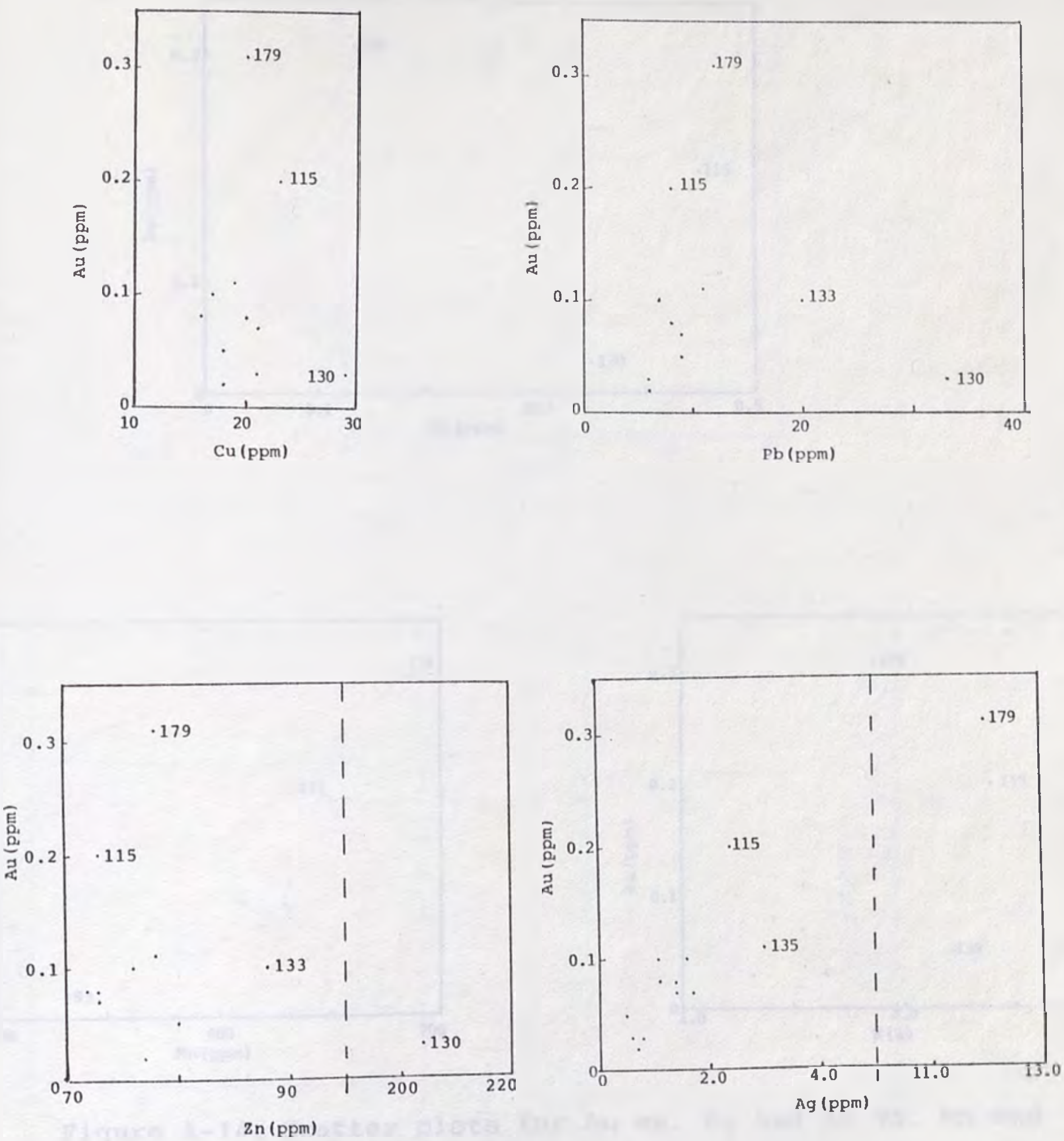

Figure A-13. Scatter plots for Au vs. Cu and Au vs. Pb and Au vs. Zn and Au vs. Ag - Gooseberry area

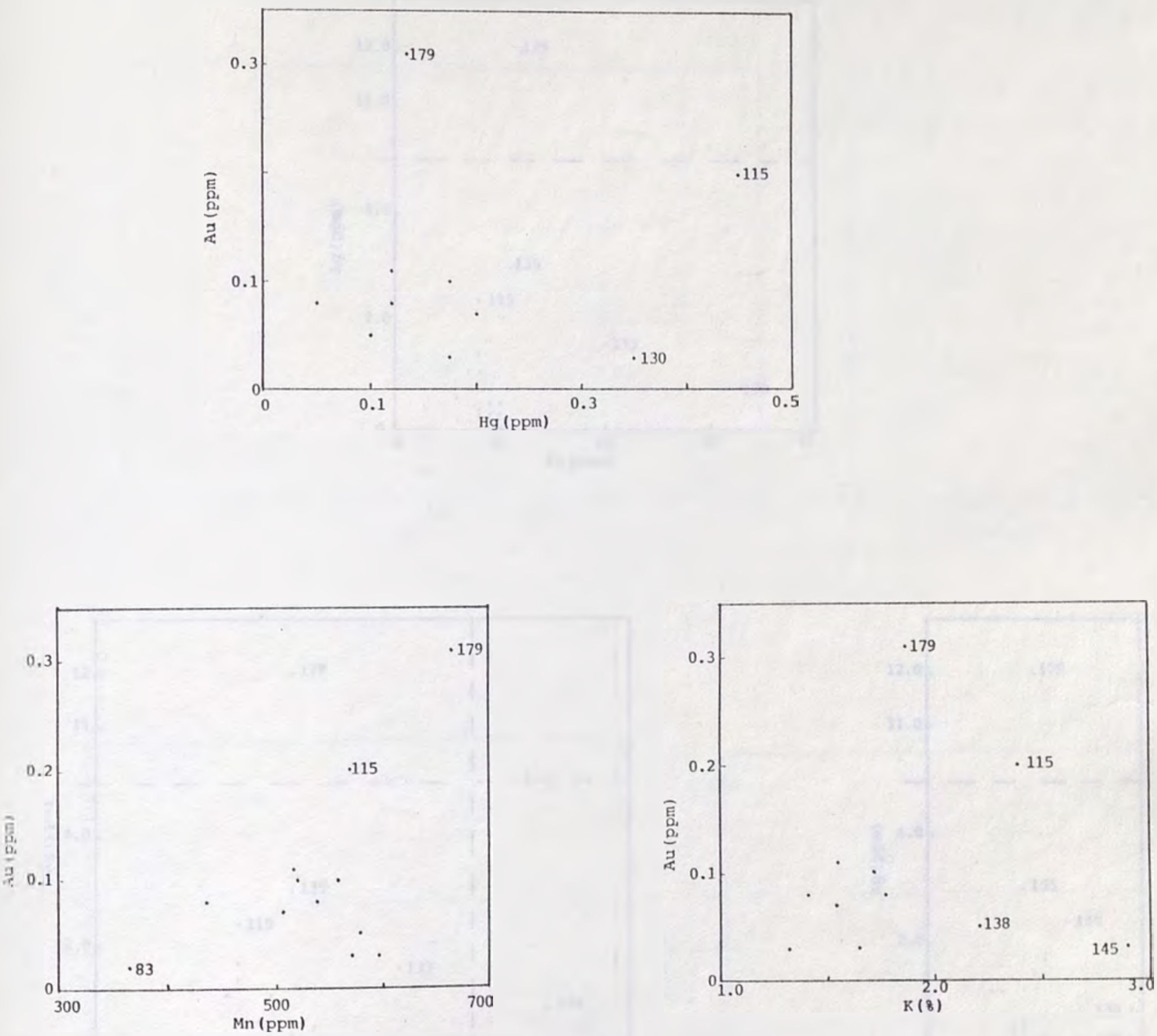

Figure A-14. Scatter plots for Au vs. Hg and Au vs. Mn and Au vs. K - Gooseberry area

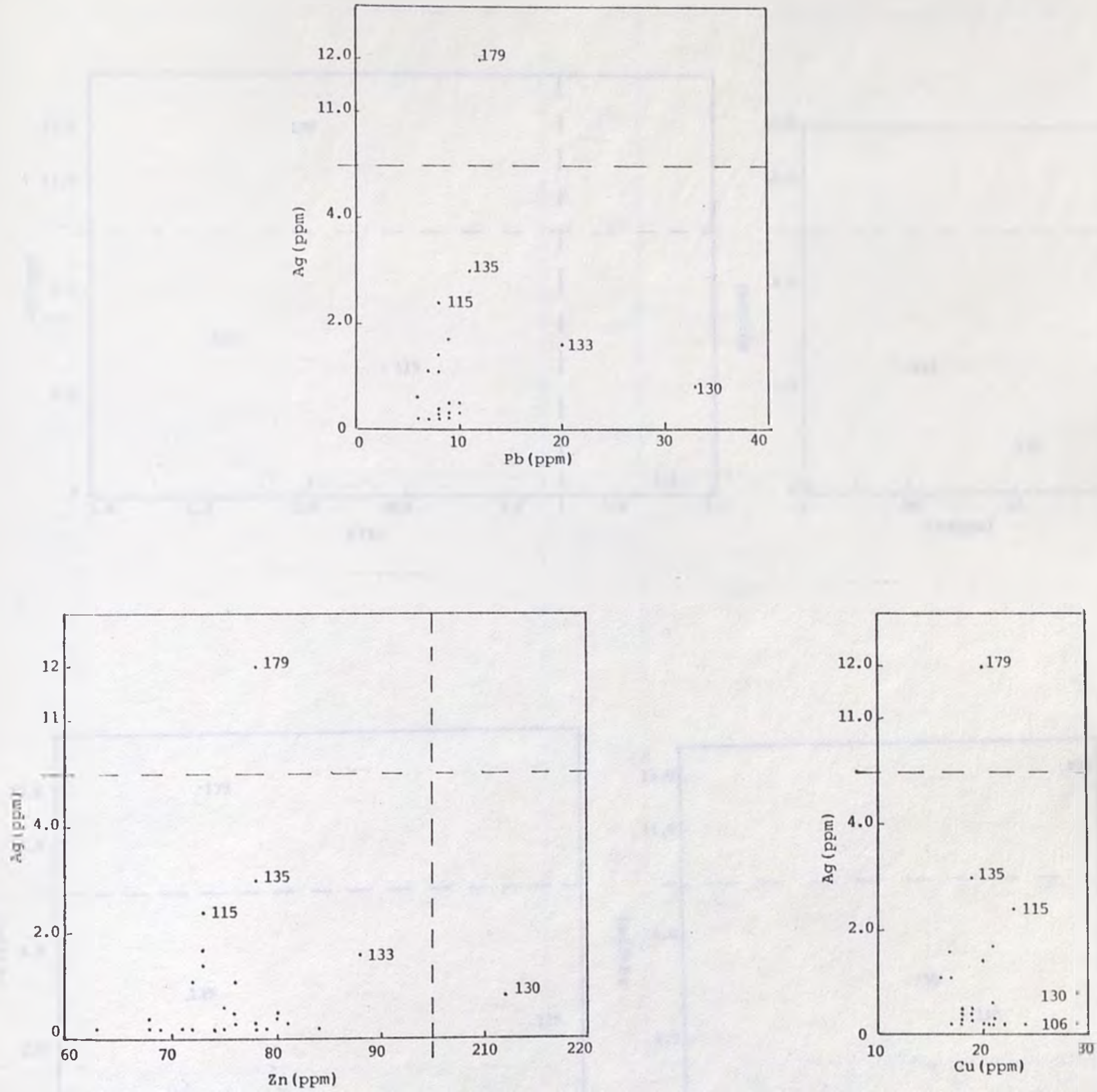

Figure A-15. Scatter plots for Ag vs. Pb and Ag vs. Zn and Ag vs. Cu - Gooseberry area

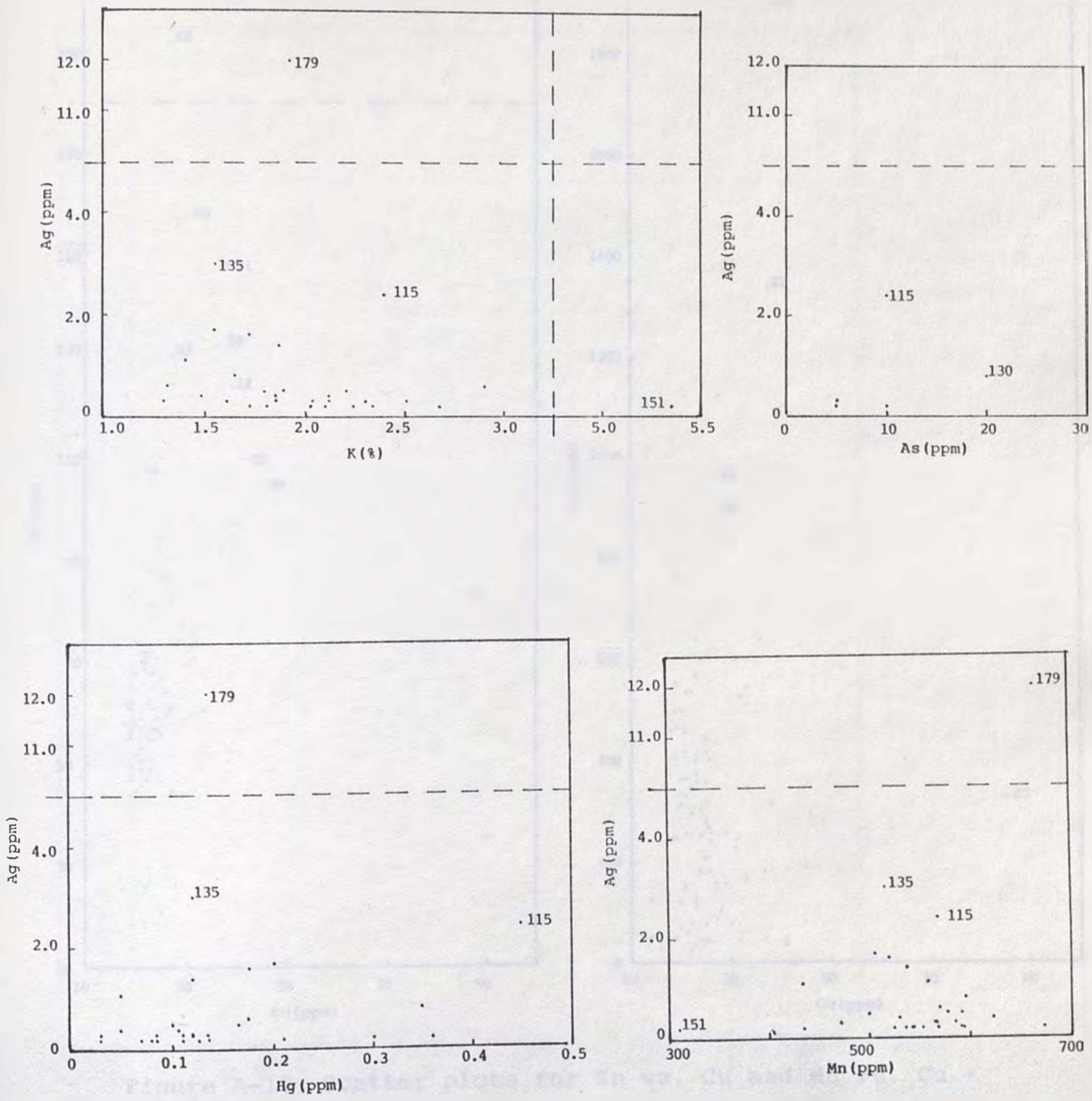

Figure A-16. Scatter plots for Ag vs. K and Ag vs. As and Ag vs. Hg and Ag vs. Mn - Gooseberry area

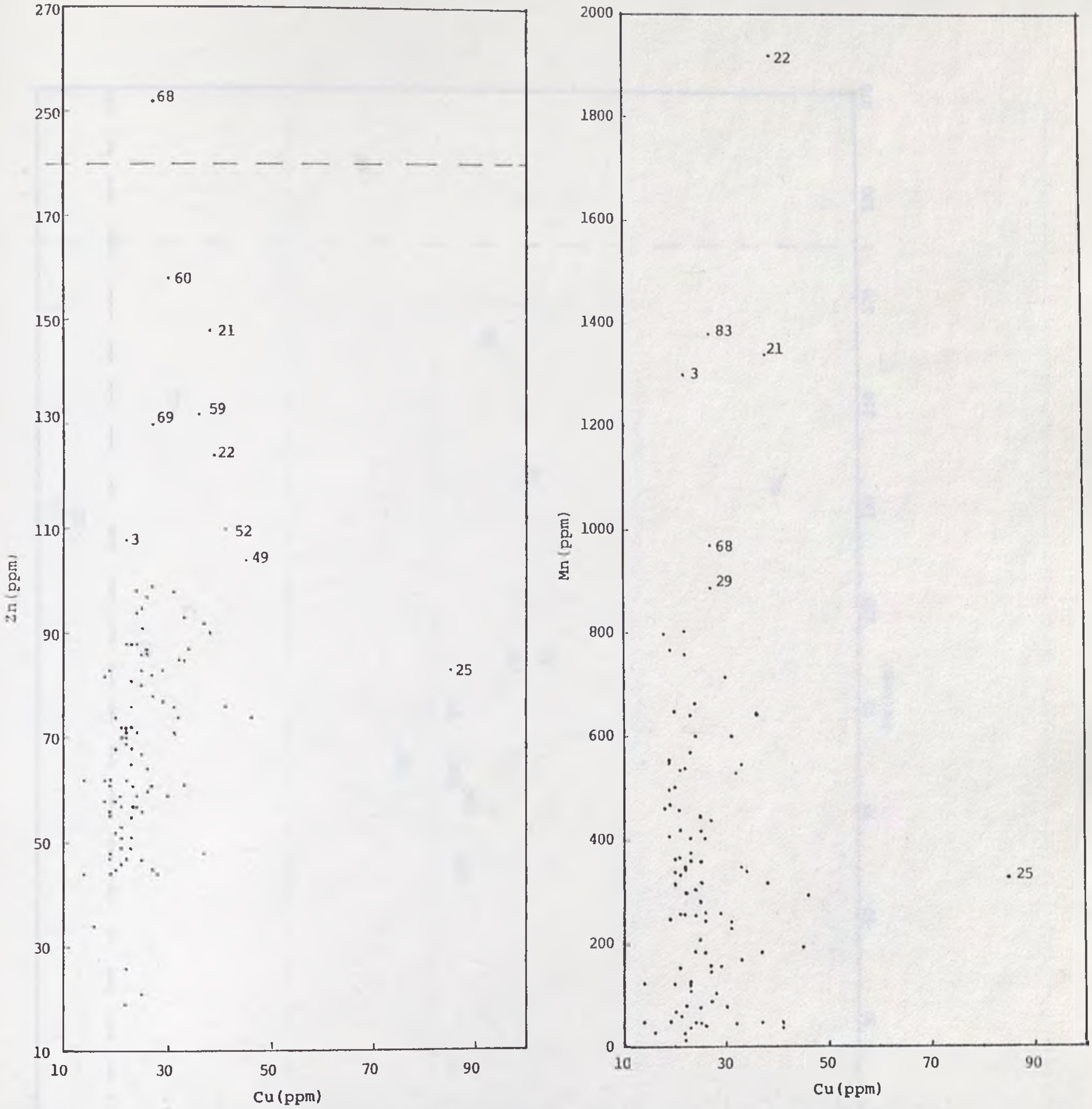

Figure A-17. Scatter plots for Zn vs. Cu and Mn vs. Cu - Red Top area

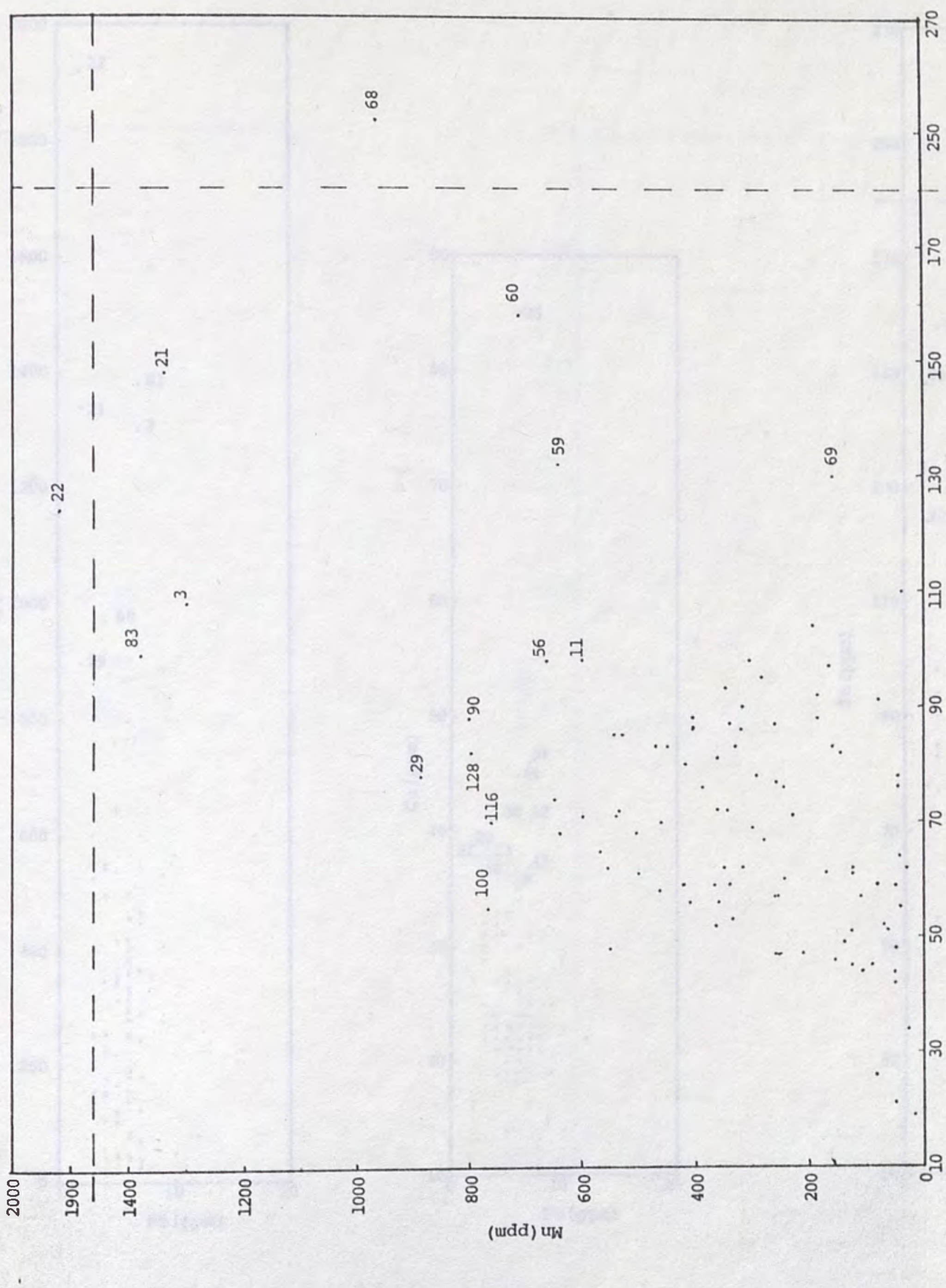

Figure A-18. Scatter plot for Mn vs. Zn - Red Top area

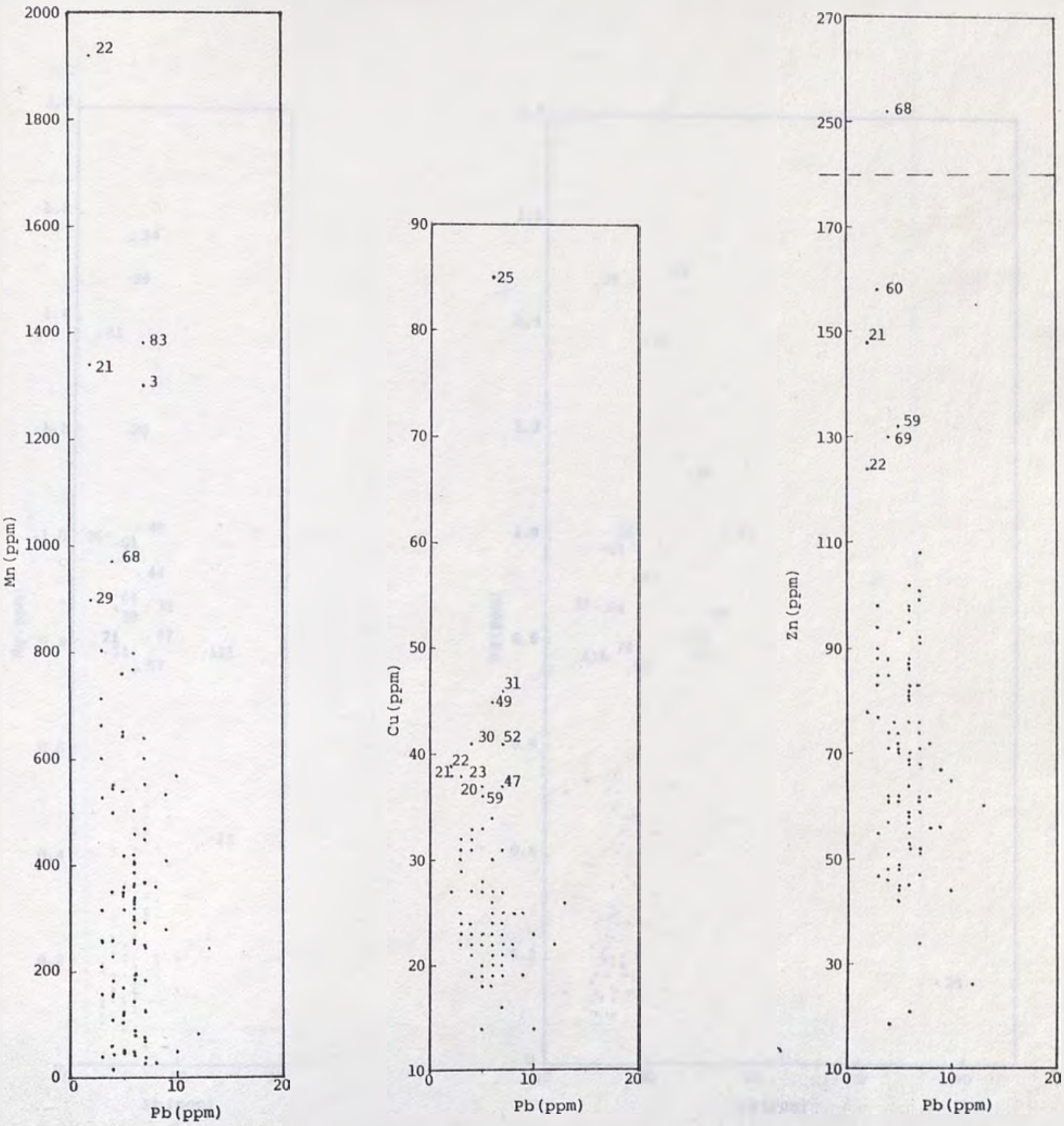

Figure A-19. Scatter plots for Mn vs. Pb and Cu vs. Pb and Zn vs. Pb - Red Top area

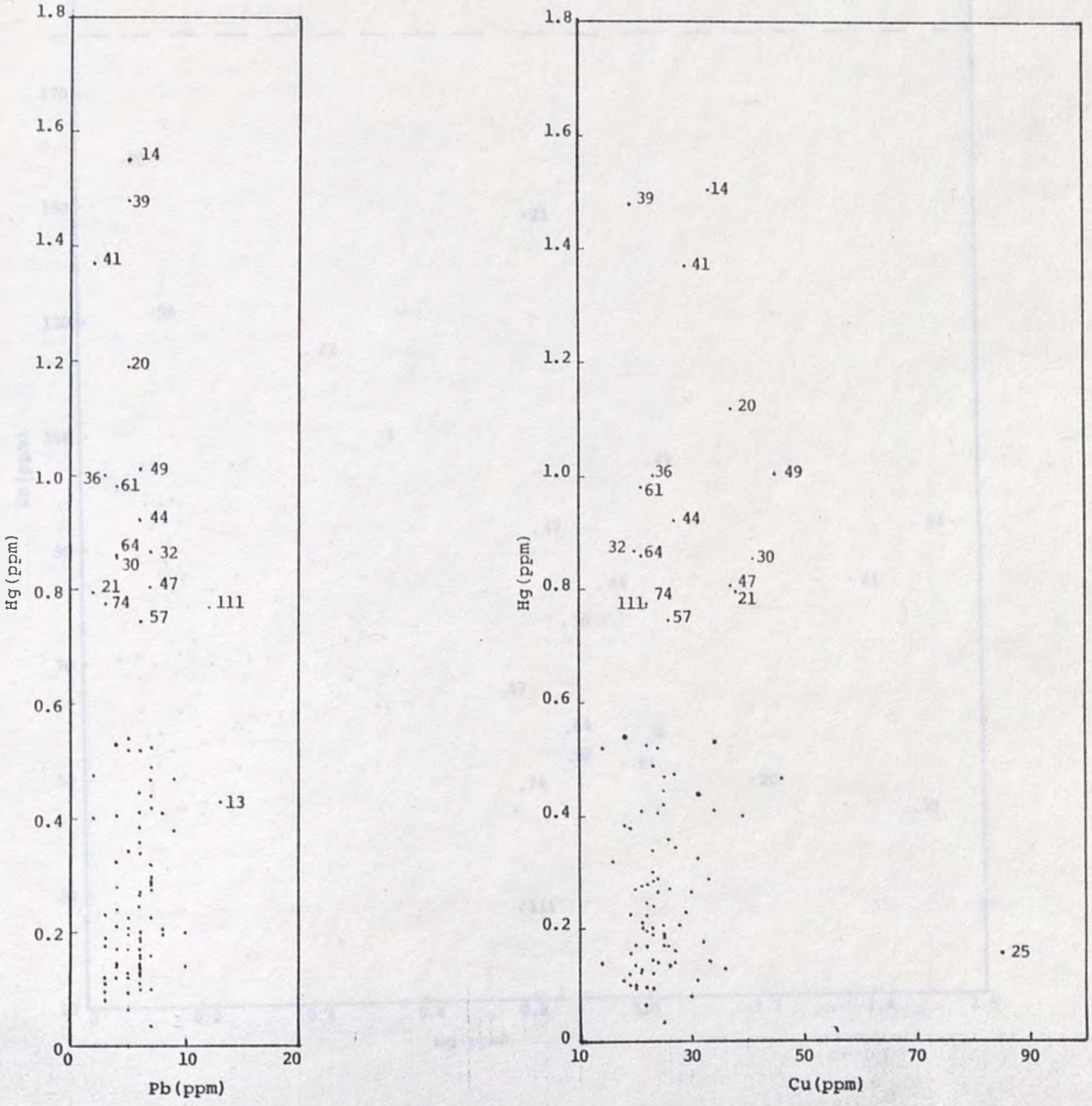

Figure A-20. Scatter plots for Hg vs. Pb and Hg vs. Cu - Red Top area

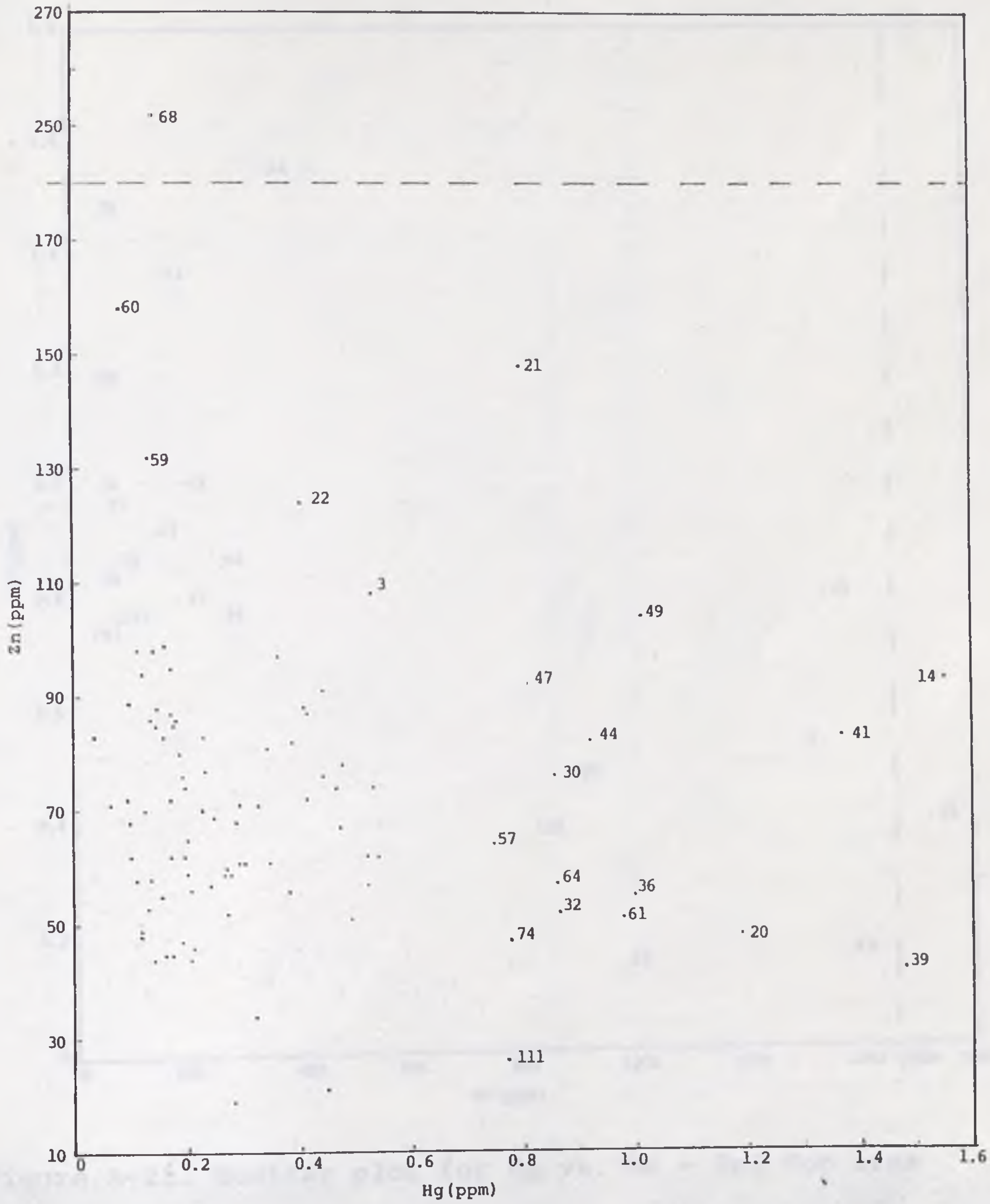

Figure A-21. Scatter plot for Zn vs. Hg - Red Top area

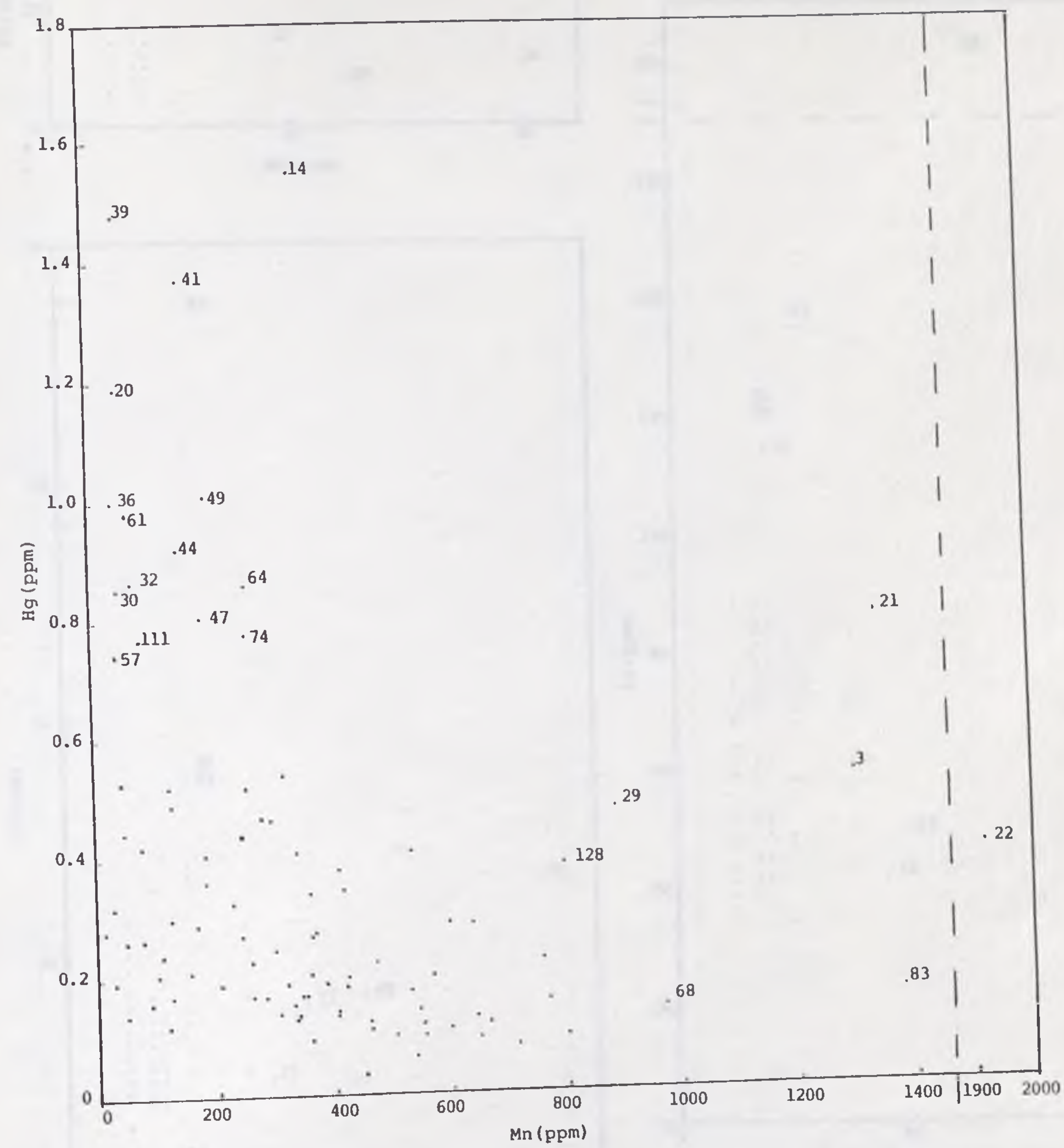

Figure A-22. Scatter plot for Hg vs. Mn - Red Top area

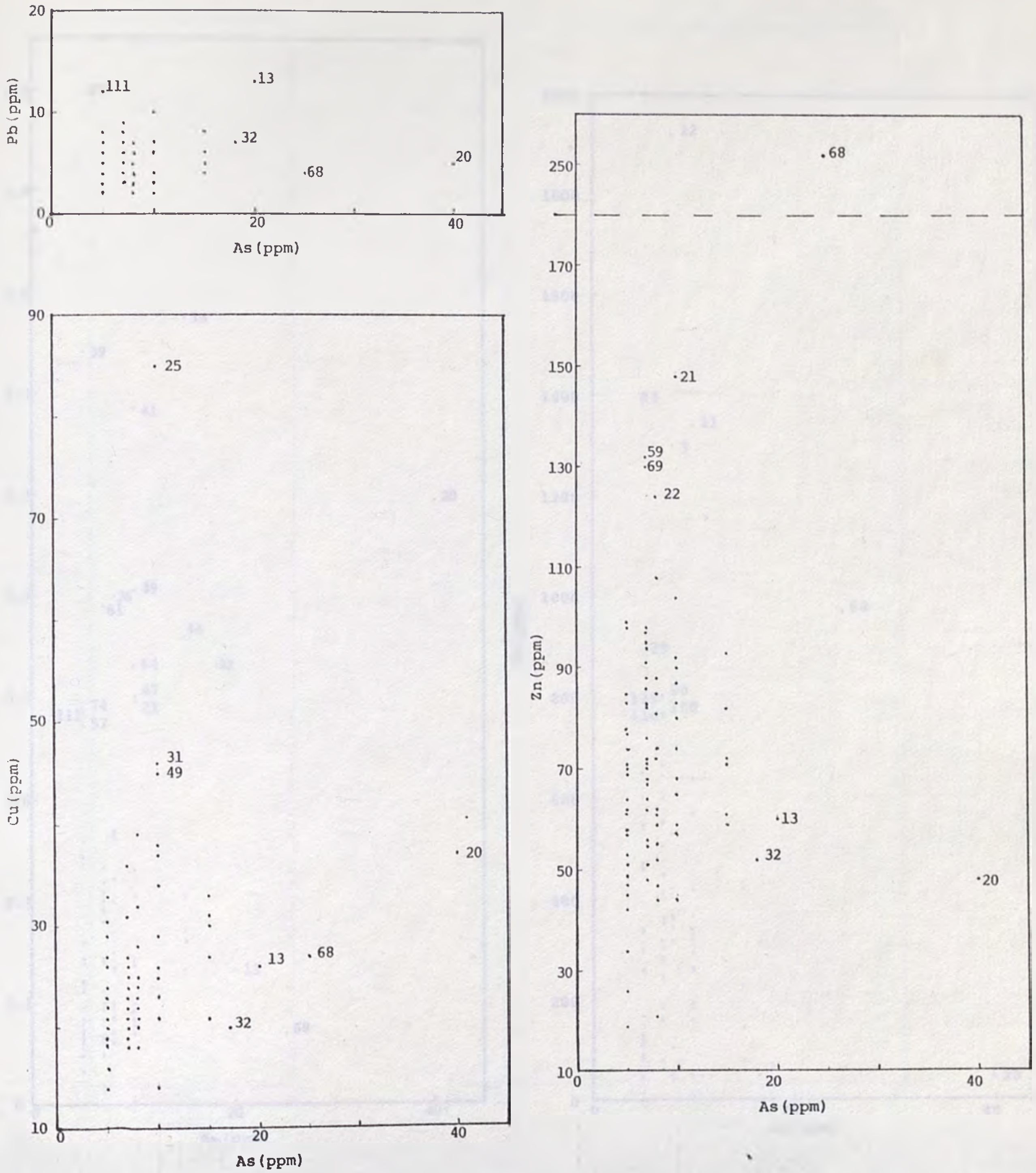

Figure A-23. Scatter plots for Pb vs. As and Cu vs. As and Zn vs. As - Red Top area

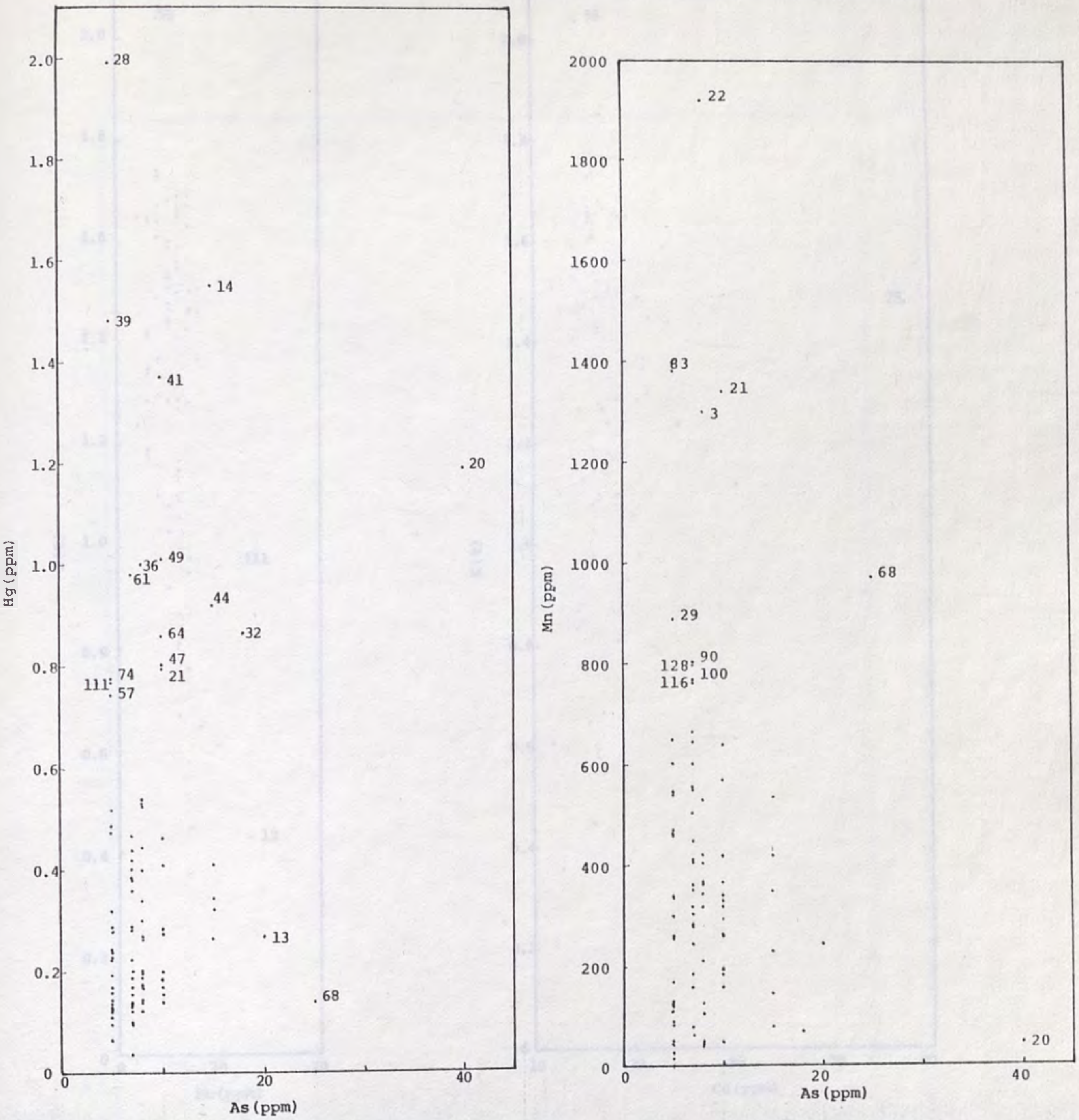

Figure A-24. Scatter plots for Hg vs. As and Mn vs. As - Red Top area

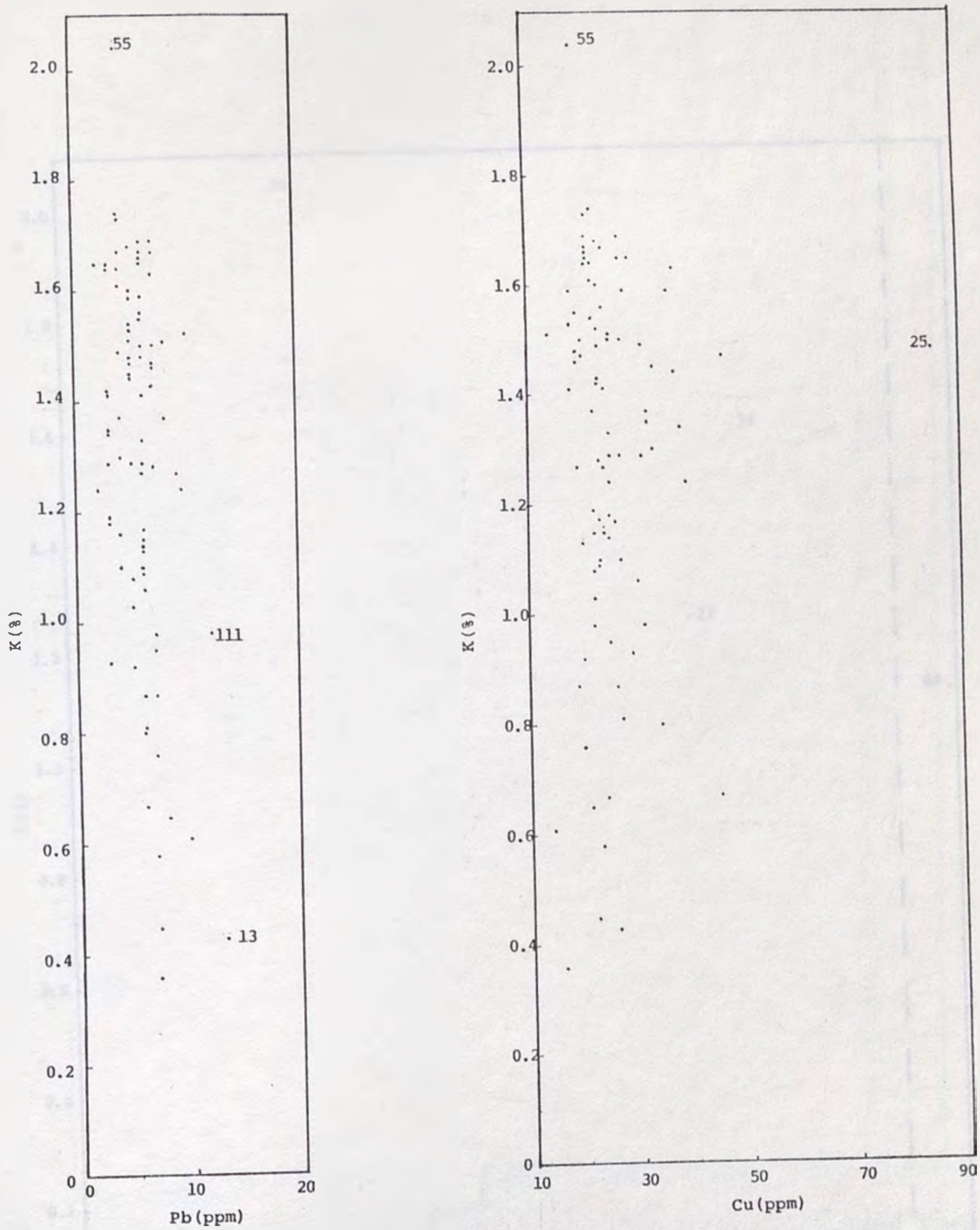

Figure A-25. Scatter plots for K vs. Pb and K vs. Cu - Red Top area

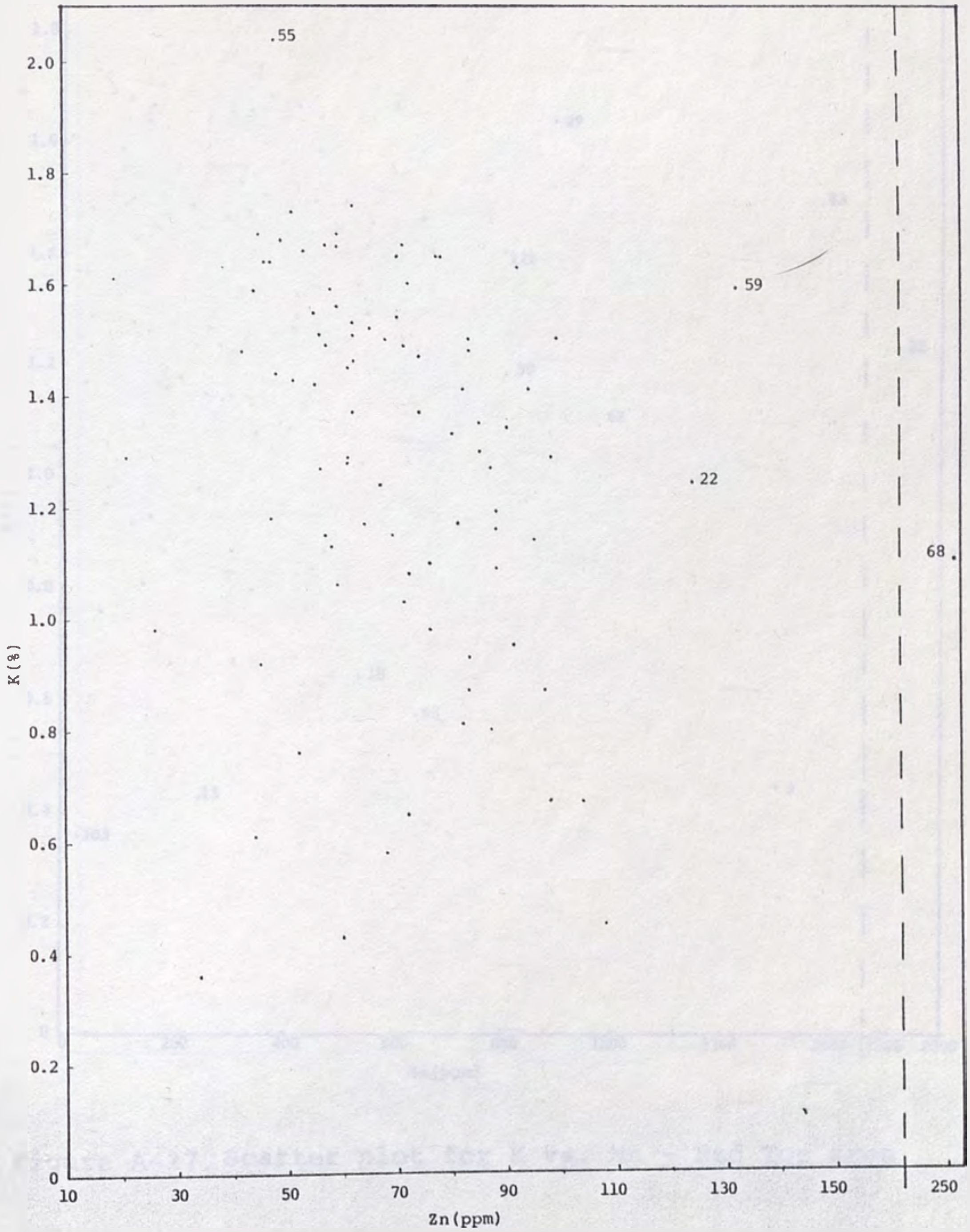

Figure A-26. Scatter plot for K vs. Zn - Red Top area

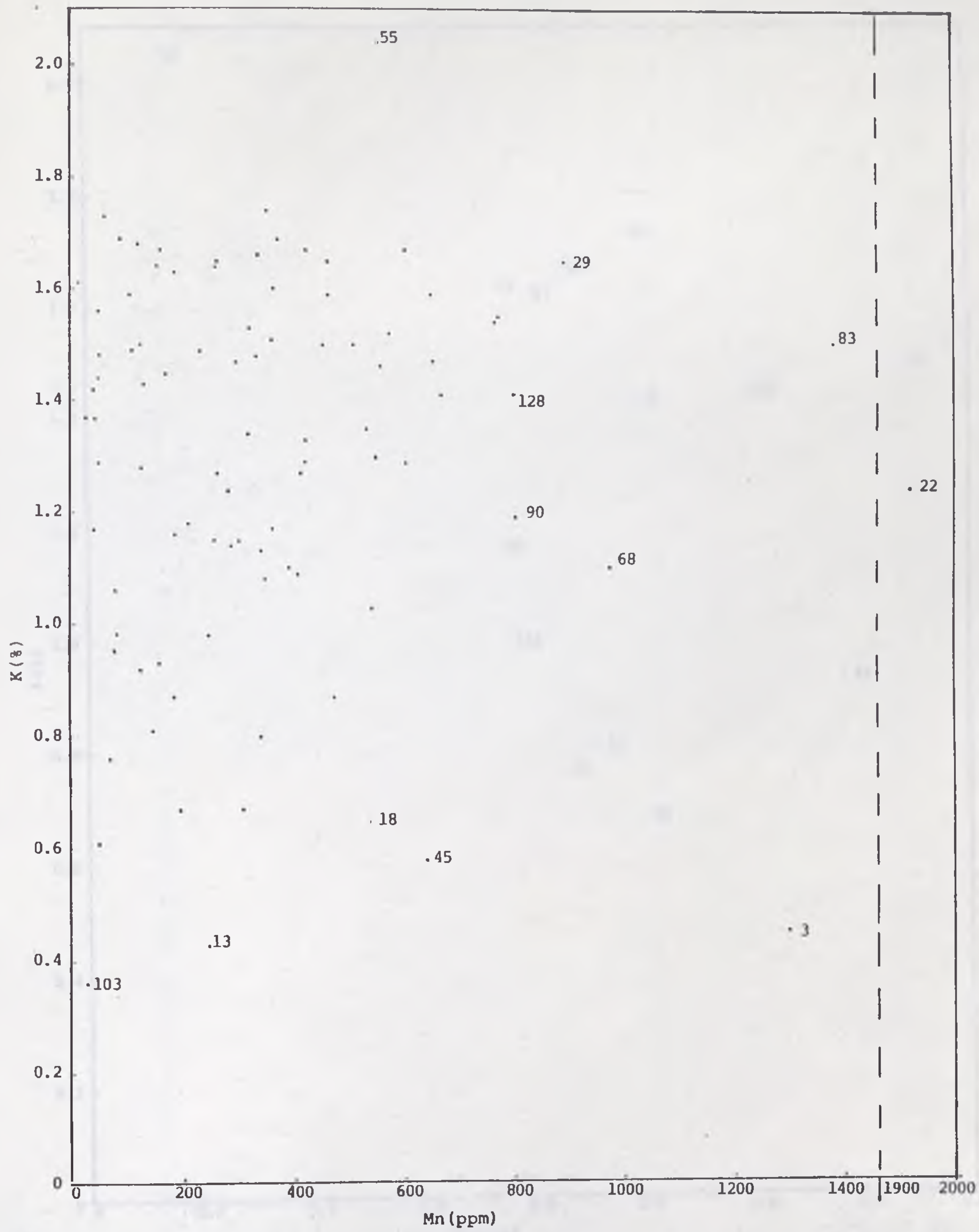

Figure A-27. Scatter plot for K vs. Mn - Red Top area

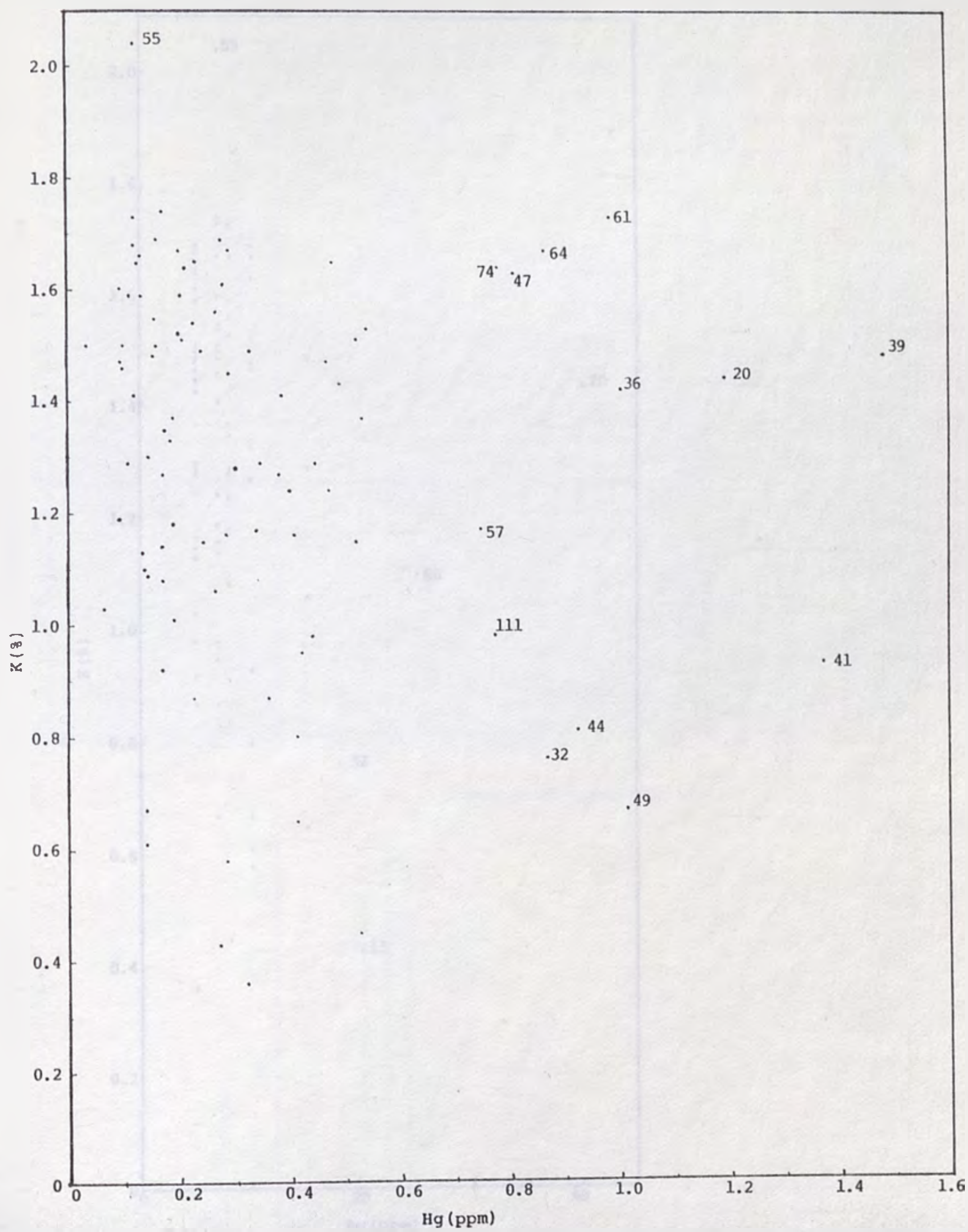

Figure A-28. Scatter plot for K vs. Hg - Red Top area

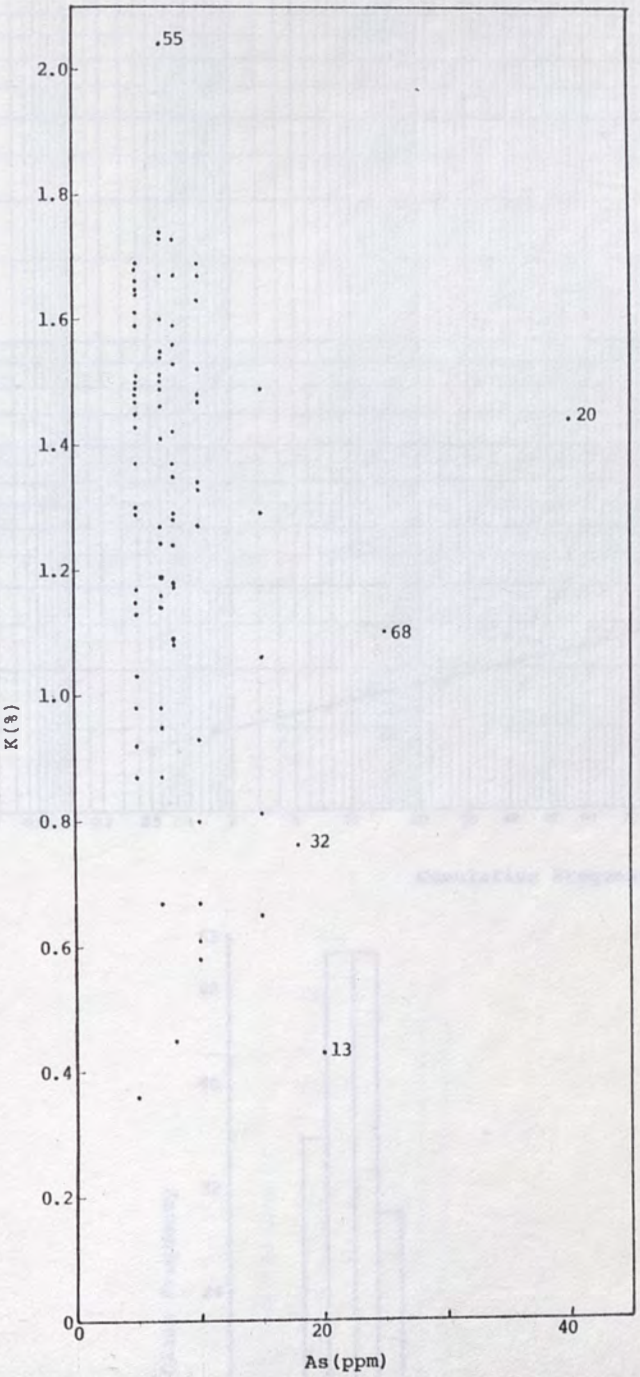

Figure A-29. Scatter plot for K vs. As - Red Top area

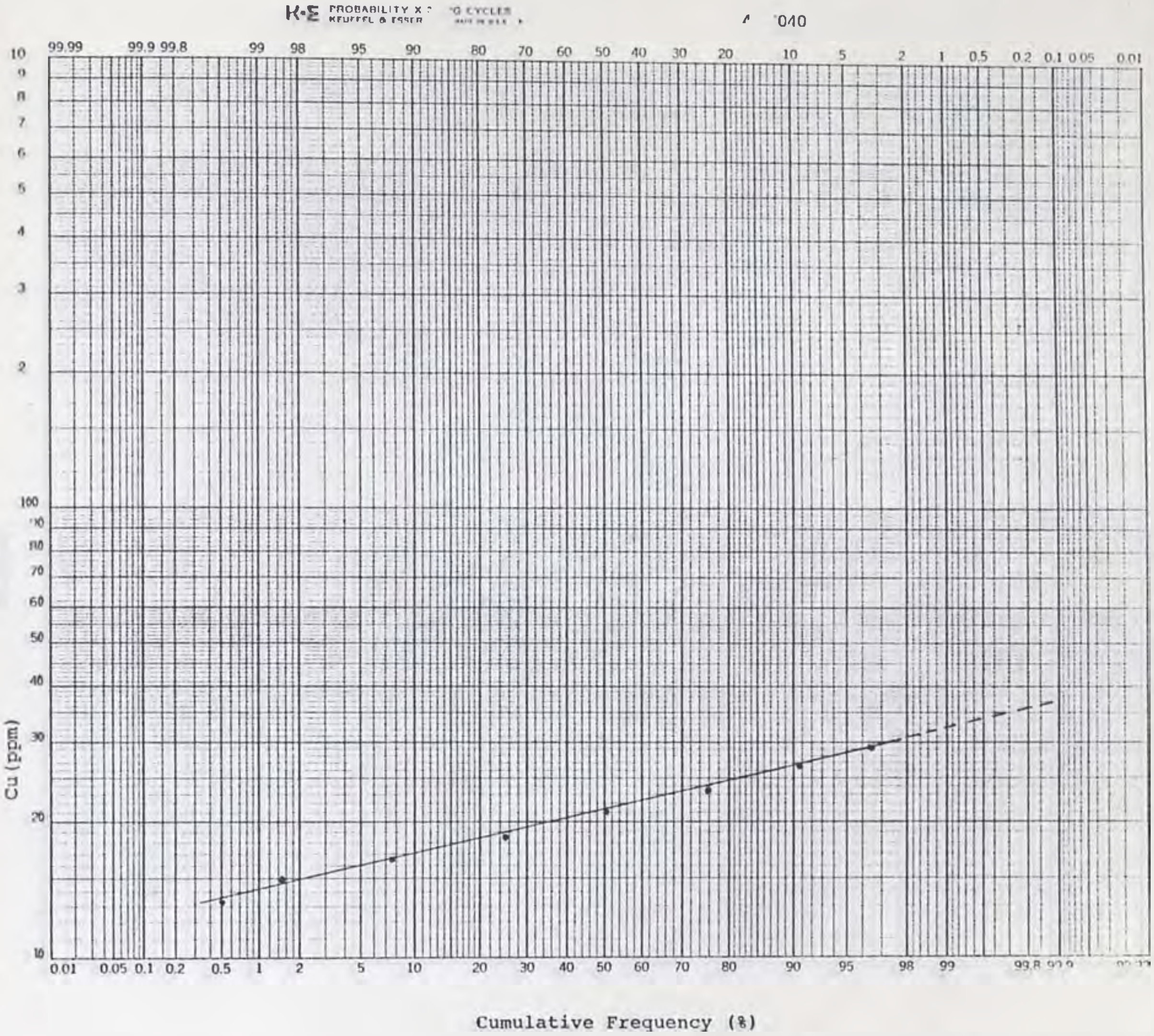

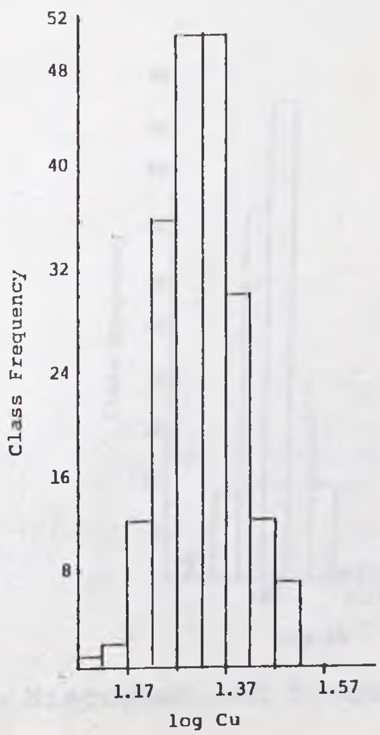

Figure A-30. Histogram and frequency plot for Cu - Gooseberry area.

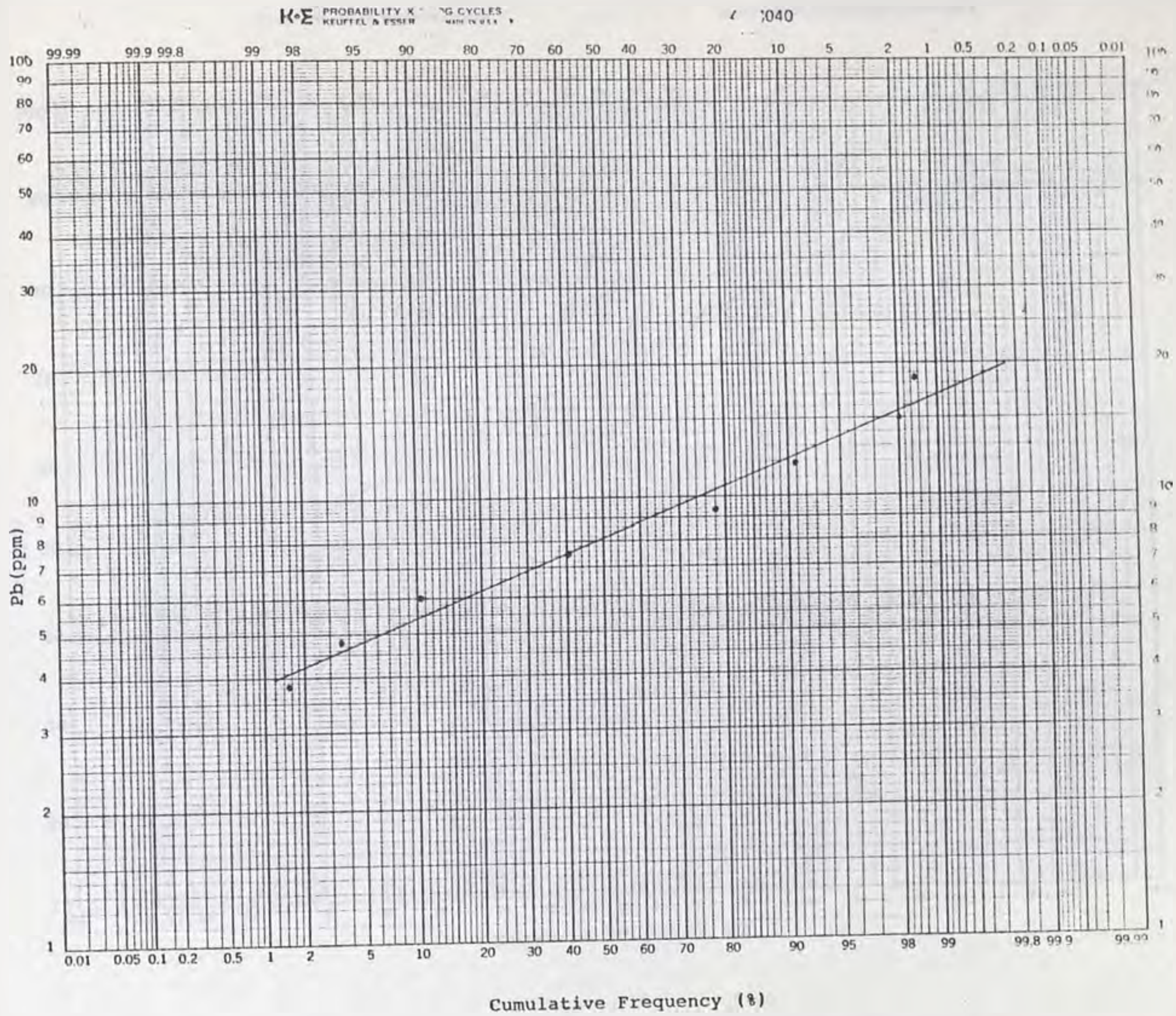

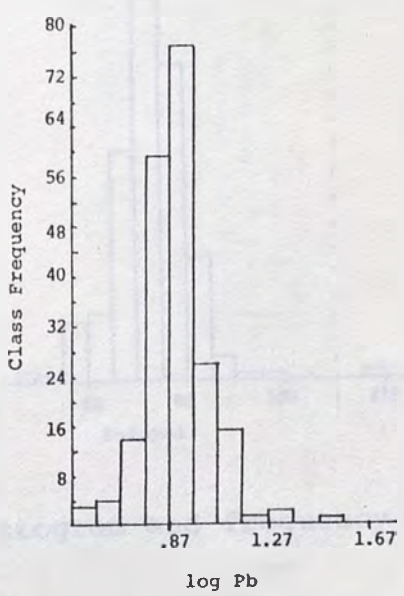

Figure A-31. Histogram and frequency plot for Pb - Gooseberry area

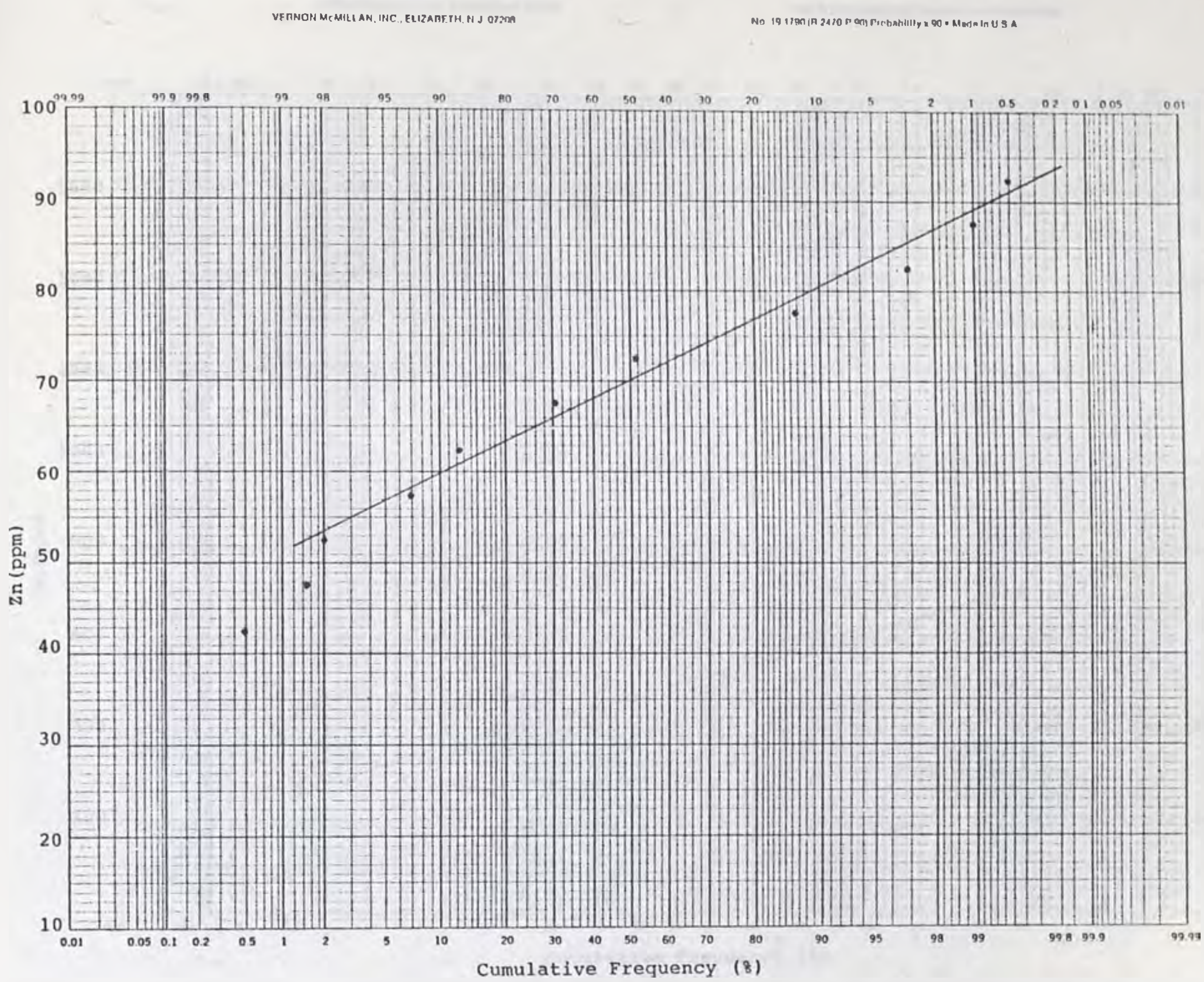

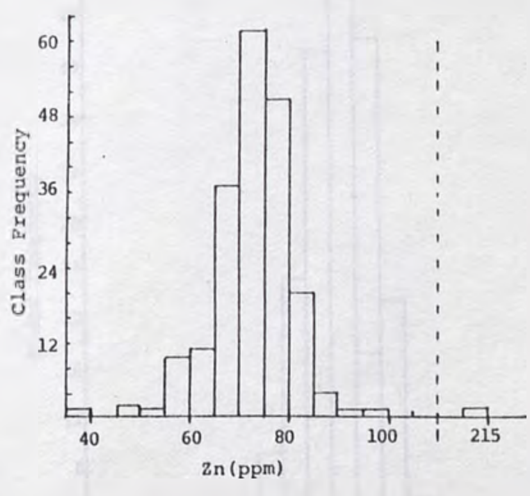

Figure A-32. Histogram and frequency plot for Zn - Gooseberry area

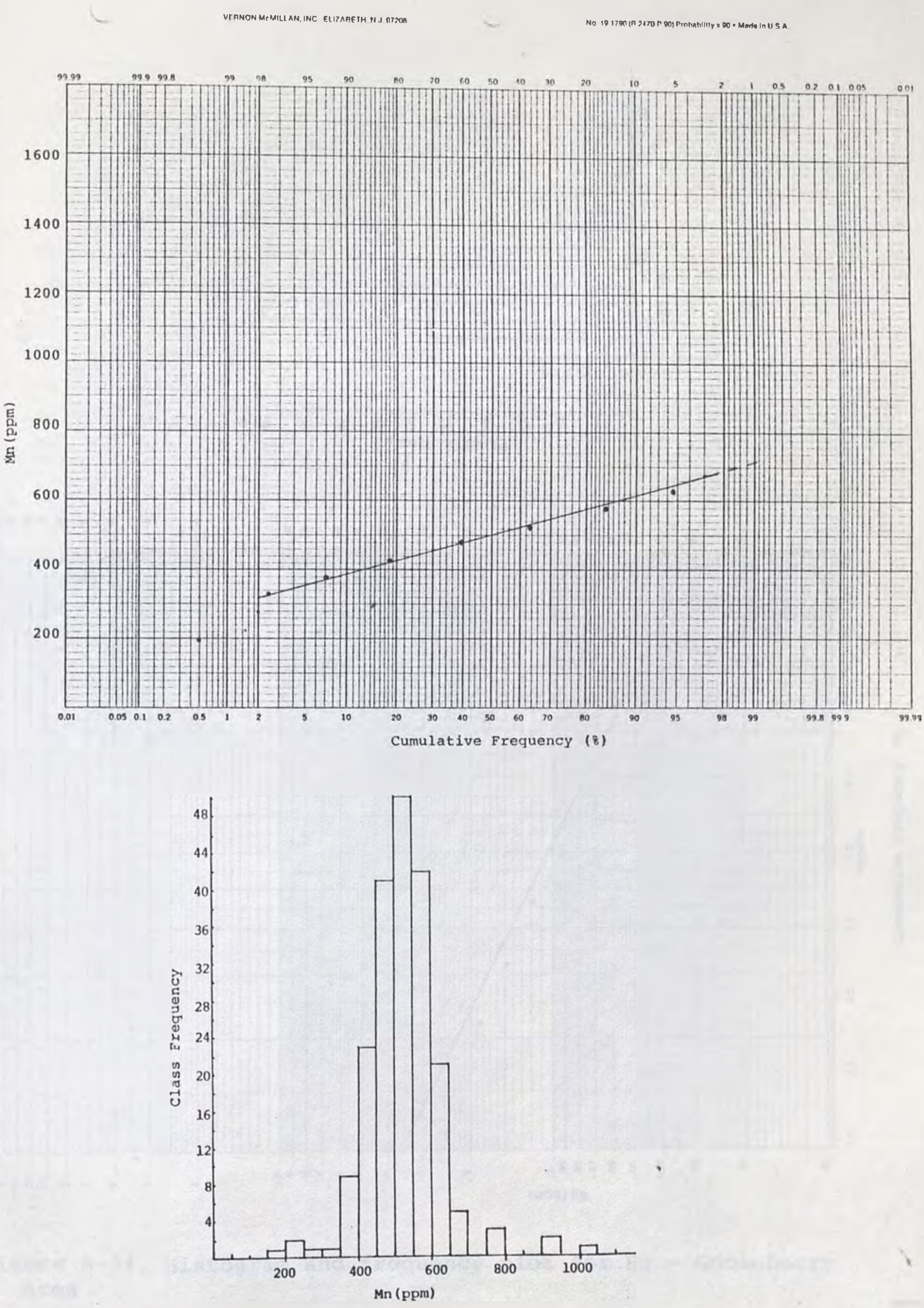

Figure A-33. Histogram and frequency plot for Mn - Gooseberry area

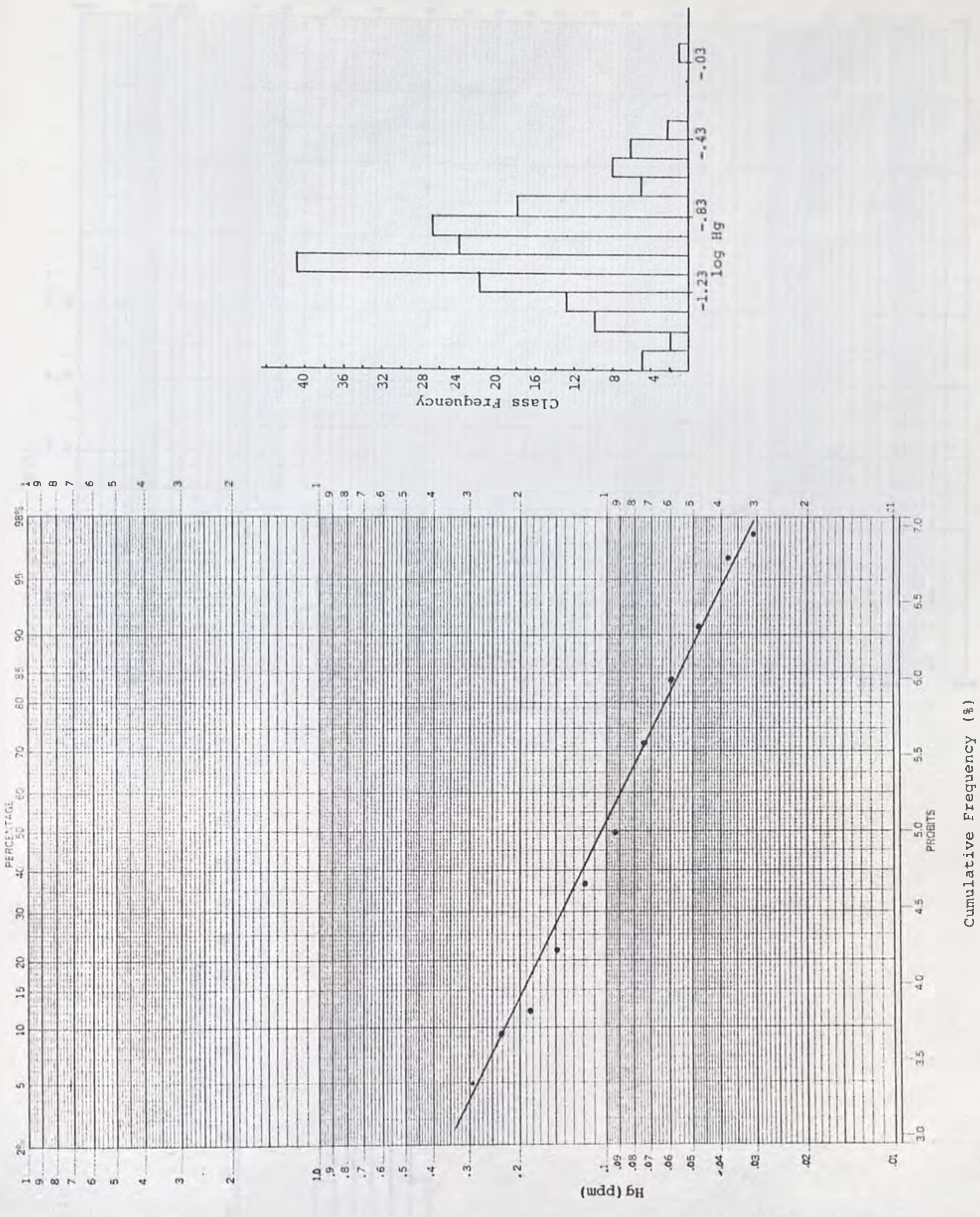

Figure A-34. Histogram and frequency plot for Hg - Gooseberry area

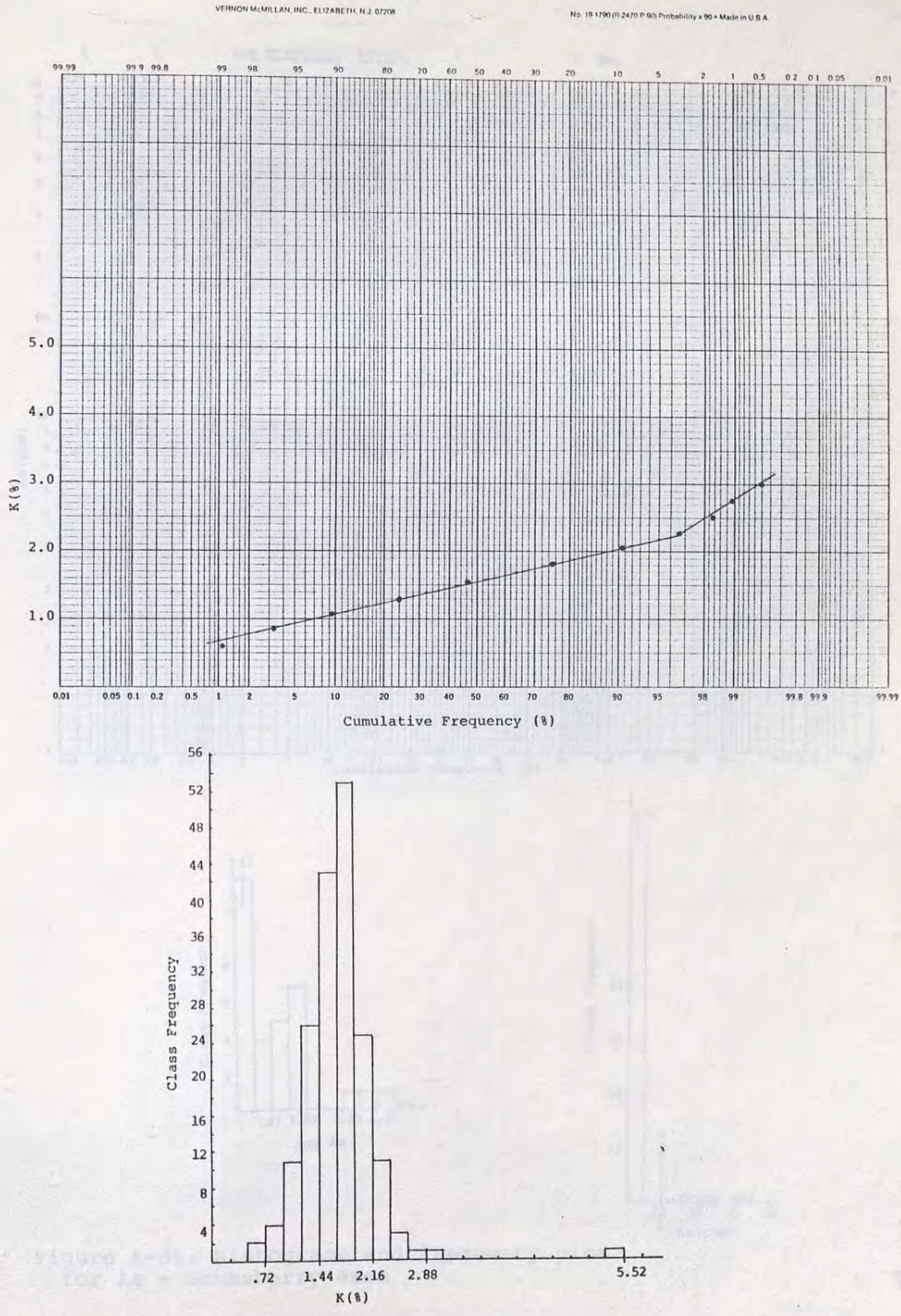

Figure A-35. Histogram and frequency plot for K - Gooseberry area

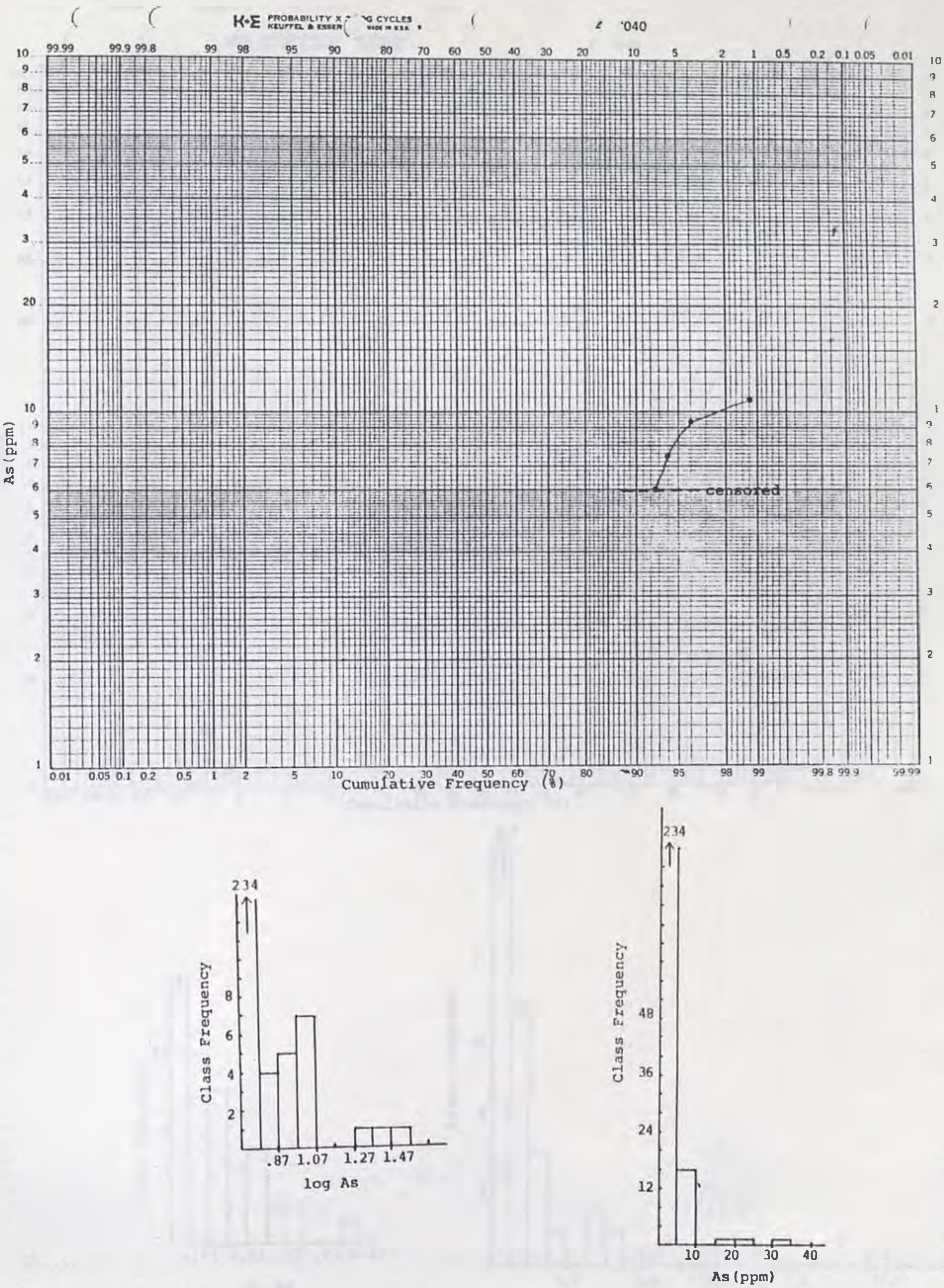

Figure A-36. Histograms and frequency plot for As - Gooseberry area

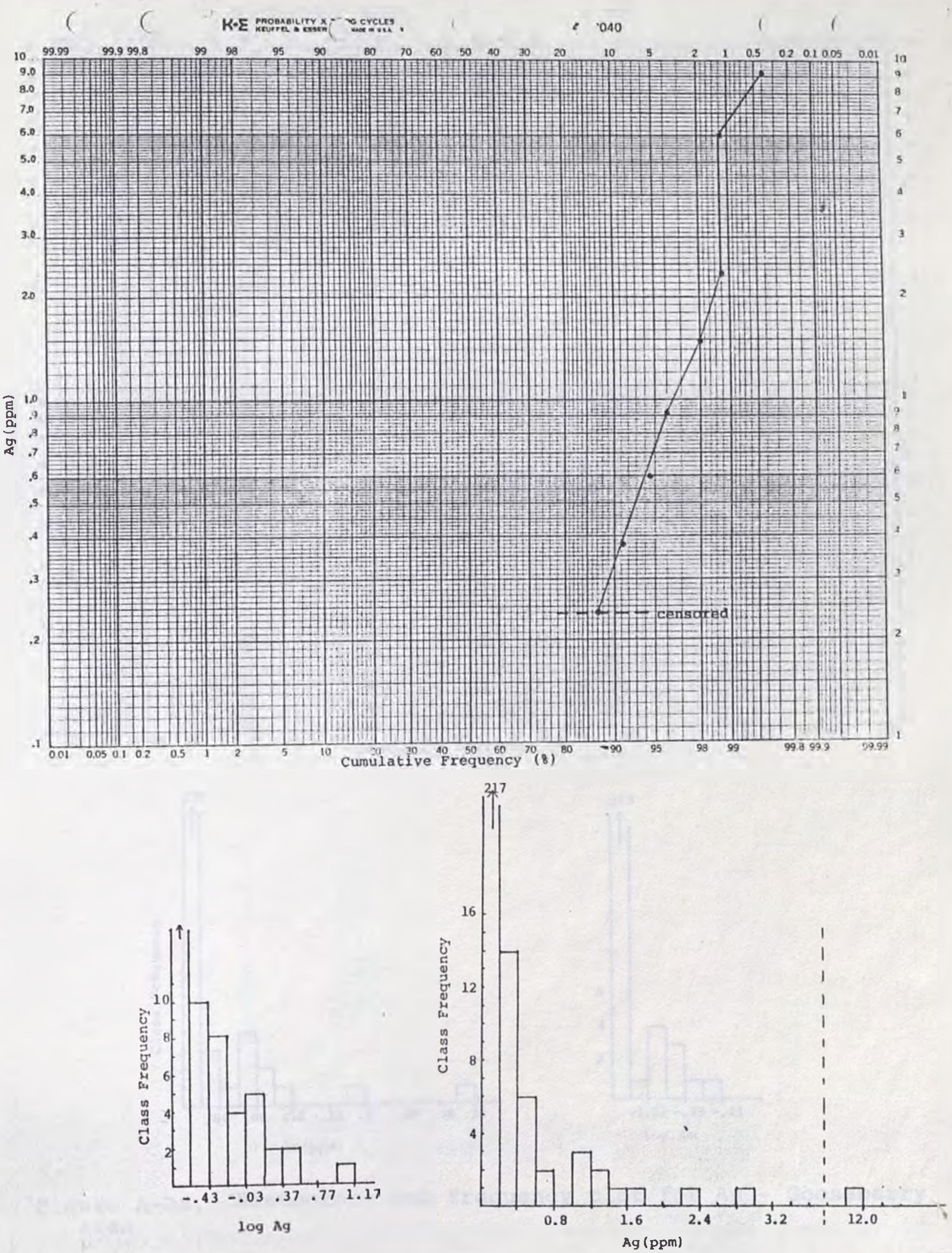

Figure A-37. Histograms and frequency plot for Ag - Gooseberry area

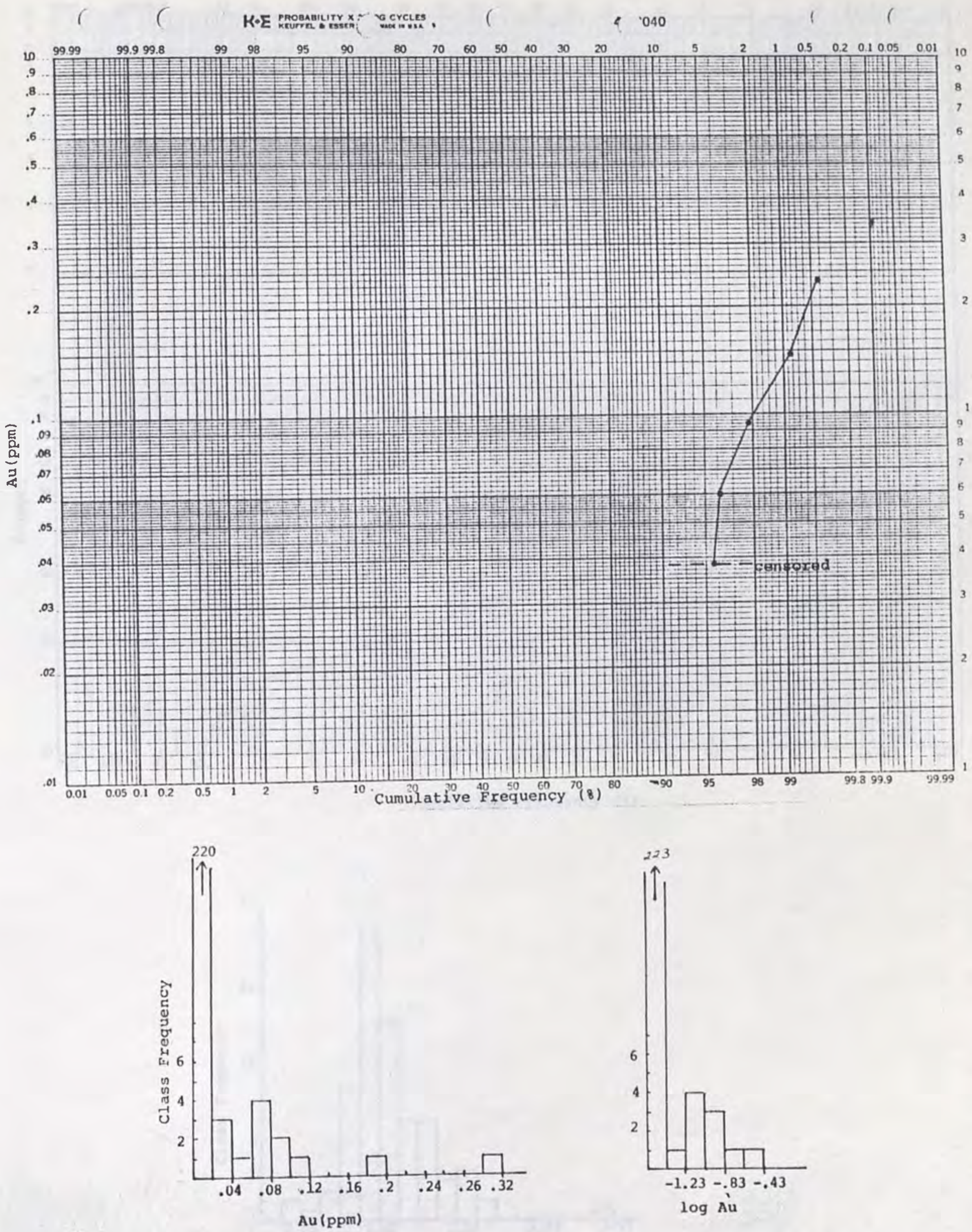

Figure A-38. Histograms and frequency plot for Au - Gooseberry area

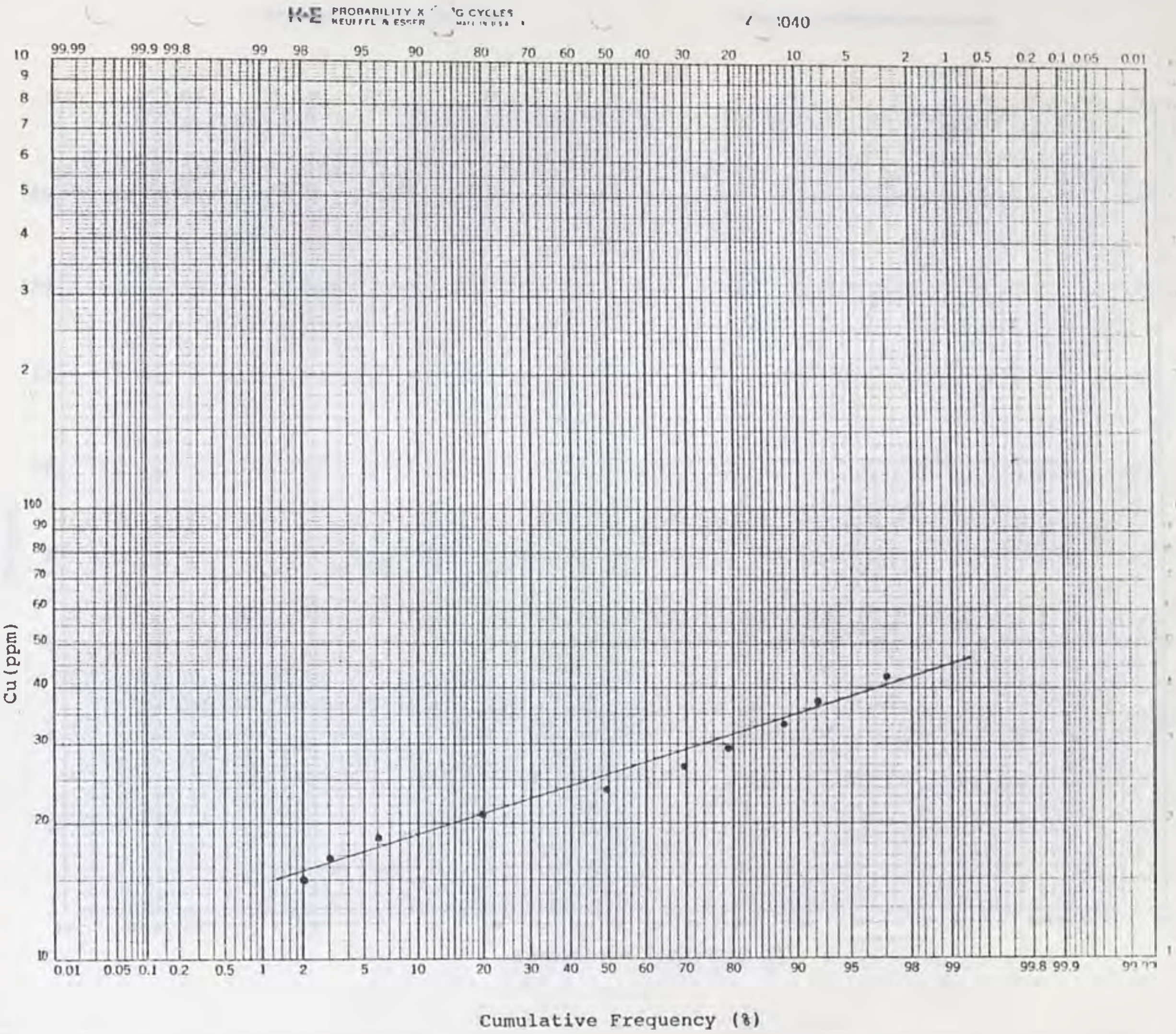

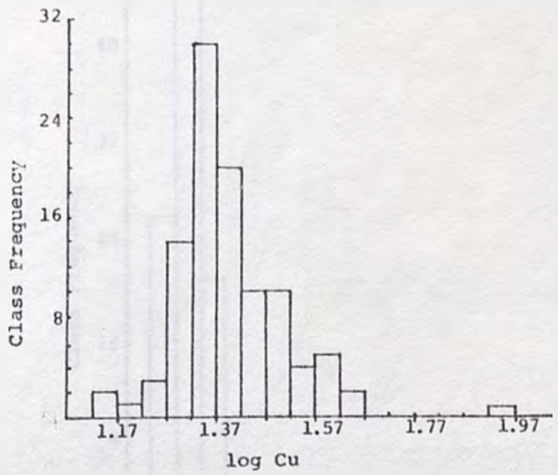

Figure A-39. Histogram and frequency plot for Cu - Red Top area

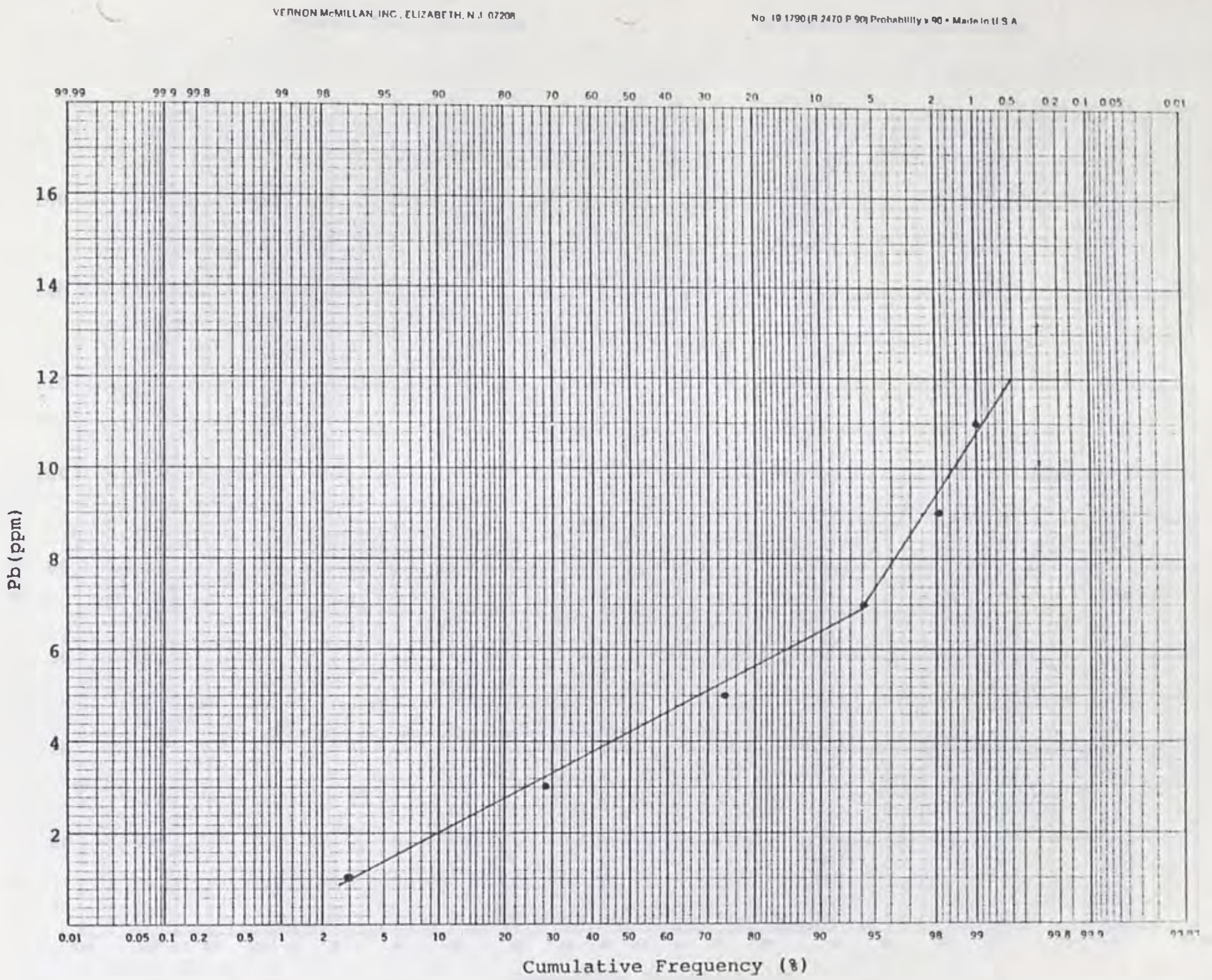

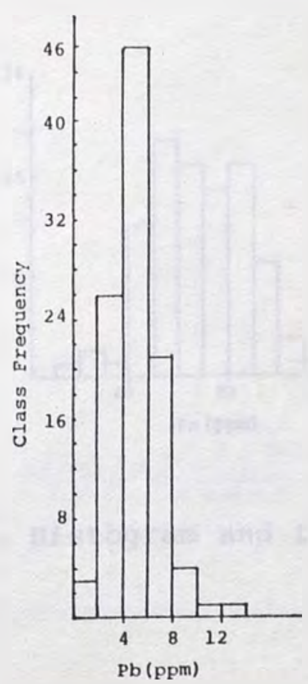

Figure A-40. Histogram and frequency plot for Pb - Red Top area

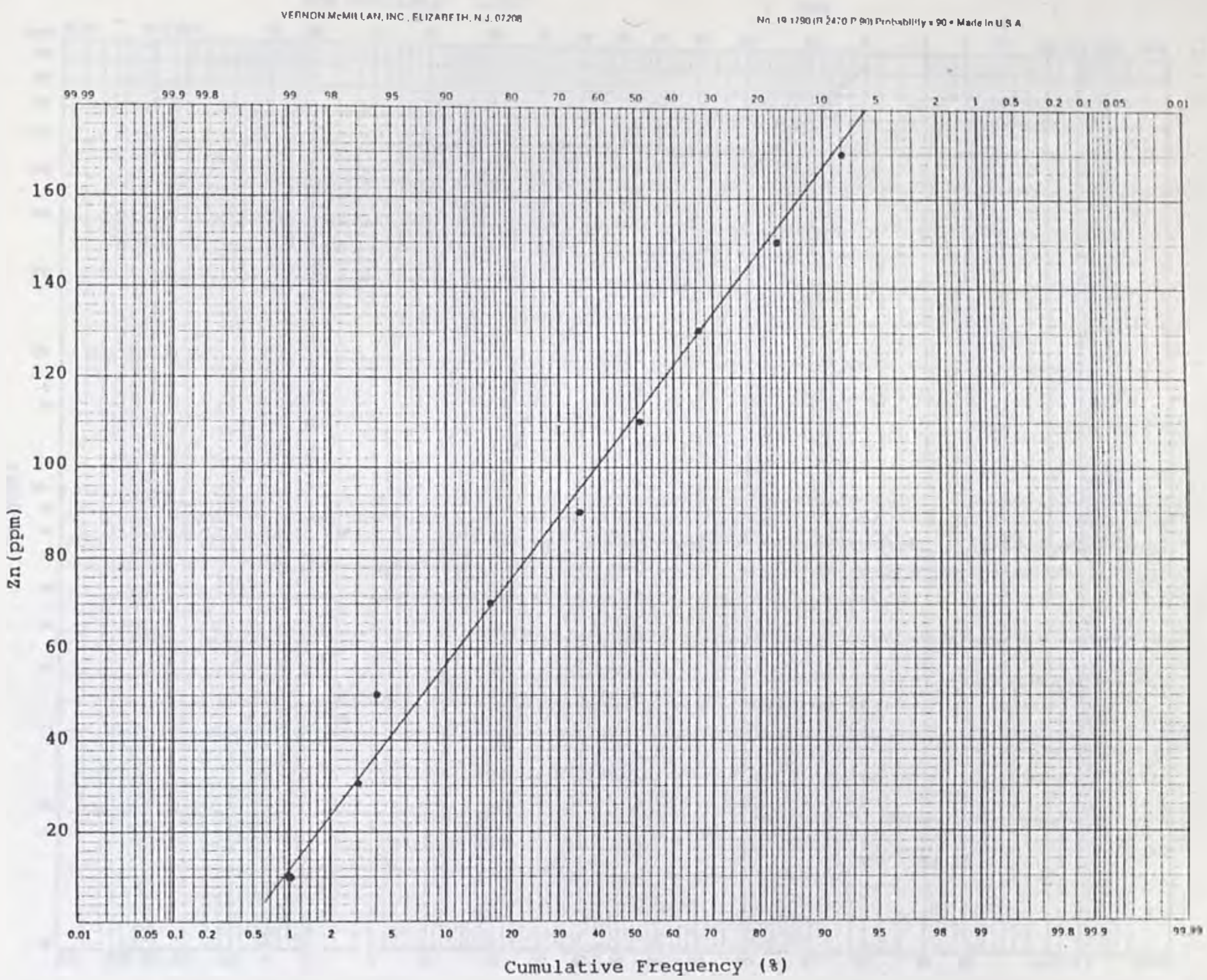

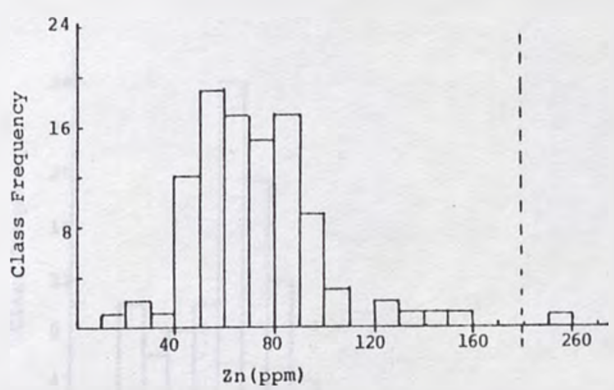

Figure A-41. Histogram and frequency plot for Zn - Red Top area

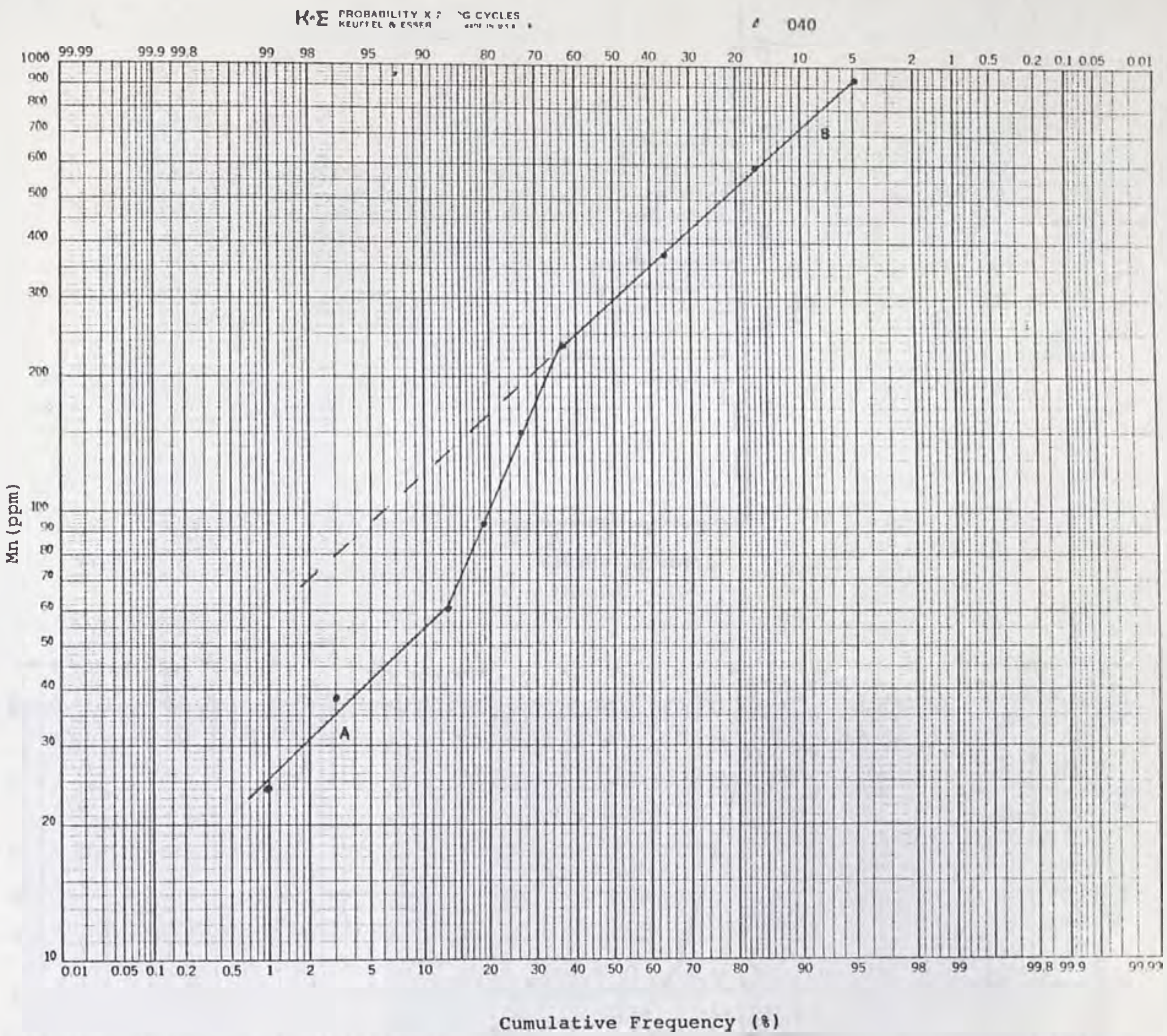

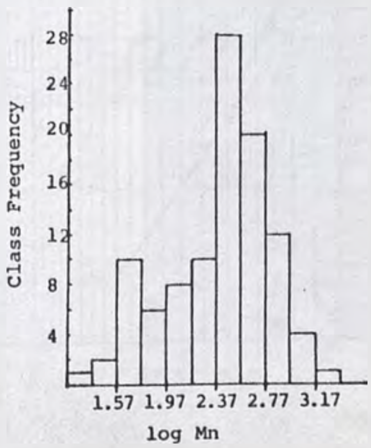

Figure A-42. Histogram and frequency plot for Mn - Red Top area

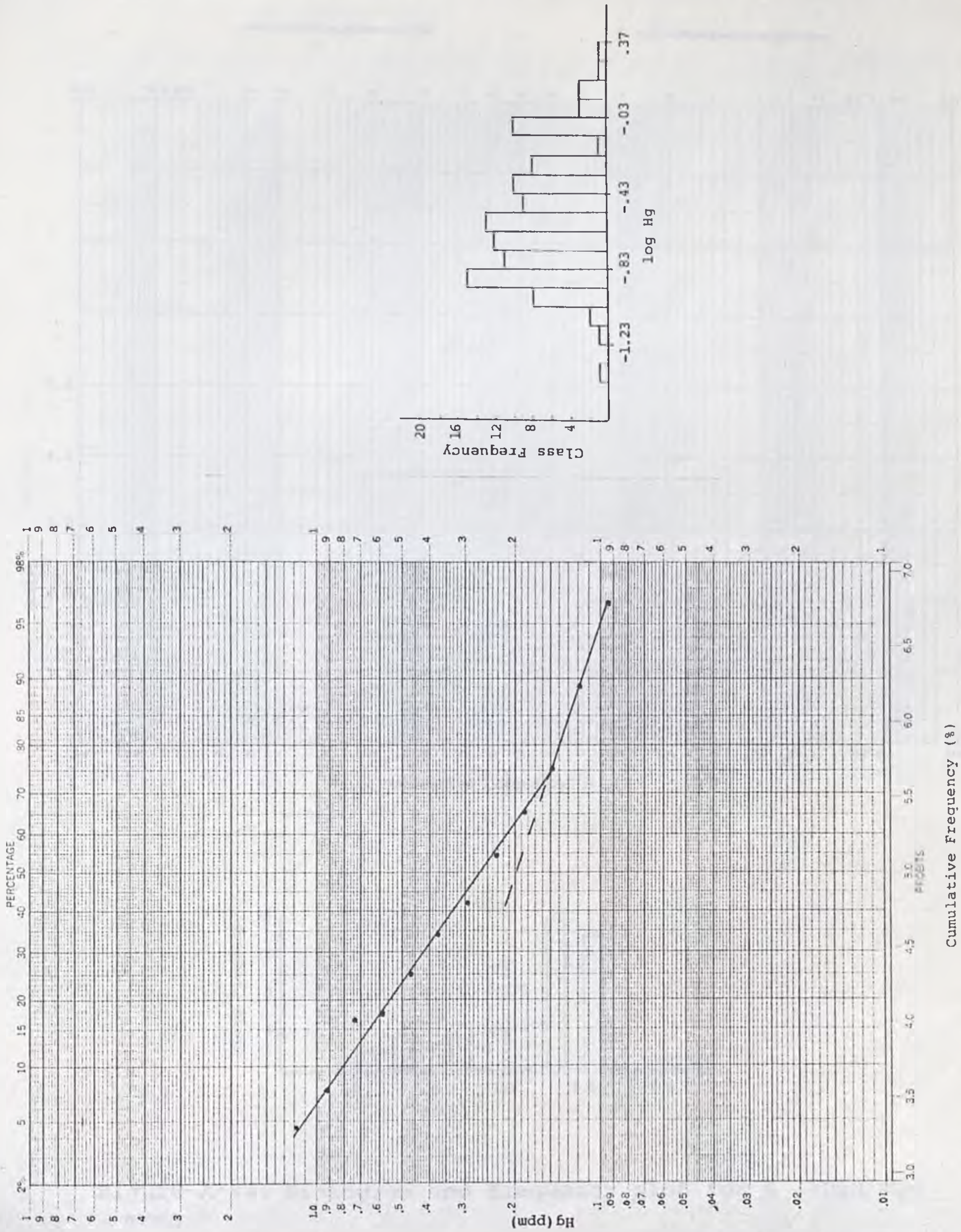

Figure A-43. Histogram and frequency plot for Hg - Red Top area

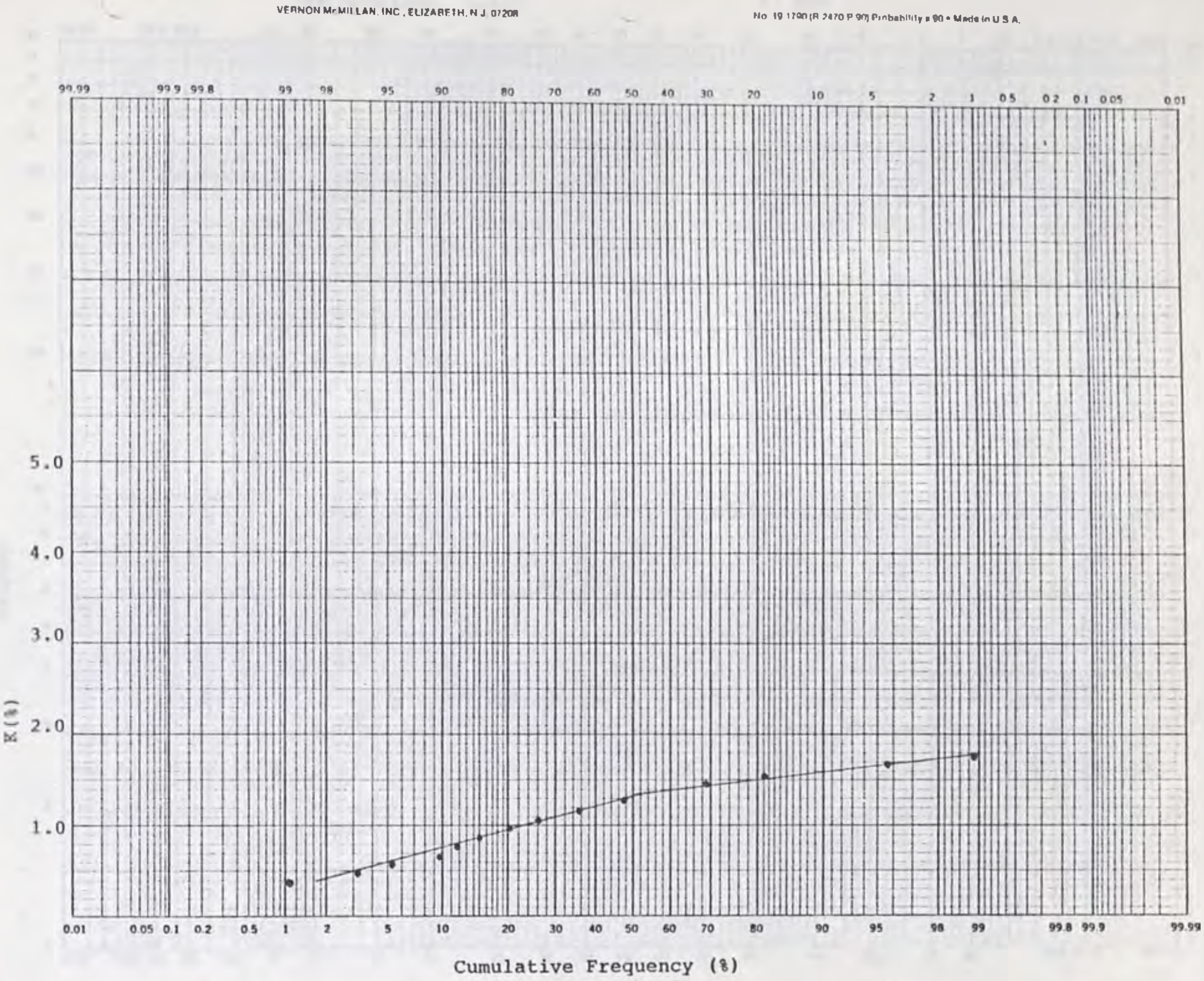

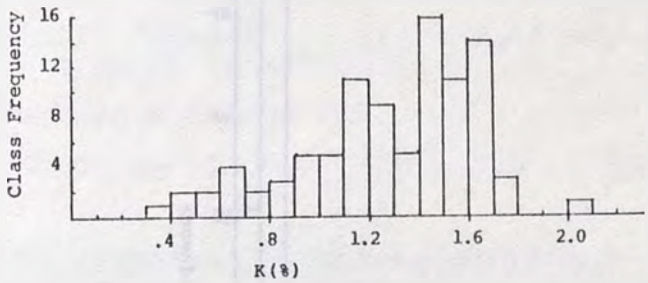

Figure A-44. Histogram and frequency plot for K - Red Top area

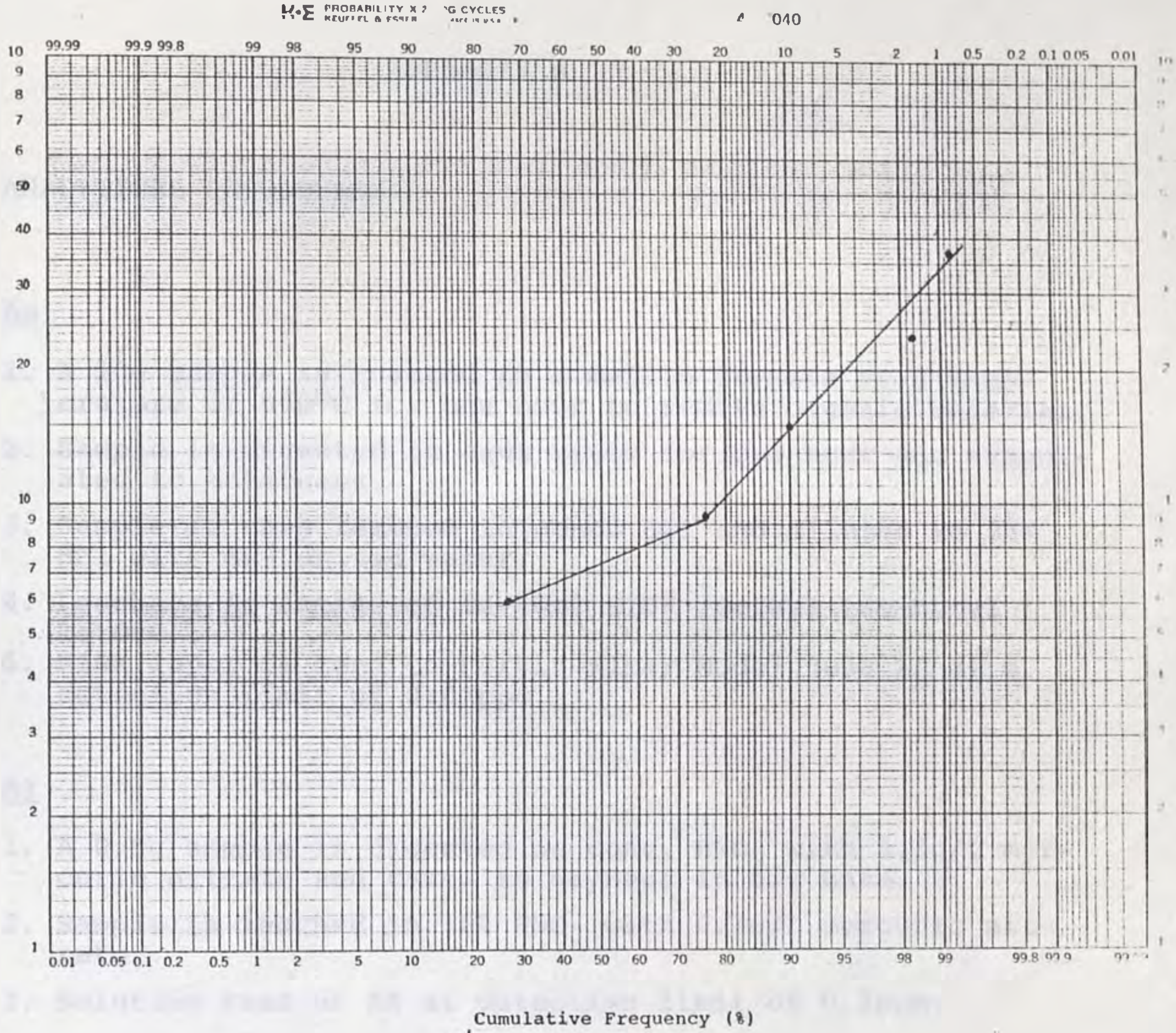

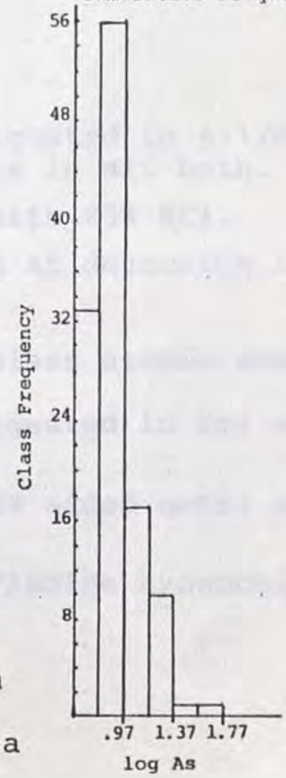

Figure A-45. Histogram and frequency plot for As - Red Top area

APPENDIX B

ANALYTICAL PROCEDURES

Au

1. A 10g sample is roasted in a muffle furnace at a temperature of 600°C for one hour to remove organic material.
2. Sample is digested in aqua regia for one hour and evaporated to moistness.
3. Sample is then leached in conc. HCl and diluted to 25% HCl with de-ionized water.
4. Leachate is extracted in 10ml MIBK (methyl iso-butyl ketone).
5. MIBK layer is read on Perkin-Elmer Model 3030 AA at a detection limit of 0.02ppm.

Ag

1. A 0.5g sample is digested on conc. HNO_3 with 0.3g/L mercuric nitrate and taken to dryness in air bath.
2. Sample is leached in 10% HNO_3 with 0.3g/L mercuric nitrate.
3. Solution read on AA at detection limit of 0.2ppm.

Cu-Pb-Zn-Mn

1. A 0.5g sample is digested in 4:1/HNO_3:$HClO_4$ solution and taken to dryness in air bath.
2. Sample is leached with 25% HCl.
3. Solution read on AA at detection limit of 1ppm.

Hg - Cold vapor, flameless atomic absorption technique

1. A 1-3g sample is digested in 5ml of HNO_3 and 5ml of H_2SO_4 for 45 minutes.
2. 5% $KMnO_4$ solution is added until solution retains a pink color.
3. 5ml of 1.5% hydroxylamine hydrochloride solution is added and mixed.

4. 5ml of 10% stannous chloride is added and immediately attached to aeration apparatus of the Hg analyzer.
5. Amount of absorbance is read and concentration is calculated by comparison to a set of standards. Detection limit 0.005ppm.

As-Sb

1. A 1g sample is digested in 10ml of 6N HCl-1% bromine solution.
2. Solution read on AA at a detection limit of 5ppm.

K

1. A 0.2g sample is fused with 1g lithium metaborate in muffle furnace at 950^{o}C for 30 minutes.
2. The beads produced are dissolved in hot 2.5% HNO_3 by stirring on a magnetic stirrer.
3. 10% lanthanum solution is added to aid in eliminating alkali interferences on the AA.
4. Solution read on AA. Detection limit of 0.05%.

APPENDIX C

Table C-1. Sichel's Table for determining $\phi(V)$ from variance

HERBERT S. SICHEL

$N = 30$

V	$\phi(V)$	δ	V	$\phi(V)$	δ	V	$\phi(V)$	δ
·0	·00000	2168	1·5	·31827	2072	3·0	·62322	1990
·1	·02168	2160	1·6	·33899	2067	3·1	·64312	1984
·2	·04328	2155	1·7	·35966	2060	3·2	·66296	1982
·3	·06483	2146	1·8	·38026	2055	3·3	·68278	1974
·4	·08629	2143	1·9	·40081	2050	3·4	·70252	1971
·5	·10772	2132	2·0	·42131	2043	3·5	·72223	1965
·6	·12904	2129	2·1	·44174	2037	3·6	·74188	1961
·7	·15033	2122	2·2	·46211	2033	3·7	·76149	1956
·8	·17155	2113	2·3	·48244	2027	3·8	·78105	1951
·9	·19268	2110	2·4	·50271	2022	3·9	·80056	1947
1·0	·21378	2102	2·5	·52293	2016	4·0	·82003	1942
1·1	·23480	2095	2·6	·54309	2011	4·1	·83945	1937
1·2	·25575	2092	2·7	·56320	2006	4·2	·85882	1933
1·3	·27667	2083	2·8	·58326	2000	4·3	·87815	1928
1·4	·29750	2077	2·9	·60326	1996	4·4	·89743	1923
1·5	·31827		3·0	·62322		4·5	·91666	

$N = 100$

V	$\phi(V)$	δ	V	$\phi(V)$	δ	V	$\phi(V)$	δ
·0	·00000	2168	1·0	·21609	2148	2·0	·43011	2128
·1	·02168	2172	1·1	·23757	2147	2·1	·45139	2128
·2	·04340	2166	1·2	·25904	2147	2·2	·47267	2125
·3	·06506	2162	1·3	·28051	2143	2·3	·49392	2122
·4	·08668	2161	1·4	·30194	2142	2·4	·51514	2122
·5	·10829	2163	1·5	·32336	2138	2·5	·53636	2120
·6	·12992	2157	1·6	·34474	2136	2·6	·55756	2116
·7	·15149	2155	1·7	·36610	2136	2·7	·57872	2115
·8	·17304	2153	1·8	·38746	2132	2·8	·59987	2114
·9	·19457	2152	1·9	·40878	2133	2·9	·62101	2112
1·0	·21609		2·0	·43011		3·0	·64213	

$N = \infty$

V	$\phi(V)$	δ	V	$\phi(V)$	δ	V	$\phi(V)$	δ
·0	·00000	2171	1·0	·21715	2171	2·0	·43429	2172
·1	·02171	2172	1·1	·23886	2172	2·1	·45601	2171
·2	·04343	2171	1·2	·26058	2171	2·2	·47772	2172
·3	·06514	2172	1·3	·28229	2171	2·3	·49944	2171
·4	·08686	2171	1·4	·30400	2172	2·4	·52115	2172
·5	·10857	2172	1·5	·32572	2172	2·5	·54287	2171
·6	·13029	2171	1·6	·34744	2171	2·6	·56458	2172
·7	·15200	2172	1·7	·36915	2171	2·7	·58630	2171
·8	·17372	2171	1·8	·39086	2172	2·8	·60801	2172
·9	·19543	2172	1·9	·41258	2171	2·9	·62973	2171
1·0	·21715		2·0	·43429		3·0	·65144	

(Sichel, 1952, p.288)

Table C-2. PERCENTAGE POINTS OF THE t_m DISTRIBUTION *

df \ α	10%	5%	2.5%	1%
1	3.078	6.314	12.706	31.821
2	1.886	2.920	4.303	6.965
3	1.638	2.353	3.182	4.541
4	1.533	2.132	2.776	3.747
5	1.476	2.015	2.571	3.365
6	1.440	1.943	2.447	3.143
7	1.415	1.895	2.365	2.998
8	1.397	1.860	2.306	2.896
9	1.383	1.833	2.262	2.821
10	1.372	1.812	2.228	2.764
11	1.363	1.796	2.201	2.718
12	1.356	1.782	2.179	2.681
13	1.350	1.771	2.160	2.650
14	1.345	1.761	2.145	2.624
15	1.341	1.753	2.131	2.602
16	1.337	1.746	2.120	2.583
17	1.333	1.740	2.110	2.567
18	1.330	1.734	2.101	2.552
19	1.328	1.729	2.093	2.539
20	1.325	1.725	2.086	2.528
21	1.323	1.721	2.080	2.518
22	1.321	1.717	2.074	2.508
23	1.319	1.714	2.069	2.500
24	1.318	1.711	2.064	2.492
25	1.316	1.708	2.060	2.485
26	1.315	1.706	2.056	2.479
27	1.314	1.703	2.052	2.473
28	1.313	1.701	2.048	2.467
29	1.311	1.699	2.045	2.462
30	1.310	1.697	2.042	2.457
40	1.303	1.684	2.021	2.423
60	1.296	1.671	2.000	2.390
120	1.289	1.658	1.980	2.358
∞	1.282	1.645	1.960	2.326

* From Table 12, Biometrika Tables for Statisticians, Volume 1, Second Edition, Cambridge University Press, 1962.

From Koch and Link (1970)

Table C-3. Percentage points of the F- distribution

$\alpha = 5\%$

df_2 \ df_1	1	2	3	4	5	6	7	8	9
1	161.15	199.50	215.71	224.58	230.16	233.99	236.77	238.88	240.54
2	18.513	19.000	19.164	19.247	19.296	19.330	19.353	19.371	19.385
3	10.128	9.5521	9.2766	9.1172	9.0135	8.9406	8.8868	8.8452	8.8123
4	7.7086	6.9443	6.5914	6.3883	6.2560	6.1631	6.0942	6.0410	5.9988
5	6.6079	5.7861	5.4095	5.1922	5.0503	4.9503	4.8759	4.8183	4.7725
6	5.9874	5.1433	4.7571	4.5337	4.3874	4.2839	4.2066	4.1468	4.0990
7	5.5914	4.7374	4.3468	4.1203	3.9715	3.8660	3.7870	3.7257	3.6767
8	5.3177	4.4590	4.0662	3.8378	3.6875	3.5806	3.5005	3.4381	3.3881
9	5.1174	4.2565	3.8626	3.6331	3.4817	3.3738	3.2927	3.2296	3.1789
10	4.9646	4.1028	3.7083	3.4780	3.3258	3.2172	3.1355	3.0717	3.0204
11	4.8443	3.9823	3.5874	3.3567	3.2039	3.0946	3.0123	2.9480	2.8962
12	4.7472	3.8853	3.4903	3.2592	3.1059	2.9961	2.9134	2.8486	2.7964
13	4.6672	3.8056	3.4105	3.1791	3.0254	2.9153	2.8321	2.7669	2.7144
14	4.6001	3.7389	3.3439	3.1122	2.9582	2.8477	2.7642	2.6987	2.6458
15	4.5431	3.6823	3.2874	3.0556	2.9013	2.7905	2.7066	2.6408	2.5876
16	4.4940	3.6337	3.2389	3.0069	2.8524	2.7413	2.6572	2.5911	2.5377
17	4.4513	3.5915	3.1968	2.9647	2.8100	2.6987	2.6143	2.5480	2.4943
18	4.4139	3.5546	3.1599	2.9277	2.7729	2.6613	2.5767	2.5102	2.4563
19	4.3808	3.5219	3.1274	2.8951	2.7401	2.6283	2.5435	2.4768	2.4227
20	4.3513	3.4928	3.0984	2.8661	2.7109	2.5990	2.5140	2.4471	2.3928
21	4.3248	3.4668	3.0725	2.8401	2.6848	2.5727	2.4876	2.4205	2.3661
22	4.3009	3.4434	3.0491	2.8167	2.6613	2.5491	2.4638	2.3965	2.3419
23	4.2793	3.4221	3.0280	2.7955	2.6400	2.5277	2.4422	2.3748	2.3201
24	4.2597	3.4028	3.0088	2.7763	2.6207	2.5082	2.4226	2.3551	2.3002
25	4.2417	3.3852	2.9912	2.7587	2.6030	2.4904	2.4047	2.3371	2.2821
26	4.2252	3.3690	2.9751	2.7426	2.5868	2.4741	2.3883	2.3205	2.2655
27	4.2100	3.3541	2.9604	2.7278	2.5719	2.4591	2.3732	2.3053	2.2501
28	4.1960	3.3404	2.9467	2.7141	2.5581	2.4453	2.3593	2.2913	2.2360
29	4.1830	3.3277	2.9340	2.7014	2.5454	2.4324	2.3463	2.2782	2.2229
30	4.1709	3.3158	2.9223	2.6896	2.5336	2.4205	2.3343	2.2662	2.2107
40	4.0848	3.2317	2.8387	2.6060	2.4495	2.3359	2.2490	2.1802	2.1240
60	4.0012	3.1504	2.7581	2.5252	2.3683	2.2540	2.1665	2.0970	2.0401
120	3.9201	3.0718	2.6802	2.4472	2.2900	2.1750	2.0867	2.0164	1.9588
∞	3.8415	2.9957	2.6049	2.3719	2.2141	2.0986	2.0096	1.9384	1.8799

$\alpha = 5\%$

df_2 \ df_1	10	12	15	20	24	30	40	60	120	∞
1	241.88	243.91	245.95	248.01	249.05	250.09	251.14	252.20	253.25	254.32
2	19.396	19.413	19.429	19.446	19.454	19.462	19.471	19.479	19.487	19.496
3	8.7855	8.7446	8.7029	8.6602	8.6385	8.6166	8.5944	8.5720	8.5494	8.5265
4	5.9644	5.9117	5.8578	5.8025	5.7744	5.7459	5.7170	5.6878	5.6581	5.6281
5	4.7351	4.6777	4.6188	4.5581	4.5272	4.4957	4.4638	4.4314	4.3984	4.3650
6	4.0600	3.9999	3.9381	3.8742	3.8415	3.8082	3.7743	3.7398	3.7047	3.6688
7	3.6365	3.5747	3.5108	3.4445	3.4105	3.3758	3.3404	3.3043	3.2674	3.2298
8	3.3472	3.2840	3.2184	3.1503	3.1152	3.0794	3.0428	3.0053	2.9669	2.9276
9	3.1373	3.0729	3.0061	2.9365	2.9005	2.8637	2.8259	2.7872	2.7475	2.7067
10	2.9782	2.9130	2.8450	2.7740	2.7372	2.6996	2.6609	2.6211	2.5801	2.5379
11	2.8536	2.7876	2.7186	2.6464	2.6090	2.5705	2.5309	2.4901	2.4480	2.4045
12	2.7534	2.6866	2.6169	2.5436	2.5055	2.4663	2.4259	2.3842	2.3410	2.2962
13	2.6710	2.6037	2.5331	2.4589	2.4202	2.3803	2.3392	2.2966	2.2524	2.2064
14	2.6021	2.5342	2.4630	2.3879	2.3487	2.3082	2.2664	2.2230	2.1778	2.1307
15	2.5437	2.4753	2.4035	2.3275	2.2878	2.2468	2.2043	2.1601	2.1141	2.0658
16	2.4935	2.4247	2.3522	2.2756	2.2354	2.1938	2.1507	2.1058	2.0589	2.0096
17	2.4499	2.3807	2.3077	2.2304	2.1898	2.1477	2.1040	2.0584	2.0107	1.9604
18	2.4117	2.3421	2.2686	2.1906	2.1497	2.1071	2.0629	2.0166	1.9681	1.9168
19	2.3779	2.3080	2.2341	2.1555	2.1141	2.0712	2.0264	1.9796	1.9302	1.8780
20	2.3479	2.2776	2.2033	2.1242	2.0825	2.0391	1.9938	1.9464	1.8963	1.8432
21	2.3210	2.2504	2.1757	2.0960	2.0540	2.0102	1.9645	1.9165	1.8657	1.8117
22	2.2967	2.2258	2.1508	2.0707	2.0283	1.9842	1.9380	1.8895	1.8380	1.7831
23	2.2747	2.2036	2.1282	2.0476	2.0050	1.9605	1.9139	1.8649	1.8128	1.7570
24	2.2547	2.1834	2.1077	2.0267	1.9838	1.9390	1.8920	1.8424	1.7897	1.7331
25	2.2365	2.1649	2.0889	2.0075	1.9643	1.9192	1.8718	1.8217	1.7684	1.7110
26	2.2197	2.1479	2.0716	1.9898	1.9464	1.9010	1.8533	1.8027	1.7488	1.6906
27	2.2043	2.1323	2.0558	1.9736	1.9299	1.8842	1.8361	1.7851	1.7307	1.6717
28	2.1900	2.1179	2.0411	1.9586	1.9147	1.8687	1.8203	1.7689	1.7138	1.6541
29	2.1768	2.1045	2.0275	1.9446	1.9005	1.8543	1.8055	1.7537	1.6981	1.6377
30	2.1646	2.0921	2.0148	1.9317	1.8874	1.8409	1.7918	1.7396	1.6835	1.6223
40	2.0772	2.0035	1.9245	1.8389	1.7929	1.7444	1.6928	1.6373	1.5766	1.5089
60	1.9926	1.9174	1.8364	1.7480	1.7001	1.6491	1.5943	1.5343	1.4673	1.3893
120	1.9105	1.8337	1.7505	1.6587	1.6084	1.5543	1.4952	1.4290	1.3519	1.2539
∞	1.8307	1.7522	1.6664	1.5705	1.5173	1.4591	1.3940	1.3180	1.2214	1.0000

From Koch and Link (1970)

REFERENCES

1. Beus, A.A. and Grigorian, S.V., 1977, Geochemical Exploration Methods for Mineral Deposits. Allied Publishing. 287pp.

2. Connor, J.J. and Shacklette, H.T., 1975, "Background Geochemistry of Some Rocks, Soils, Plants, and Vegetables in the Conterminous United States"; USGS PP 574-F.

3. Davis, J.C., 1973, Statistical and Data Analysis in Geology. Wiley, N.Y. 543pp.

4. Glover, J.E., Groves, D.I., and Smith, R.E. (eds), 1979, "Mercury Pathfinder Techniques in Minerals Exploration"; Pathfinder and Multi-element Geochemistry in Mineral Exploration; The Geology Dept. and Extension Service, Univ. of Western Australia, Publication no. 4, p.99-116.

5. Govett, G.J.S. (ed), 1983, Handbook of Exploration Geochemistry, v.2 - "Statistics and Data Analysis in Geochemical Prospecting". Elsevier Scientific, N.Y. 437pp.

6. Koch, G.S. and Link, R.F., 1970, Statistical Analysis of Geological Data, v.1. Wiley, N.Y. 365pp.

7. Koch, G.S. and Link, R.F., 1971a, Statistical Analysis of Geological Data, v.2. Wiley, N.Y. 468pp.

8. Koch, G.S. and Link, R.F., 1971b, "The Coefficient of Variation- a guide to the sampling of ore deposits"; Econ. Geol. v.66, pp.293-301.

9. Lepeltier, C., 1969, "A Simplified Statistical Treatment of Geochemical Data by Graphical Representation"; Econ. Geol. v.64 no.5, pp.538-550.

10. Levinson, A.A. (ed), 1974, Introduction to Exploration Geochemistry. Applied Publ. 601pp.

11. Miesch, A.T., 1967, "Methods of Computation for Estimating Geochemical Abundance"; USGS PP 574-B, 15pp.

12. Miesch, A.T., 1976, "Geochemical Survey of Missouri- Methods of Sampling, Laboratory Analysis and Statistical Reduction of Data"; USGS PP 954-A.

13. Obial, R.C. and James, C.H., 1972, "Use of Cluster Analysis in Geochemical Prospecting with Particular Reference to Southern Derbyshire, England"; Geochemical Exploration 1972, pp. 237-257.

14. Oliviera, Jose, 1981, Unpublished report for Westcoast Oil & Gas Corp.

15. Polikarpochkin, V.V. and Kitaev, N.A., 1971, "Endogenic Halos of Epithermal Gold-Bearing Deposits", Canadian Institute of Mining and Metallurgy Special v.11, pp.381-383.

16. Rose, 1969, Nevada Bureau of Mines Bull. 71.

17. Rose, A.W., Hawkes, H.E. and Webb, J.S., 1979, Geochemistry in Mineral Exploration. Academic Press. 635pp.

18. Schafer, Robert W., 1976, "The Mineralogy, Structure and Alteration Pattern of the Gooseberry Mine, Storey County, Nevada"; Miami University-Oxford, Ohio, M.S. Thesis, 79pp.

19. Scherkenbach, Daryl A. and Noble, Donald C., 1984, "Potassium and Rubidium Metasomatism at the Julcani District, Peru"; Econ. Geol. v.79, pp.565-572.

20. Sichel, H.S., 1952, "New Method in the Statistical Evaluation of Mine Sampling Data"; London Institute Mining & Metallurgy, Trans. v.61, pp.261-288.

21. Silberman, M.L., 1977, Isochron/West Bulletin no. 20.

22. Sprecher, Terry A., 1985, "Wall-rock Alteration, Vein Structure, and Preliminary Fluid-inclusion Studies, Gooseberry Mine, Storey Couny, Nevada; Univ. of Nevada, M.S. Thesis, 93pp.

23. Tennant, C.B. and White, M.L., 1959, "Distribution of Some Geologic Data"; Econ. Geol. v.54, pp.1281-1290.